BIOCHEMICAL ANALYSIS OF THE REGULATION OF VESICLE FUSION, PEROXISOMAL PROTEIN IMPORT AND PROTEOLYTIC PROCESSING IN EUKARYOTES

by

Antionette L. Williams

A dissertation submitted in partial fulfillment
of the requirements for the degree of
Doctor of Philosophy
(Cellular and Molecular Biology)
in The University of Michigan
2008

Doctoral Committee:

Associate Professor Laura J. Olsen, Co-Chair
Associate Professor Jesse C. Hay, Co-Chair, Univ. of Montana
Professor John W. Schiefelbein, Jr.
Associate Professor Amy Chang
Assistant Professor Matthew R. Chapman

"…Being confident of this very thing, that He which hath begun a good work in you will perform *it* until the day of Jesus Christ…"
Phillipians 1:6

For Mom.
Your Roonie's a doctor now!

ACKNOWLEDGEMENTS

First and foremost, I give honor to God the Father. I thank You for Your love, the gift of eternal salvation, and Your Son, Jesus Christ. I've come this far by faith in Him and great is His faithfulness unto me. I shall **never** be ashamed.

I am thankful to my thesis co-advisors, Dr. Laura J. Olsen and Dr. Jesse C. Hay for guidance and support over the years. I would like to thank my committee members Dr. John Schiefelbein, Dr. Amy Chang and Dr. Matthew Chapman for their invaluable contributions to my growth and success – committee meetings were a total trip! I would also like to thank the faculty, staff and students of the Program in Cellular and Molecular Biology. A special thanks is extended to the Department of Molecular, Cellular and Developmental Biology – your adoption afforded me a home on central campus. Thanks also to Dr. Janine Maddock, Dr. Santhadevi Jeyabalan, and Dr. Marcus Ammerlaan for the opportunities to teach and mentor students. I appreciate your confidence in me. The students couldn't have been in safer hands (if I must say so myself -- wink).

I would also like to thank my former lab mates Dr. Ashwini Joglekar, Dr. Dalu Xu, Dr. Haruki Hasegawa, Nicola Harrison-Lowe, Katherine Drake, Stephanie Gardiner, Brandon Wojcik (my son), Margaret Du, Jennifer Rothstein (my lab genie), Jessica Farber, Daniel Holbrook (shall we clone?), Zachary Bay

and Christopher Dobson – let us do a happy lab dance! To my friends across all departments, disciplines and graduate levels – it's time to party ya'll!

Tyrone L. Odister, you are someone very special to me. Thanks for your friendship and more. Who'd ever think we'd be… crazy, huh?

I am forever indebted to Biza and Titos Sompa and the Bichini Bia Congo Dance Theater Company. I can't thank you enough for how you have enriched my life. You are my family.

Thanks to the best child I've ever known, my daughter Latrece Antionette Brabson. You are the physical manifestation of the best of me. Thank you for your understanding and support, even when you didn't realize you were giving it. Thank you for your unconditional love. You will never again have to sleep in the lab, I promise!

Shawn and Kim – we are Mom and Poppy's three musketeers. What we do alone, we do together. All for one and… well, you know the rest. That's how mom raised us to be. Let us continue to make her proud. Remember when Poppy used to say, "I don't know, check it out?" Perhaps that's what sparked my interest in research (ha!). How can it ever be enough to say thank you? You have both invested so much in your little sis. I adore you both and cherish our sisterhood bond. Together forever, "ReeRee's girls".

TABLE OF CONTENTS

LIST OF FIGURES

LIST OF TABLES

Table

ABSTRACT

My dissertation research provides major contributions to the current understanding of intracellular protein trafficking in two important areas: vesicular fusion and peroxisome biogenesis.

I began with a study of SNAREs, highly conserved proteins that form the core fusion machinery within secretory and endosomal trafficking systems. I examined the regulation of an integral member of this protein machinery, syntaxin 5, by its mammalian endoplasmic reticulum/Golgi Sec1/Munc18 protein binding partner rSly1. To address their functional relationship, I produced a conformation-specific monoclonal antibody to use in immunostaining experiments and *in vitro* ER-to-Golgi transport assays. Results from the manipulation of rSly1/syntaxin 5 interactions indicate that rSly1 function is intimately associated with syntaxin binding, not promoting availability of the SNARE motif, but perhaps supporting a later step in SNARE complex formation.

My research continued with an examination of peroxisome matrix protein import, a mode of protein transport that utilizes two distinct peroxisomal targeting signals (PTS1 and 2) to bind exclusively to two different cytosolic receptors that define separate import pathways. A few matrix enzymes contain a PTS2 that is cleaved off after import, in plants and mammals. The identity of the PTS2

processing protease is unknown. Bioinformatic analysis of the Arabidopsis genome revealed a 76kDa Deg-protease, AtDEG15, predicted to be peroxisomal**.** Analysis of protein extracts from Arabidopsis plants with a knockout mutation in *atdeg15* reveals that the precursor form of the PTS2 protein thiolase (THL) was not processed. Using reverse transcription, I isolated and cloned *AtDEG15*. *In vitro* peroxisome import, protease assays, and mutagenic analysis demonstrated that AtDEG15 is a novel PTS2-specific processing protease.

Two proteins found in *Arabidopsis thaliana* have been identified that possess both a putative PTS1 and a PTS2, long-chain acyl-CoA synthetase 7 (LACS7) and alpha-crystallin domain protein 31.2 (ACD31.2). While both proteins have been localized to the peroxisome, the PTS responsible for their localization remains unclear. Mutagenic analysis and standard *in vitro* import assays showed that either the PTS1 or PTS2 is sufficient to direct ACD31.2 and LACS7 import.

Thus, using cellular and molecular biological techniques, my research has expanded the current understanding of intracellular protein trafficking.

CHAPTER ONE

The Study of Intracellular Protein Trafficking In Eukaryotes

INTRODUCTION

The complexity of the eukaryotic cell lies in its system of membranes that provide the very boundaries within which life exists. The plasma membrane provides the physical demarcation between the cellular biochemical activities and the extracellular world. Within the cell, membranes separate and organize different biochemical processes to avoid interference between them, generating compositionally and morphologically distinct compartments that characterize the eukaryotic cell. Therefore, a major mystery of the eukaryotic cell is its capacity to transfer material between distinct compartments without compromising their individual integrity or functionality. Cell biology is an area of biological science concerned with explaining individual cell function in logical terms of cell structure. Its roots lie in the commonality of all cells and its success is due to the great number of scientific approaches and technological advances employed. In particular, cell biologists' general understanding of biological membranes and the

trafficking of proteins between them has been one of the greatest scientific advancements for more than a century.

Notably, the study of intracellular protein trafficking began with the functional definition of the secretory pathway whereby secretory proteins are translocated across the membrane of the endoplasmic reticulum (ER), traverse through the Golgi and undergo exocytosis at the plasma membrane (Figure 1). One of the most significant observations was that transport steps within the secretory pathway are mediated by transport vesicles that carry proteins from membrane-to-membrane and lumen-to-lumen, or extracellular space (156). In fact, the notion of membranous sacs carrying and delivering proteins to different organelle compartments is how we currently define the mechanism of secretory protein transport.

Additional experiments revealed that distinctive signal sequences, or targeting signals, located on newly translated proteins permit movement from the cytosol across ER membranes (17-19). Translocation across ER membranes takes place during synthesis, i.e. co-translationally, and proteins are transported across the ER membrane into the ER lumen. However, signal-dependent translocation across membranes is more robust, flexible, and applicable to a wider range of intracellular locations than originally thought. It was later realized that the nucleus, mitochondria, chloroplasts, and peroxisomes also utilize destination-specific targeting signals to import their nuclear-encoded proteins released in the cytosol after synthesis, i.e. post-translationally (71, 107, 124, 146, 204) (Figure 1).

Work on protein translocation led to the development of *in vitro* assays to reconstitute the insertion of proteins into the ER or the import of proteins into peroxisomes, chloroplasts, or mitochondria (8, 20, 27, 59, 231). These *in vitro* assays helped facilitate the stepwise dissection and identification of important components required for complex biochemical events. Coupled with genetic studies to identify mutants with trafficking defects, molecular cloning techniques, and the aforementioned morphological studies, *in vitro* assays have become one of the most powerful tools used to reveal the machinery involved in such trafficking processes as membrane fusion, vesicle formation, organelle biogenesis and protein sorting.

The cell biological analysis of human diseases was perhaps the lone force that helped to catapult the protein trafficking field to the forefront of scientific attention. Mutations that result in defects in protein trafficking are the molecular basis of many hereditary and autoimmune diseases. For example, diabetes mellitus results from mutations in the receptor that binds to insulin thereby impairing its transport from the ER (5, 6, 93). Familial hypercholesterolaemia is a consequence of a host of transport defects ranging from failure of the low-density lipoprotein receptor to exit the ER to its failure to recycle back to the cell surface following endocytosis (5, 6, 93). Peroxisomal import and biogenesis defects cause neurodegenerative diseases and mental retardation such as those found in Zellweger's Syndrome and rhizomelic chondrodysplasia puntata (203, 225). Taken together, the work uncovering trafficking malfunctions associated with human diseases led to the incorporation of genetics into the mainstream of cell

biology. It was this transition that has taken the field of cell biology to the level of scientific research that we know today. The current generation's cell biologists are concerned with understanding the mechanisms of membrane trafficking at the molecular and biochemical levels. This transition was characterized by the addition of cell culture systems, enveloped viruses, and yeast genetics to the previously established tools of the trade. Moreover, immunoelectron microscopy, antibody probes, and immunoflourescence microscopy upgraded the traditional tools.

Given the number of techniques developed to study membrane transport, it seems reasonable to think that the basic mechanisms that govern individual trafficking events are now quite well understood. But a number of underlying details remain controversial and have yet to be resolved. While biochemical assays can measure the production of budded vesicles (12, 183, 191), they are inadequate in measuring the intermediates leading to them. The same can be said for *in vitro* reconstitution of fusion events (186, 234) that occur at rates too slow to account for additional mediators and regulatory factors that increase fusion rates *in vivo*. In the area of protein trafficking, the task at hand is to translate the results of the genomic, genetic, and biochemical understanding of the last two decades into useful information that leads to a comprehensive, mechanistic understanding of intracellular protein transport systems.

PART 1: PROTEIN TRANSPORT THROUGH THE ENDOMEMBRANE SYSTEM REQUIRES VESICLE FUSION

Due to the pioneering efforts of the 70's and 80's on the biochemistry of synaptic vesicles, the genetic dissection of secretion in yeast, and the *in vitro* reconstitution of Golgi transport, scientists have come to generally understand the basic mechanism of vesicular transport. First, budding vesicles from a "donor" membrane, loaded with the appropriate cargo, travel and become tethered to a potential target membrane. Second, upon proper "recognition", the loosely tethered vesicle becomes tightly docked. Finally, a mutiprotein complex facilitates fusion of the two membranes to complete cargo delivery (22). A more detailed version of the steps of vesicular transport is shown in Figure 2. Several families of proteins have been implicated in controlling the specificity and mechanism of vesicle targeting and fusion events. Among these, soluble N-ethylmaleimide sensitive factor attachment protein receptors (SNAREs) are presently accepted as the core machinery for the job of executing fusion (94, 128, 198).

SNAREs as Mediators of Vesicle Fusion

SNAREs form a superfamily of small membrane associated proteins (18-42kDa) with 25 members in *Saccharomyces cerevesiae*, 36 members in humans and 54 members in *Arabidopsis thaliana* (21, 92). They have a simple domain structure distinguished by a stretch of 60-70 amino acids arranged in heptad repeats termed SNARE motifs. At their carboxyl terminus, most SNAREs have a

single transmembrane domain that is connected to the SNARE motif by a short linker region. Although this structural prototype refers to most SNAREs, there are subsets that lack the transmembrane domain. Instead, these SNAREs are post-translationally modified with hydrophobic structures that mediate membrane anchorage. These SNAREs include a small group that is represented by the neuronal SNARE SNAP-25 (25 kD synaptosome-associated protein), which contains two different SNARE motifs joined by a flexible linker that is palmitoylated (81, 84, 95, 117, 184). SNARE Ykt6 also lacks the transmembrane domain. Instead, Ykt6 is associated with the membrane by a CAAX box that is farnesylated and perhaps also palmitoylated (60, 82, 127).

SNAREs were initially given functional distinctions as either vesicle-associated (v-SNARE) or associated with the target membrane (t-SNARE) (4, 210, 230). However, v-SNAREs and t-SNAREs can also be structurally distinguished as R- or Q- types, respectively, based on the residue positioned at the zero ionic layer of the four-helix bundle formed during complex formation and subsequent fusion (4, 55, 61, 210). Analysis of SNARE complex formation in reconstituted lipid vesicles revealed that t-SNAREs can be further designated as either a heavy chain, Qa or light chains Qb and Qc derived from either the same or from two different SNARE proteins (4, 55, 61, 210) (Table 1). One member of each subfamily contributes a single SNARE motif to the resulting Qa:Qb:Qc:R configuration of the functional SNARE complex (21, 92, 97, 235).

How SNAREs are distributed between the membranes or which combinations of SNAREs are fusogenic is still a matter of debate. In both

constitutive and regulated exocytosis, the R-SNARE is predominantly localized on the vesicle donor membrane, whereas the Q-SNAREs function as acceptors located on the plasma membrane. For intracellular fusion events, the SNARE topologies are less clear. With experiments reconstituting heterotypic fusion of SNARE-containing liposomes, Rothman and colleagues demonstrated that only a single 3:1 combination of SNAREs is fusogenic, with exquisite specificity conferred by precise cognate SNARE pairing mediated by the SNARE motif (30, 128, 157, 159). In contrast, SNAREs mediating homotypic fusion of early endosomes fuse liposomes in five out of seven possible combinations (242). This finding led to the idea that, at least in the case of homotypic fusion, the conserved SNARE structure allows for flexibility in intermediates needed for fusion rather than specificity as initially thought.

To appreciate the role of SNAREs in vesicle fusion we must first review the interaction of SNARE complexes and the SNARE conformational cycle. Simply put, SNAREs present on opposing membranes combine and engage in coiled-coil interactions that bridge two opposing membranes about to undergo fusion (Figure 3). These interactions result in a metastable “trans” complex of four interacting SNARE motifs oriented at very close proximity to the membrane surface. Assembly of the four-helix bundle is thought to supply enough free energy to bring opposing membranes close enough to fuse, resulting in a cis-SNARE complex in the fused membrane (34, 81, 230). α-SNAP, or soluble NSF associated protein, then binds to the SNARE complex and recruits NSF, N-ethylmaleimide sensitive factor (176). ATP hydrolysis by NSF dissociates the cis-

SNARE complex, releasing it for further rounds of vesicle fusion (125). Confidence in this SNARE-mediated model of fusion comes from the fact that it is structurally analogous to the activated form of viral fusogen proteins (96). In addition, reconstitution experiments showed that v- and t-SNAREs present on the surface of different liposomes was enough to promote fusion in vitro (94, 230).

Regulation of SNARE-Mediated Vesicle Fusion

As the molecular events leading to fusion become more clear, it is evident that a number of additional factors are required to bring about SNARE-mediated fusion *in vivo*. Biophysical fusion assays demonstrate that only the biologically relevant, specific and precise pairing between v- and t-SNARE combinations result in membrane fusion *in vitro* (128, 157). However, *in vitro* reconstituted fusions are much slower than *in vivo* fusion events, implying that there must be some other factors involved that accelerate the fusion process (230). Each fusion event must satisfy two fundamental physical requirements: 1) be fast enough or occur at a high enough probability to meet the physiological requirements of that trafficking step, and 2) be specific enough such that vesicles release their contents after fusing with the appropriate target membrane (96). To this end, there is considerable interest in uncovering potential SNARE regulatory factors necessary to provide specificity, help with SNARE complex assembly or help with the fusion event itself (96, 180).

A plethora of accessory proteins have been implicated in regulating the action of SNAREs (67) (Table 2). For example, cytosolic factors such as Gate-16

and LMA1 bind to SNAREs, subsequent to α-SNAP/NSF-mediated dissociation, keeping them inactive until the next round of fusion (49, 141, 236). Another potential regulatory mechanism comes from the putative Ca2+ sensor, synaptotagmin, which interacts with SNAREs and promotes synaptic vesicle fusion in response to the influx of Ca2+ (56, 96, 209). Synaptotagmin also acts in cooperation with other neuronal proteins Complexins I, II and Munc13, which help to provide spatial and temporal regulation of neuronal synaptic exocytosis through the stabilization and priming of SNARE complexes (16, 29, 67, 79, 172, 177, 181, 219).

Regulation by amino-terminal domains

Perhaps the most interesting mechanism of SNARE complex regulation lies within the structures of the individual SNARE proteins. Several SNAREs possess amino (N)-terminal domains (NTDs) that have critical functions in regulating fusion events. Certain v/R-SNAREs are further classified as 'longins' or long based on possession of a highly conserved stretch of 120-140 amino acids with a profilin-like fold called the longin domain (LD) at their amino terminus (57, 182) (Figure 4). Bioinformatic analysis has identified three subfamilies of longins in mammals: Ti-VAMP/VAMP7, Ykt6, and Sec22b. The crystal structures of both Ykt6 (214) and Sec22b (70) have revealed a five-stranded beta sheet packaged by three alpha helices longin domain structure (57). In the case of Ykt6, a SNARE capable of functioning in multiple transport steps (118), the LD contains a hydrophobic patch that can fold back to interact intramolecularly with the SNARE motif to influence Ykt6 SNARE pairing and subcellular localization

(214). The LD of ER/Golgi SNARE Sec22b also contains a hydrophobic patch in a similar spatial orientation as that of Ykt6 (70). The crystal structure of the mammalian Sec23/24-Sec22b complex reveals that interaction between the Sec22b SNARE motif and its LD serves as a conformational transport signal for packaging into COPII vesicles (120). Although it has not yet been solved, the structure of the Ti-VAMP/VAMP7 LD is assumed to have a similar profilin-like fold that has also been implicated in SNARE complex formation and protein localization (122).

Conformation-dependent regulation of SNARE-mediated fusion by the NTD has also been suggested to occur among the syntaxin-like t/Q-SNAREs (215). In general the regulatory unit, or the NTD, of syntaxins exists autonomously from the SNARE motif and consists of a short unstructured amino-terminal peptide sequence followed by alpha helices, called Ha,b and c, that fold into a three-helix bundle (Figure 4). The NTD of plasma membrane syntaxins, neuronal syntaxin1A and yeast Sso1, have an additional groove that can accommodate the SNARE motif to facilitate a “closed” conformation of the SNARE (84, 130). The Habc bundle packs with the amino-terminal half of the syntaxin SNARE domain and prevents the SNARE motif from entering into SNARE complexes (24, 84, 121, 143). Removal of this apparently negative regulatory domain has been shown to accelerate SNARE complex formation *in vitro* (147, 158, 235). In the case of Sso1 the closed conformation is an important intermediate that prevents fast SNARE pairing (142, 143). Like the plasma membrane syntaxins, mammalian syntaxin 5 appears to display a similar

negative effect of its amino-terminal domain on ER/Golgi SNARE complex formation *in vitro* (84, 235). But how conserved is the negative regulatory function of this domain across the 12 mammalian, 7 yeast and 24 *Arabidopsis* syntaxins? Although this domain seems promising towards understanding the regulation of SNAREs, it remains highly controversial. Indeed not all syntaxins are capable of adopting closed conformations. The endosomal and vacuolar syntaxins 7, 13, Pep12p and Vam3p as well as Golgi syntaxins 16 and Tlg2p all contain the Habc bundle but have been found to reside primarily in the open conformation (47, 84). Therefore we must question the role that this domain plays, if any, in SNARE complex regulation as a whole *in vivo*.

Although auto-regulatory inhibition to prevent fast SNARE pairing is reserved for the Habc domain of plasma membrane syntaxins, other roles are likely. Recently, it was shown that the Habc domain of plasma membrane syntaxin is also responsible for the trafficking and cluster distribution of syntaxin1A on the plasma membrane (54). Members of the Sec1/Munc-18 family of proteins, collectively referred to as SM proteins, are major binding partners of some syntaxin NTDs and have also been implicated in regulating the activity of SNAREs. In this way, the Habc domain could be the site for direct binding for SM protein-mediated chaperone activities required to allow specific assembly of t-SNARE complexes (161), prevent the degradation of unstable SNARE complex intermediates (31), or trigger fast exocytosis (180). One final provocative hypothesis is that the NTD domain of syntaxin is an escort to bind and guide SM proteins to their site of action at a later stage in trafficking (42, 195). However, a

recent look at the amino-terminal region of the yeast plasma membrane syntaxin, Sso1p, shows that the required function of the NTD can be circumvented when t-SNARE complex formation is made intramolecular (218). These results suggest that the essential function of the NTD of syntaxins is to regulate efficient t-SNARE complex formation.

Regulation by SM proteins

SM proteins were first discovered during screens for membrane trafficking mutants in yeast and *C. elegans* (1, 149). Less abundant than SNAREs, (four in yeast, seven in both mammals and *Arabidopsis*), all SM proteins are conserved hydrophilic proteins of about 60-70 kDa that appear to function at a variety of intracellular membrane fusion steps (64). Loss- of- function mutations of any SM protein invariably leads to a block of intracellular fusion and a lethal phenotype, illustrating the indispensable role these factors play in fusion (64, 162, 180, 215). But, in contrast to the consensus and clarity about SNARE proteins, previous data on SM proteins in different systems produce perplexing ideas about their exact role, site of action and relationship to SNARE proteins.

The unifying hallmark of all SM proteins is their high binding affinity and specificity for syntaxins. To date, the crystal structures of two SM proteins have been solved: munc18-1 and Sly1p complexed with their cognate SNAREs syntaxin1A and Sed5p, respectively (25, 131). Despite high structural homology, these structures reveal two very different modes of SM/syntaxin binding. In the crystal structure of the munc18-1/syntaxin1A complex, syntaxin 1A is found in a “closed” conformation, with its amino-terminal Habc domain folded over onto the

SNARE interaction domain. “Closed” syntaxin1A is inserted into the cleft of munc18-1 in a 1:1 complex that precludes binding to the other presynaptic SNAREs or α-SNAP (131) (Figure 5, panel I). In this way, Munc18 acts as a negative regulator of SNARE complex formation by binding monomeric syntaxin1A and locking it in the closed conformation. In stark contrast, Sly1p is bound only to the short amino-terminal peptide sequence that precedes the Habc domain of Sed5p by a small groove on the surface of the SM protein, with no involvement of the central cleft (25) (Figure 5, panel II). This binding modus allows simultaneous interaction of SM proteins and syntaxins alongside SNARE complex members, supporting the participation of all proteins in fusion.

Other SM protein/SNARE interactions, described in various trafficking steps of the ER, Golgi, TGN and early endosomes, also support the latter binding mode whereby SM/syntaxin association occurs despite SNARE complex formation. Indeed, the yeast syntaxin, Sso1, also adopts a “closed” conformation but its corresponding SM protein, Sec1, appears to favor interaction in the context of either the binary t-SNARE complex or the fully assembled ternary SNARE complex over a weak 1:1 complex that was also observed (33, 142, 194) (Figure 5, panel III). Binding in a 1:1 complex was also revealed in the crystal structure of Sly1 bound to its Golgi syntaxin Sed5p (25) but Sly1 also can associate with a fully assembled SNARE complex (160). The SM protein Vps45 binds its syntaxin, Tlg2, in a manner analogous to that captured by the Sly1-Sed5 crystal structure whereby the NH2-terminal peptide of the syntaxin binds with high affinity to its cognate SM protein (32). In addition, Vps45 also binds Tlg2-

containing SNARE complexes via a second mode that involves neither the amino terminus of Tlg2 nor the region of Vps45 that facilitates this interaction (32). More interestingly, a yeast SM protein, Vps33, is part of a homotypic fusion, protein-sorting complex (VpsC complex) that functions in Golgi-to-vacuole transport that indirectly interacts with the syntaxin homolog Vam3 (113). It appears that this interaction is required to allow a coordinated transition from priming of SNARE complexes to their subsequent docking at the target membrane prior to fusion (188, 228) (Figure 5, panel IV).

Thus, the binding between Munc18 and syntaxin1A appears to be somewhat of an enigma within the SM protein family. Although a negative regulatory role is implied *in vitro*, it is hard to reconcile the phenotypic findings obtained from munc18 deletion, overexpression or otherwise manipulated mutants *in vivo* (64). For the most part, except in *Drosophila*, these manipulations support an activator role of SM proteins. Therefore it seems a matter of debate as to whether or not the interaction of Munc18 to a “closed” syntaxin1A really represents a bona fide *in vivo* entity or is just an artifact produced by *in vitro* circumstances, particularly because no other SM protein interferes with the formation of SNARE complexes. In fact, neuronal SNARE complexes can be isolated from membranes in a complex with Munc18, consistent with the idea that SM/syntaxin interactions occur in the presence of SNARE complex formation (36). In native membranes, munc18-1 stabilizes a half-closed conformation of syntaxin1A that is still capable of participating in SNARE complex assembly (241). Recent evidence indicates that Munc18 is also able to participate in other

binding modes that are not inhibitory but rather promote assembly of SNARE complexes. Arachidonic acid was identified as a vehicle to disrupt the Munc18/syntaxin1A interaction through fatty acid metabolism, in an attempt to uncover a potential molecular mechanism for the release of syntaxin1A from Munc18-imposed control (178). However, it was later revealed that this release of inhibition is due to a stimulation of syntaxin1A alone and that Munc18 remains associated with syntaxin1A after arachidonic acid-induced syntaxin1A binding to SNAP25 (36). Furthermore, munc18-1 stimulates SNARE-mediated membrane fusion in reconstituted liposome fusion assays (195), and can bind directly to the assembled SNARE complex (45, 179) (Figure 5, panel III). A third mode of munc18-1/syntaxin1A interaction was discovered that involves binding at an evolutionarily conserved motif at the amino terminus of syntaxin (103, 179). This low-affinity binding is considered to be an intermediate between the two previous interaction modes (103) (Figure 5, panel II). Such binding modes are perfectly compatible with other SM proteins that associate with partially or even fully assembled SNARE complexes.

Much remains to be learned about the precise mechanism of vesicle fusion. However, a picture is emerging as to the unifying connections between individual SM/syntaxin interactions that lead to one complete functional model for SM/SNARE protein-protein interactions. Perhaps each of the interactions observed *in vitro* represent intermediate stages of a SM protein-controlled molecular pathway of specific SNARE complex assembly that results in

membrane fusion while also contributing to SNARE proofreading, syntaxin localization or even organelle morphology (46, 103, 161, 237) (Figure 5).

PART 2: TRANSLOCATION OF FULLY SYNTHESIZED CYTOSOLIC PROTEINS ACROSS BIOLOGICAL MEMBRANES

Post-translational protein import does not require the budding and fusion of vesicles to translocate proteins across organelle membranes. Instead, newly synthesized proteins released into the cytosol are marked with targeting information, or signal sequences, specific to the proper organelle destination. In some cases, corresponding receptor proteins located in the cytosol exclusively recognize targeting sequences, bind, and transfer the proteins to the correct organelles.

In vitro import assays were developed by adding isolated organelles to protein synthesis extracts for prokaryotic plasma membranes, ER, mitochondria, chloroplasts and peroxisomes (8, 19, 27, 35, 119, 139, 140, 231). Through manipulation of the conditions for import, these reconstitution systems helped uncover energy requirements, chaperones and other mechanistic factors necessary for import. Much of what is known about the basic mechanisms of post-translational import comes from the well-studied mitochondria and chloroplast import models. Subsequent to membrane association, proteins are threaded through the organelle membrane in a process that requires energy. In some cases, chaperones bind to the translocating proteins and, through multiple rounds of binding and release, result in the ‘pulling’ of peptide chains through the membrane. Finally, other proteins within the organelle catalyze the folding of the newly imported proteins into their final functional conformation (reviewed in (2,

116, 126, 232)). A basic schematic of protein transport into ER, bacteria plasma membrane, mitochondria and chloroplast is depicted in Figure 6.

Protein import into the peroxisome also occurs by signal dependent post-translational import. Results from the progress made over the past five decades in understanding the peroxisome suggests that the actual translocation event may proceed in manner very different from that defined for the other organelles. Despite extensive research uncovering proteins involved in peroxisome protein import, a peroxisomal translocation pore has not yet been defined. Nevertheless, folded or oligomeric proteins are capable of traversing the peroxisome membrane (83, 115, 126, 205, 221, 223). It has been demonstrated, however, that oligomeric protein import in peroxisomes is less efficient *in vitro* than the import of semi-folded or monomeric proteins (37). Still, the fact that large structures can be incorporated into peroxisomes is clear from the finding that even a 9.0nM gold particle conjugated to a peroxisome targeting signal is able to traverse the membrane (223). Therefore, the elucidation of peroxisomal protein import and translocation mechanisms will add new insights to the general scheme of protein translocation and organelle biogenesis.

Peroxisomes

First recognized in electron micrographs of animal tissues in the late 1950s, peroxisomes are structurally and functionally related organelles that are found in virtually every eukaryotic cell (175). Peroxisomes were named after identifying hydrogen peroxide metabolism as one of the organelle's conserved

functions (13, 39). Now we understand that the peroxisome is a highly versatile, metabolically active organelle and the site of many vital biochemical reactions.

Peroxisomes are morphologically simple organelles of approximately 0.1-1 μm in diameter. They are composed of a proteinaceous matrix, sometimes containing a paracrystalline core, enclosed by a single membrane (Figure 7). Metabolic tasks of peroxisomes vary and are widespread throughout the eukaryotic kingdom amongst evolutionarily diverse organisms. Three conserved functions are generally found: β-oxidation of fatty acids, metabolism of hydrogen peroxide, and defense against oxidative stresses. Other specialized roles vary depending on the organism and cell type. Peroxisomes have been implicated in synthesis of plasmologens, isoprenoids, and cholesterol; purine and pyrimidine metabolism; nitrogen metabolism; biosynthesis of lysine; methanol degradation (87, 88, 185, 224, 226). These organelles also contain enzymes that participate in the glyoxylate cycle, pentose phosphate pathway, photorespiration and seedling development in plants (87, 88, 111, 129, 174, 226). Peroxisomes also play key roles in hormone signaling both plants and yeast (9, 212).

In plants, peroxisomes are characterized according to tissue location, developmental stage and enzymatic composition (98). Plant peroxisomes can be classified into four main types: glyoxysomes, leaf peroxisomes, root peroxisomes and unspecialized peroxisomes (14, 87, 89, 150). Glyoxysomes are mainly found in seedlings where the breakdown of fatty acids takes place through fatty acid β-oxidation and the glyoxylate cycle (15, 150). When seedlings begin photosynthesis, glyoxysomes are transformed into leaf peroxisomes, by

exchanging sets of enzymes within the organelle (89, 150, 213). Leaf peroxisomes house the glycolate and glycerate pathways of photorespiration. When leaves undergo senescence, the reverse transformation back to glyoxysomes is observed (89). A third type of peroxisome is found in the uninfected cells of nodules on legume roots. These peroxisomes contain uricase, one of the last enzymes of ureide biosynthesis (80, 150). The final class of peroxisomes comprise uncharacterized smaller organelles, found in most plant organs including roots, that mostly contain the enzymes necessary for hydrogen peroxide metabolism (150). Because other specific metabolic roles that this class of peroxisomes may play remain unknown, they are classified as “unspecialized” (150).

Peroxisomes lack DNA and ribosomes. Their nuclear-encoded proteins are synthesized on free ribosomes in the cytosol and function after post-translational import into pre-existing peroxisomes. During peroxisome proliferation, as existing peroxisomes enlarge and divide to make new ones, there is a constant influx of proteins. Genetic studies have produced a wealth of information regarding the genes required for peroxisome biogenesis. To date 32 genes encoding peroxins (PEX genes) in plants, mammals and yeast, have been identified whose products are involved in matrix protein import, membrane biogenesis, and organelle proliferation (Table 3). The following discussion will examine the current knowledge regarding the mechanisms involved in peroxisome matrix protein import.

Peroxisome Matrix Protein Import

Targeting of peroxisomal matrix proteins occurs via one of two pathways requiring evolutionarily conserved peroxisomal targeting signal (PTS) sequences present within newly synthesized polypeptides. Two different PTSs exist for matrix proteins: PTS1, a carboxyl terminal tripeptide and PTS2, a loosely conserved, amino-terminal nonapeptide sequence. The principal role of each targeting signal, PTS1 and PTS2, is to mediate recognition of the newly synthesized polypeptide by the necessary factors to effect specific import into peroxisomes. A few proteins possess putative internal signals that resemble neither PTS1 nor PTS2 but are sufficient to direct matrix protein import (150, 217). However, an interaction between these signals and an import receptor has not been shown. Therefore, these putative internal PTSs will not be discussed further.

Peroxisome Matrix Targeting Signals

Peroxisome Targeting Signal 1 (PTS1)

Most of the known peroxisomal matrix enzymes possess a PTS1 that, unlike the well-studied import mechanisms of the ER, mitochondria and chloroplasts, is not removed after import into peroxisomes (207). In addition, peroxisomal matrix enzymes bearing a PTS1 must be fully synthesized in the cytosol prior to import because of the signal's extreme carboxyl terminal location (205, 206). The PTS1 location is key since placing the PTS1 elsewhere within the protein sequence does not lead to peroxisomal targeting (72, 75, 205). Also,

the extension of the carboxyl terminus by the addition of residues beyond the tripeptide sequence eliminates targeting of proteins to peroxisomes (75, 87, 133, 151).

The first PTS1 described was Ser-Lys-Leu (SKL) located at the carboxyl terminus of firefly luciferase that was both necessary and sufficient to direct its peroxisomal targeting (72, 75, 102). In fact, the SKL motif is located on proteins targeted to the peroxisomal matrix throughout eukaryotic evolution from trypanosomes (63, 199, 200) to yeast (3, 43), plants (11, 86, 151, 220), and mammals (72, 75, 222).

Despite consideration as the prototypical PTS1, many permissible substitutions within this tripeptide sequence still effectively target PTS1 proteins to peroxisomes (28, 173). For this reason, it became more acceptable to consider the PTS1 tripeptide as adhering to an “S-K-L rule,” i.e. small-basic-hydrophobic residues (75, 211). This seemingly tolerant consensus was still too simplistic to describe, in total, the characteristics of a PTS1. First, not all functional PTS1s match the original small-basic-hydrophobic consensus. SQL, KKL, SSL, and NKL are all capable of targeting alanine glyoxylate aminotransferase 1 to peroxisomes in human cells (134). Second, not all variations on the PTS1 theme are functional in all species (51, 75, 132, 208). PTS1 variants SKF and SKI direct catalases to peroxisomes in yeast, *Saccharomyces cerevisiae* and *Hansenula polymorpha*, respectively (41, 109). Yet these same sequences, found at the carboxyl termini of luciferases in monkey kidney cells, fail to reach peroxisomes. Third, residues adjacent to the

tripeptide carboxyl terminus play key roles in the competency of the terminus to act as a PTS1 (28, 138, 145, 173). For example, while most plant PTS1s conform to the SKL motif, there are a few that possess nonconforming residues (Figure 8). In these cases, accessory residues present upstream of the signal enhance efficiency of peroxisomal targeting (138, 145, 173). Particularly, plant and mammalian catalases require the basic residue immediately adjacent and upstream of the tripeptide for functionality, the former ending -RPSI and the latter –KANL (138, 166). These auxillary residues are thought to improve binding to the PTS1 receptor for translocation or to mediate conformational changes in the PTS1 protein itself that make the PTS1 more accessible to the receptor (28). Whatever the reasoning, it is clear the PTS1 must be considered as more than just a terminal tripeptide sequence.

Peroxisome Targeting Signal 2 (PTS2)

Few peroxisomal matrix enzymes possess a PTS2. First discovered in the protein sequence of the β-oxidation enzyme 3-ketoacyl-CoA thiolase in rat liver, the PTS2 sequence is located within the first ~30-40 amino acids of the amino terminus, which is usually cleaved during, or shortly after, translocation (152, 211). Initial comparison of the sequences of the functional PTS2 of other peroxisomal enzymes with similar sequences amongst different species led to the recognition of a conserved nonapeptide, $RLx_5(H/Q)L$, that appears to be the consensus PTS2 (40, 53, 69, 216). Important elements of this sequence, however, are still being determined.

Site-directed mutagenesis focusing on the first two and the last two amino acids of the nonapeptide sequence of rat liver thiolase, *S. cerevisiae* thiolase, and watermelon malate dehydrogenase demonstrated that these amino acid positions are critical for targeting (53, 69, 216). From these studies it was determined that a basic amino acid is essential at position 1, whereas the leucine at position 2 could be replaced by glutamine. Basic residues could not be tolerated at position 8 and subtle changes of the leucine at position 9 significantly impaired PTS2 function. Moreover, functional conservation of the PTS2 was established when the watermelon enzyme could be imported into the peroxisomes of *H. polymorpha* (53). As more naturally occurring PTS2s were discovered, recognition of the sequence variability led to a broadening of the accepted PTS2 consensus (169, 173).

Sequence comparisons of 32 diverse eukaryotic peroxisomal proteins shed some additional light on the nature of the PTS2: the idea that certain amino acid substitutions within the PTS2 sequence are functional based on the species in which the enzymes are contained. For example, the mammalian thiolases have the original consensus, RLx_5HL, but the plant thiolases all differ with a glutamine at position 2 (58, 173). Interestingly, rat thiolase correctly targets to tobacco glyoxysomes, but this targeting is abolished when residue 2 is changed to the plant-specific glutamine (58). Surprisingly, coupling mutations in rat thiolase that change the valine in position 5 of the nonapeptide to a leucine, and the leucine in position 2 of the nonapeptide to a glutamine to form RQQVLLGHL,

restores its PTS2 function within the context of the tobacco cells. Thus, position 5 may add further constraints on the structure of the PTS2.

The length of the PTS2 seems to be precisely fixed to nine amino acid residues. An 11 amino acid peptide, RIx_7HL, is found within the amino terminus of enoyl-CoA isomerase in *S. cerevisiae* (238). Though this sequence matches the PTS2 consensus, the 2 additional amino acids render it nonfunctional.

Large-scale genomic sequencing and bioinformatics permit a more detailed analysis of the PTS2 sequence. When applied to plants, for which there is a complete sequence of the Arabidopsis and *Oryza sativa* genomes and more than 20,000 expressed sequence tags for 27 higher plant species, a total of 137 enzymes containing a PTS2 were revealed (173). These studies demonstrated several features of plant PTS2s. First, three of the four residues of the original PTS2 consensus (positions 1,8 and 9) are highly conserved. In plants, most of the variation occurs at residue 2 (173). Second, RLx_5HL and RIx_5HL represent the most widely present PTS2 sequences, with RQx_5HL restricted to only the plant thiolases. In fact, Q was not present at position 2 in any mammalian or yeast PTS2 (173). Conversely, some amino acid residues found in PTS2s of other eukaryotes were not observed at all in plants, such as Q at residue 8 (173). Finally, the regions bordering the PTS2 sequence showed conservation, with proline frequently present immediately downstream of the PTS2 and alanine, leucine and valine commonly found just before the nonapeptide (173). The significance of these residues has not yet been determined. The amino acid residues frequently found in plant PTS2 sequences are summarized in Figure 9.

Combining the experimental data from the literature on permissible amino acid changes within the PTS2 sequence of all the organisms studied thus far, has led to the resulting consensus of R-(L/V/I/Q)-xx-(L/V/I/H)-(L/S/G/A)-x-(H/Q)-(L/A) (163). With this much variability, it seems safe to conclude that the analysis of the PTS2 sequence structure is far from over.

The PTS Receptors and Matrix Protein Import

Receptor PEX5 and PTS1 protein import

The receptor PEX5 interacts with matrix proteins containing a carboxyl-terminal PTS1 (73, 91, 167, 208). In mammals and rice, this receptor exists in two isoforms generated through alternate splicing: PEX5L (long) and PEX5S (short), which differ in length by a 37 amino acid insert (26, 114, 123, 153, 233). Interestingly, only the short form of PEX5 exists in yeast while Arabidopsis contains only the long form.

The carboxyl terminus of PEX5 typically contains a highly conserved tetratricopeptide repeat (TPR) domain essential for PTS1 binding (65, 66, 105). The crystal structure of the seven TPRs of human PEX5L co-crystallized with a PTS1-containing peptide reveals two clusters of three TPRs (1-3 and 5-7) almost completely enclosing the peptide (65). This peptide-binding site is lined by a set of highly conserved asparagines that form direct hydrogen bonds with the PTS1 motif (65, 66, 105). Upon cargo binding, the conformation of the carboxyl terminal part of the receptor changes to a slightly more restrictive shape (65, 201) to close the gap between TPR domains in the presence of PTS1-containing cargo.

The amino terminus of PEX5 contains a seven-fold repeated pentapeptide WXXXF/Y motif that has been implicated in an intricate work of additional protein-protein interactions distinct from PTS1 binding (106, 108, 148, 155, 187, 193). These interactions, although not completely understood, have been implicated in receptor-cargo complex docking, complex translocation, and PTS receptor recycling.

One interesting fact about PEX5 is that it changes its location with respect to the membrane during the PTS1 protein import cycle. In the beginning during cargo recognition, PEX5 is soluble in the cytosol. Upon docking at the peroxisome membrane, it behaves like an integral membrane protein (77). Finally, at the end, PEX5 resides in the peroxisome matrix; although it is not clear whether it does so in its entirety as a part of a receptor-cargo complex that completely traverses the membrane or by partially extending itself into the matrix just enough to deliver cargo (38, 78, 110). Accumulating evidence reveals the participation of PEX5 in virtually every major step of the PTS1 protein import pathway, also known as the PEX5 receptor cycle (Figure 10). PTS1 protein import is widely accepted to occur by an “extended shuttle” model of four major steps: 1) cargo recognition in the cytosol, 2) receptor-cargo docking at the peroxisomal membrane, 3) translocation and subsequent cargo delivery across the membrane, and finally 4) monoubiquitin-mediated receptor recycling for further rounds of PTS1 import (136, 164, 165, 196).

Receptor PEX7 and PTS2 import

PEX7 is a protein, composed almost entirely of WD-40 (B-transducin related) repeats, that binds specifically to PTS2 proteins and is the receptor for PTS2 matrix protein import (50, 170, 239). In all species, mutants lacking PEX7 are incapable of PTS2 matrix protein import, but are entirely normal for the import of PTS1 proteins (50, 170, 239).

Like the PTS1 receptor PEX5, the PTS2 receptor PEX7 resides in the cytosol, the peroxisomal membrane, and the peroxisome matrix (26, 135, 144, 233, 239). The import mechanism indicates that PEX7, like PEX5, is a primarily cytosolic receptor that brings PTS2 cargo to the peroxisome (144). But, unlike PEX5, the specifics of the PEX7 receptor cycle are less straightforward. Although PEX7 is necessary to bind and direct the targeting of PTS2-containing peptides, it is not sufficient to do this job on its own (192). Rather, it requires additional species-specific soluble chaperones to be fully active (192). These proteins fulfill key roles in the import of PTS2 proteins and are referred to as PTS2 co-receptors (192).

The PTS2 co-receptors are a group of peroxins, first described in yeast (PEX18/21/20p), whose structural and functional homologs include PEX5 in plants and PEX5L in mammals and rice (26, 123, 153, 154, 192, 233) (Figure 11). The PTS2 co-receptors share evolutionarily conserved structural domains; among which exists a 20-30 amino acid domain exclusively responsible for PEX7 binding (44, 116). The co-receptors are responsible for peroxisomal targeting and membrane association (44, 48, 51, 52, 74, 76, 77, 116, 153, 187, 189). In fact, in

the absence of PEX18/21p, epitope-tagged PEX7 is completely localized to the cytosol in *S. cerevisiae* (168). In mammals and plants, PEX5L and PEX5 respectively, act as PTS2 import co-receptors and the amino-terminal 214 amino acids have been shown to be sufficient to direct the PEX7/cargo complex to the peroxisome (26, 44).

Caution must be taken, however, when assigning the role of targeting exclusively to the PTS2 import co-receptors. Exceptions exist that demonstrate that PEX7 does not necessarily require an additional targeting module. In *P. pastoris*, the association of either PEX7 or PEX20 with the peroxisomal docking complex can be independent of the other protein and neither peroxin significantly affects the localization of the other (116). Moreover in *S.cerevisiae*, co-immunoprecipitation and *in vitro* binding assays show that PEX7 interacts with the membrane docking machinery, regardless of the presence of PEX18 or PEX21 (202).

A model for the PTS2 matrix protein import pathway consistent with that of PTS1 protein import has been proposed: 1) PEX7 recognizes PTS2 cargo in the cytosol. This receptor-cargo complex then travels and binds the PTS2 co-receptors also present in the cytosol; 2) this complex docks onto the peroxisomal membrane via the docking machinery; 3) the PTS2 transport complex is translocated into the peroxisome matrix; and 4) both PEX7 and the co-receptors recycle back to the cytosol for further rounds of PTS2 protein import (Figure 12).

PTS2 Matrix Proteins are Processed After Import

Though the mechanisms of PTS2 protein import appear to be conserved among most species, one difference concerns the fate of PTS2 proteins following import into the peroxisomes matrix. In plants and mammals, the PTS2 import presequence appears to be cleaved off subsequent to matrix protein import (85, 90, 100, 101, 112, 150, 152, 211). A completely conserved cysteine residue 35-45 amino acids downstream of the PTS2 has been suggested for the cleavage site of PTS2-containing precursor proteins (85, 90, 100, 101) (Table 4).

Although attempts have been made to establish its identity, little is known about the enzyme responsible for PTS2 processing. Likely candidates must fulfill certain criteria: 1) since PTS1 import defects result in a lack of processing of PTS2 proteins and mutations that result in a lack of PTS2 import result in the accumulation of precursor protein in the cytosol, potential proteases must possess a PTS1 signal for peroxisome matrix (10, 100); 2) because yeast do not have proteolytically processed PTS2 proteins, potential candidates are not expected to have functional homologs in yeast (137); and 3) finally, the candidate protein must contain a proteolytic domain within its amino acid structure.

An insulin-degrading enzyme of the metalloproteinase family was localized to peroxisomes in mammalian fibroblasts cells (7). Although this protease, renamed PP110 for peroxisomal protease of 110kDa, was capable of degrading a synthetic presequence of thiolase, it failed to process full-length thiolase *in vitro* (7). In plants, a 35kDa cysteine endopeptidase was isolated from the glyoxysomes of germinating castor bean endosperm via its capacity to

specifically process the precursor form of the PTS2 protein malate dehydrogenase *in vivo*; the same endopetidase was unable to cleave thiolase at the proper processing site *in vitro* (68). Next, an ATP-dependent Lon protease, distinct from the mitochondrial isoform, was identified in rat liver peroxisomes (104). Like its bacterial and mitochondrial homologs, however, this protease is likely to function as a chaperone, degrading unfolded proteins (104).

Recently, more promising candidates for processing the PTS2-containing precursor peptide have been recognized. A novel PTS1-targeted protein, called Tysnd1 (trypsin domain containing protein 1), was identified in mouse peroxisomes. Tysnd1 was responsible for both the removal of the PTS2-containing leader sequence from prethiolase and for specific processing of PTS1 proteins involved in the peroxisomal β-oxidation pathway of fatty acids in mammals (112). Using a cell-based assay, these authors show that Tysnd1 overexpression led to the *in vitro* processing of the peroxisomal enzymes to fragments identical to the sizes described for their endogenous forms (112). Moreover, Tysnd1 itself is reported to undergo processing in a cysteine-dependent manner similar to its substrates, perhaps as an auto-activating mechanism (112).

In plants, the Tysnd1 homolog is a protease-related protein belonging to a group of ATP-independent trypsin-like serine proteases for which the *E. coli* DegP is the prototype (90). This protease, referred to as Deg15, has been partially purified from the fat-storing cotyledons of watermelon (*Citrullus vulgaris*) and examined for its ability to act as a glyoxysomal processing protease (GPP)

(90). In watermelon, DEG15 functions in two forms, a 72kDa monomer and an 144kDa dimer, whose equilibrium can be shifted in the presence of Ca^{2+} in favor of the dimeric GPP/Deg15 form, reportedly responsible for cleavage of the PTS2 presequence of malate dehydrogenase at the proper, cysteine-containing location (90). The monomer, on the other hand, acts as a general peptidase that cleaves denatured peroxisome matrix proteins (90).

In Arabidopsis, a knockout mutation in *DEG15* prevents processing of glyoxysomal malate dehydrogenase to its mature form (90). Although the presence of unprocessed malate dehydrogenase in *deg15* mutants provides evidence that DEG15 may be the PTS2 peroxisomal processing protease in plants, its peroxisomal localization and specific cleavage of PTS2 proteins *in vitro* have not yet been experimentally defined.

Redundancy of Matrix Protein Import Pathways

Our general understanding of peroxisomal matrix protein import is based on the premise that targeting is governed by a single PTS present on the newly synthesized protein released into the cytosol. This PTS-containing protein is then recognized by a specific import receptor that guides it to the peroxisome. Attempts to identify the proteins associated with peroxisomes have led to the identification of unique enzymes that contain both a PTS1 and PTS2.

PEX8, the yeast importomer complex linker protein, contains both a PTS1 and PTS2 sequence (171, 227, 229). Mutants in *Hansenula polymorpha* lacking PTS2 import, revealed that the PTS1 and its interaction with PEX5p were

required for targeting of PEX8 (240). In addition, deletion of the PTS2 motif on PEX8 results in PEX5-directed PTS1 import (240). Conversely, PEX8 lacking its PTS1 sequence follows the PTS2 pathway. In this case, the targeting depends on both PEX7 and PEX20 and PEX8 interacts with PEX20 directly (197, 240). Since PEX20 interacts with PEX7, it is presumed that all three proteins, PEX8, PEX7 and PEX20, form a cargo/receptor/co-receptor complex that aids in the PTS2-dependent entry of PEX8 into peroxisomes (116, 197, 240).

Two proteins identified in *S. cerevisiae,* Dci1 and Eci1, belong to the isomerase/hydratase family and share 50% sequence identity. Both of these proteins are localized to peroxisomes, and both contain sequences that resemble PTS1 and 2 (99). It was demonstrated that the putative PTS1 is not required for the peroxisomal localization of either of these proteins (99). Furthermore, the correct targeting of Eci1 and Dci1 occurs in the absence of either receptor PEX5 or 7, although PEX5 interacted in two-hybrid assays with Eci1 (99, 238). It was later reported that the carboxyl-terminal tripeptide of Dci1 can function as a PTS1, and is capable of targeting both Dci1 and Eci1 (238). Interestingly, although Eci1 peroxisomal targeting follows the PTS1 pathway, it does not require a PTS1 of its own. It was suggested that the PEX5-dependent import of Eci1 is due to interaction and co-import with its partner Dci1 (238).

Other dual PTS-containing proteins have been identified in plants, however their targeting has not been completely characterized. Long-chain acyl-CoA synthetase (LACS) 7 possesses both a putative PTS1 and PTS2 and has been localized to the peroxisome by fluorescent microscopy (62). In addition, this

localization is dependent upon both targeting signals (62). However, in studies involving yeast two-hybrid analysis and co-immunoprecipitation, AtLACS7 was shown to interact only with the PTS1 receptor PEX5 (23). The lack of interaction with PEX7 could be explained by fusion of the Gal4 binding domain to the amino terminus of LACS7, resulting in a bait protein with a PTS2 sequence buried too deep into the protein sequence of LACS7 to be an effective targeting sequence. On the other hand, there are documented examples of amino-terminal fusions to enzymes that can still be recognized as PTS2 import proteins in yeast two-hybrid systems (50). Still, subcellular localization studies of PTS-dependent variants of the green fluorescent protein (GFP) reveal that both the PTS1 and PTS2 of AtLACS7 appear necessary to direct its peroxisome entry (62).

A screen for novel low-abundance proteins of plant peroxisomes, identified a gene in the Arabidopsis genome, At1g06460 or ACD31.2, (190) possessing an α-crystallin domain, characteristic of small heat-shock proteins, and putative targeting signals for both peroxisome protein import pathways (173). Upon transient gene expression of full-length and deletion constructs of ACD31.2 by fluorescent microscopy, this protein is targeted to peroxisomes in a PTS2-dependent fashion (173). Though these experiments seem to yield definitive evidence for peroxisome localization of ACD31.2, further investigation by *in vitro* import assays may be useful. First, localization determined by fluorescence microscopy does not distinguish between intra-organelle localization and organelle-membrane association. As discussed earlier, PTSs that deviate from the canonical sequence also require accessory residues that assist in protein

import. Therefore, careful consideration of the nature of the deletion constructs must be taken. In the analysis involving ACD31.2 localization, only the non-canonical carboxyl terminal tripeptide sequence was eliminated in the deletion construct. In this way, the remaining accessory proteins could still potentially aid in receptor/membrane association even though matrix translocation may be defective – a result not easily discriminated by fluorescence microscopy alone. Also, the construct made to test ACD31.2 import dependence on the PTS2 not only possessed a mutated PTS2 sequence, but also a carboxyl-terminal fluorescent tag, the presence of which has been previously shown to eliminate PTS1 import (75, 133).

CONCLUDING REMARKS

The dynamic trafficking of proteins is a critical function of all eukaryotic cells. Trafficking defects lead to numerous life-threatening diseases in humans. Understanding the mechanisms involved in this fundamental process has direct applications for understanding disease states and engineering therapeutic interventions in human medicine. In the 200 years since its inception, the field of intracellular protein trafficking has seen a lot of action. By the start of the new millennium, many of the trafficking systems studied in the past century, if not entirely solved, have at least logical, biochemically-defined mechanisms. Indeed, we now believe we know the fundamental steps involved in protein transport to and between organelles. Nevertheless, gaps remain.

It is clear that SNARE assembly is the key to fusion of secretory and endosomal membranes in eukaryotes. As such, SNARE structure and assembly must be tightly regulated to ensure proper timing and function. Many proteins have been implicated. Most interesting among them are the SM proteins. SNAREs and SM proteins interact in regulating membrane fusion through tight control of the conformational cycle of SNARE fusion complex formation by SM proteins. Until recently, quite divergent and conflicting models existed for one central role of SM proteins in vesicular fusion and SNARE regulation. Chapter two addresses the question of how SM proteins might favor SNARE complex assembly; specifically investigating the proposed regulatory role for SM proteins as being responsible for maintaining an available open and/or monomeric pool of syntaxin molecules for SNARE complex formation. With the use of conformation-

specific monoclonal antibodies, live-cell imaging, immunocytochemistry and *in vitro* reconstitution of vesicular transport to address the functional relationship of the mammalian ER/Golgi SM protein rsly1 and its SNARE binding partner syntaxin5, this work will no doubt contribute to the reconciliation of how each of these binding modes cooperates to create one complete functional model for SM/SNARE protein-protein interaction.

Peroxisomal matrix protein import is a mode of protein transport that requires two discrete peroxisomal targeting signals (PTSs) to bind exclusively to two distinct cytosolic receptors to define two separate import pathways. Little is known about the import pathway of matrix enzymes that contain an amino-terminal PTS2. In plants and mammals, these enzymes are imported as precursor proteins that are processed to their mature forms subsequent to matrix entry. The identity of the peroxisomal protease required for processing of PTS2 proteins is still unknown. High-throughput genomic and proteomic screening methods have identified potential candidates. *In vitro* peroxisome import and proteolytic cleavage assays will help to uncover a peroxisomal protease with exciting PTS2 protein processing capabilities. Chapter three directly addresses the question of the identity of the processing protease.

Attempts to identify the proteins associated with peroxisomes have led to the identification of unique enzymes, possessing both a PTS1 and PTS2, whose import has not yet been fully characterized. Using deletion constructs, mutagenic analysis, and *in vitro* import assays, chapter four addresses the question of which import pathway proteins with redundant targeting signals choose.

Overall, the work presented in this thesis represents significant contributions to the broader field of protein trafficking. These contributions include: 1) a better understanding of SM/SNARE protein interactions as it relates to the regulation of vesicle fusion, 2) the identification and initial characterization of the PTS2 protein processing protease, AtDEGP15, and 3) the determination of signa dependence for two peroxisomal proteins with apparent dual signaling capabilities. Each of these accomplishments will serve as foundations for future research endeavors.

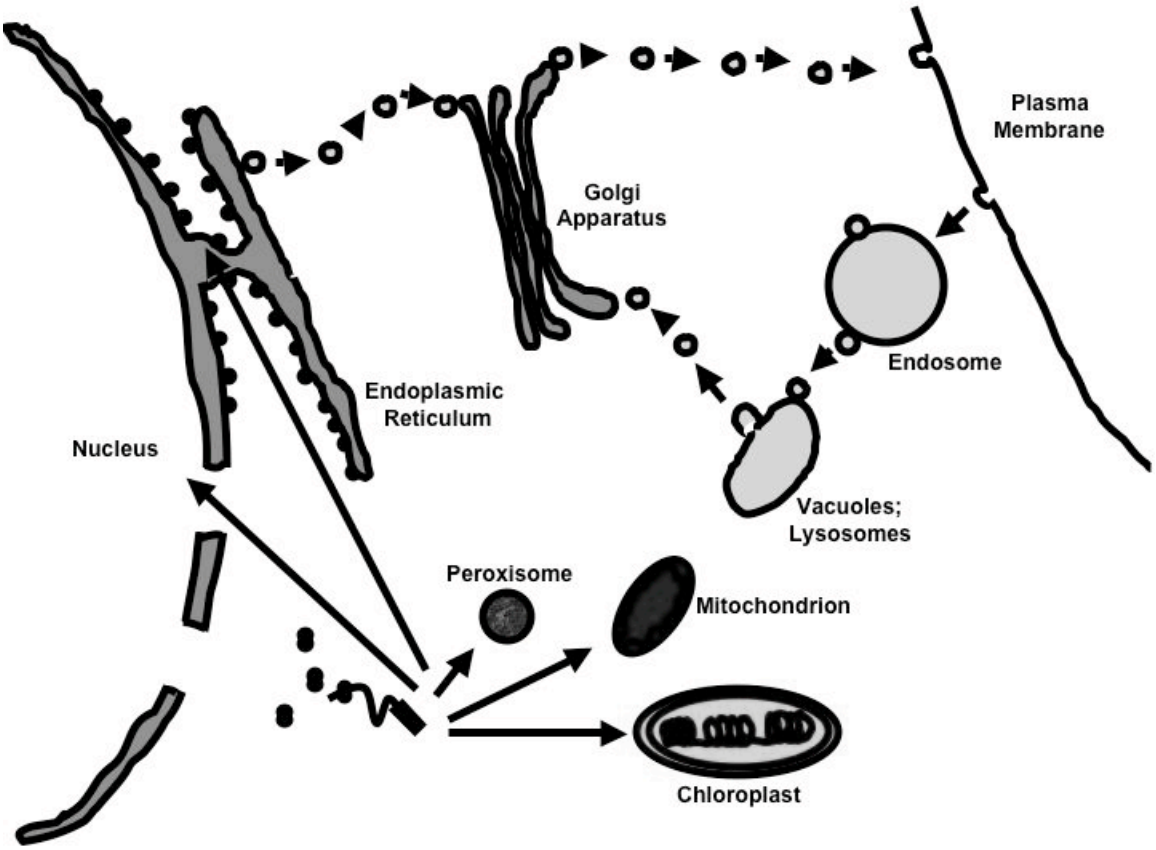

Figure 1.1. Eukaryotic intracellular protein trafficking. This scheme is a general depiction of protein trafficking between the organelles of the secretory, lysosomal and endocytic pathways. Post-translational import of matrix proteins into the mitochondria, chloroplast and peroxisome is also shown. Arrows indicate transport steps.

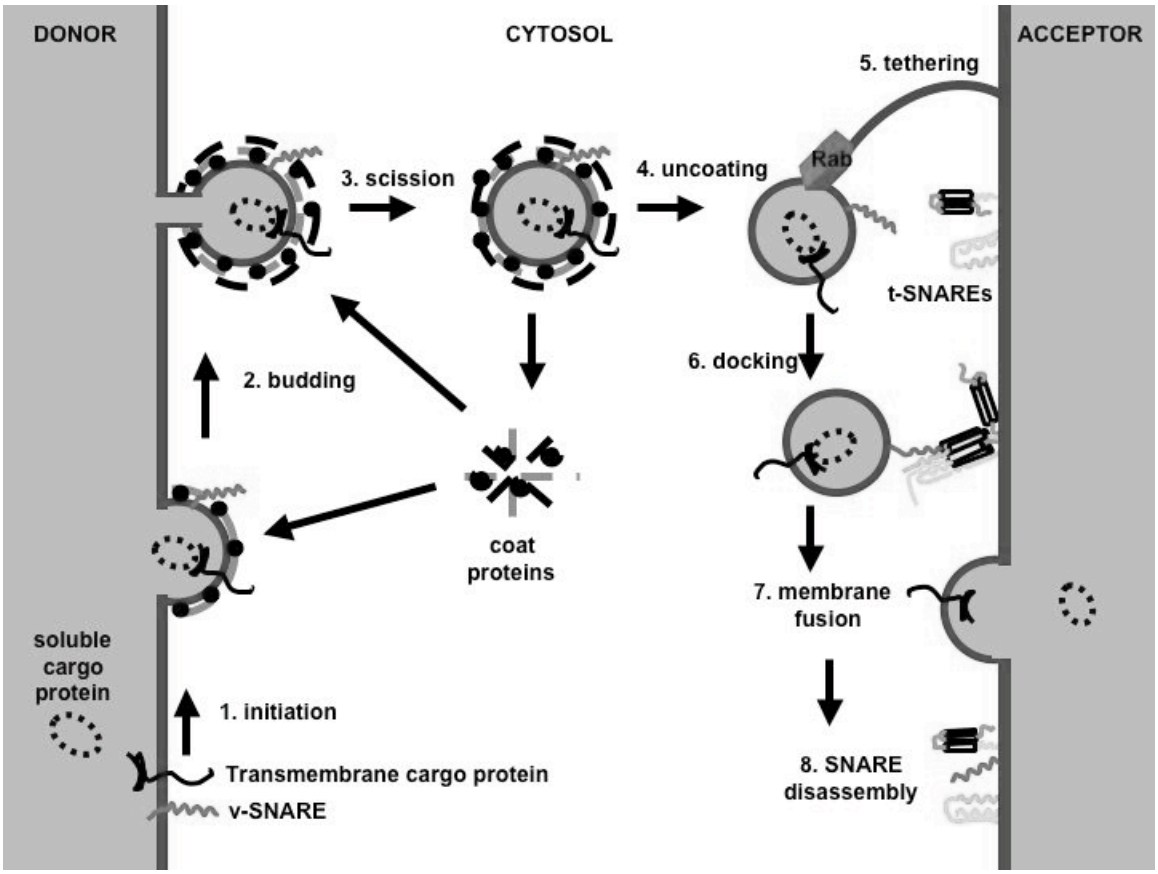

Figure 1.2. Basic steps of Vesicular Transport. 1) Initiation. Membrane coat components (gray) are recruited to the donor compartment. Transmembrane cargo proteins (black squiggle) and SNAREs (red) begin to gather at the assembling coat. 2) Budding. More membrane coat components (black) are added to the newly formed vesicle. The cargo becomes concentrated and membrane curvature increases. 3) Scission. The neck between the vesicle and donor compartments is severed. 4) Uncoating. The vesicle loses its coat and the cytosolic coat proteins are recycled for additional rounds of budding. 5) Tethering. The vesicle is tethered to the acceptor compartment by the combination of a GTP bound Rab (purple) and a tethering factor (blue). 6) Docking. The v- and t-SNAREs assemble into a four-helix bundle. 7) This "*trans*-SNARE complex" promotes fusion of the vesicle and acceptor membranes resulting in a "*cis*-SNARE complex". Cargo is transferred to the acceptor compartment and 8) the SNAREs are disassembled. This depiction of vesicular transport is adapted from Bonifacino and Glick (2004).

Functionally	v-SNARE		t-SNARE		
Sub-classification			Heavy chain & Light chain		
Structurally	R-SNARE		Q-SNARE		
Further sub-classification	Brevins (short)	Longins (long)	Qa	Qb	Qc

Table 1.1. Classification of SNAREs. Functionally SNAREs can be classified into v- and t-SNAREs according to their association with either the vesicle or target membrane, respectively. A t-SNARE is assembled from one heavy and two light chains of SNARE domains. The two light chains can be contributed from one or two SNARE proteins. Based on the residue in the zero layer within the four-helical bundle of the SNARE interaction domain, SNAREs can be structurally divided into R-SNAREs (those having an R/arginine residue) or Q-SNAREs (those having a Q/glutamine residue). Q-SNAREs are further divided based on the amino acid sequence of the SNARE domain into Qa-, Qb-, and Qc-SNAREs. Table adapted from Hong (2005).

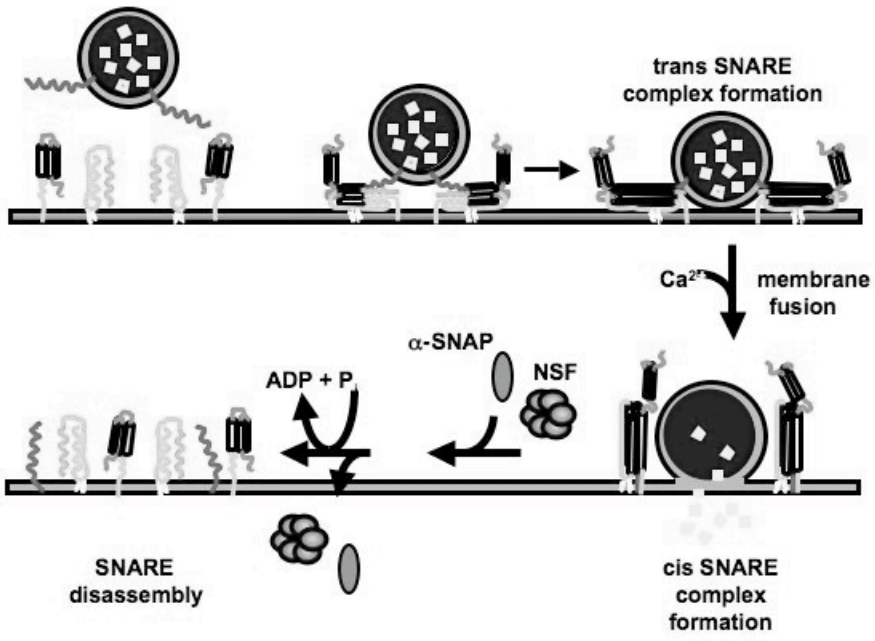

Figure 1.3. SNARE conformation cycle. Monomeric v-SNARES on the vesicle bind to olgiomeric t-SNAREs on the target membrane to form the *trans*-SNARE complex, a stable four-helix bundle that promotes fusion. Formation of the *cis*-SNARE complex in the same membrane is a consequence of the fusion event. α-SNAP (pink) binds to this complex and recruits NSF (blue), which hydrolyzes ATP to disassociate the complex. This depiction of the SNARE cycle is adapted from Jahn, Lang and Sudhof (2003).

Regulator	Target	Trafficking step
Sec1/Munc18 (SM proteins)	Syntaxin, SNARE complex	All
Synaptotagmin	Syntaxin, SNARE complex	Regulated exocytosis
Munc13	Syntaxin	Regulated exocytosis
GATE16/Apg8 (UFT proteins)	Golgi transport SNAREs	Golgi transport, Golgi reassembly, autophagy
LMA1/EEA1	Vam3 (syntaxin homolog)	Vacuolar membrane fusion (yeast)
Complexins	Syntaxin, SNAP-25, SNARE complex	Regulated exocytosis
Snapin	SNAP-25	Regulated exocytosis
Synaptophysin	VAMP	Regulated exocytosis
Amisyn/Tomosyn/ Sro proteins	Syntaxin, SNAP-25 ortholog (yeast)	Constitutive and regulated exocytosis
Vsm1	VAMP and Syntaxin orthologs	Constitutive exocytosis (yeast)

Table 1.2. Common SNARE regulators. Shown here is partial list of SNARE-interacting proteins that have been identified to play critical roles in SNARE-mediated fusion events. Adapted from Gerst (2003).

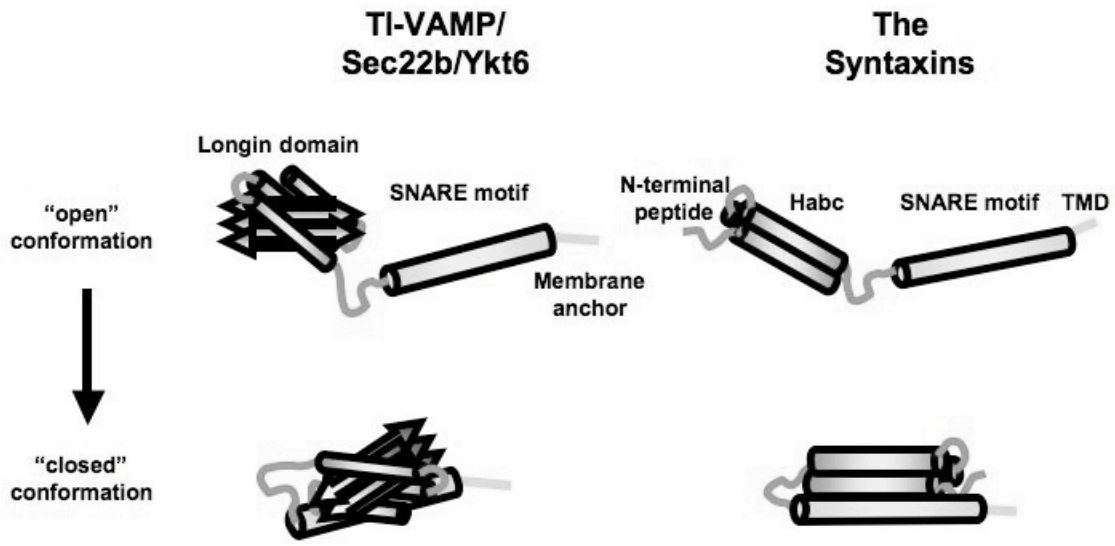

Figure 1.4. Schematic representation of the domain architecture of Longins and Syntaxins. All SNAREs contain the distinguishing SNARE motif (beige). R-SNARE longins share a long NTD with a profilin-like fold characterized by a five-stranded, anti-parellel beta sheet flanked by alpha helices that can influence the kinetics and proper assembly of SNAREs (214, Gonzalez, 2001 #63). Syntaxins have a domain structure set apart by a Habc domain with potential auto-inhibitory function to regulate SNARE function in membrane fusion (147, 158, 235). Most SNAREs have TMDs, but the Ykt6 longin associates with the membrane by prenylation (60, 82).

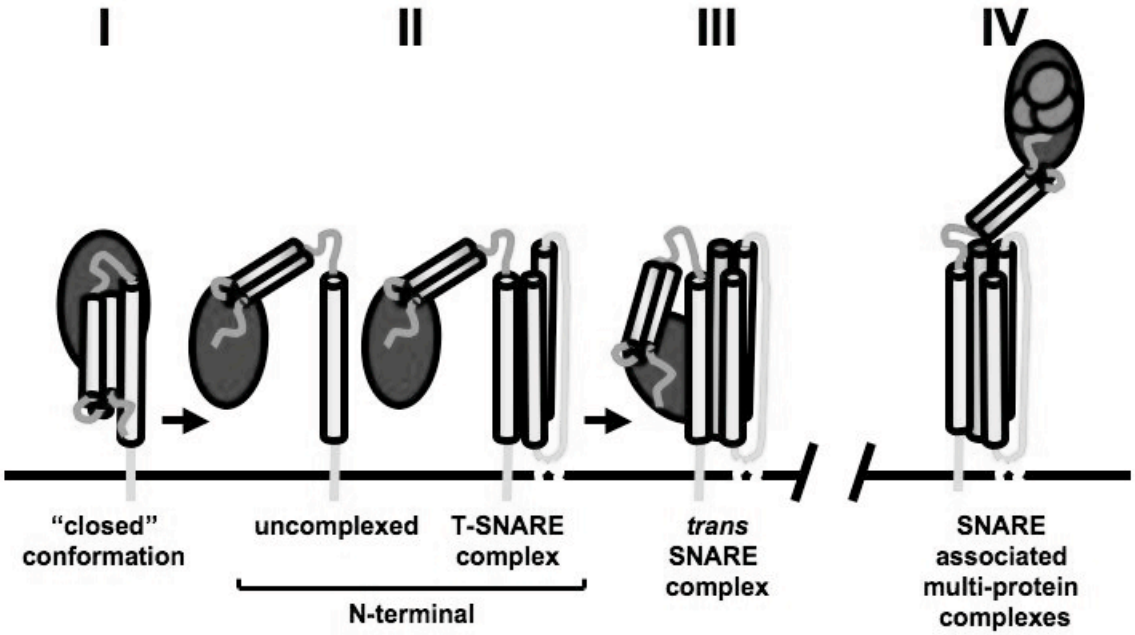

Figure 1.5. SM/SNARE protein binding modes. The following SM interactions with monomeric and assembled SNAREs have been proposed. From left, panel I represents SM protein binding to a "closed" form of syntaxin (Misura, 2000), to the amino terminus of syntaxin in panel II (Bracher, 2002), and to the assembled SNARE complex in panel III (Peng, 2004). It is possible that each interaction represents an intermediate on an SM protein-controlled molecular pathway of specific SNARE complex assembly. Panel IV represents a special case in which the interaction between syntaxins and SM proteins is indirect through association with a large complex that binds directly to the syntaxin (Laage, 2001). The arrows indicate states occurring as a series of interactions on a molecular pathway rather than each existing as separate states.

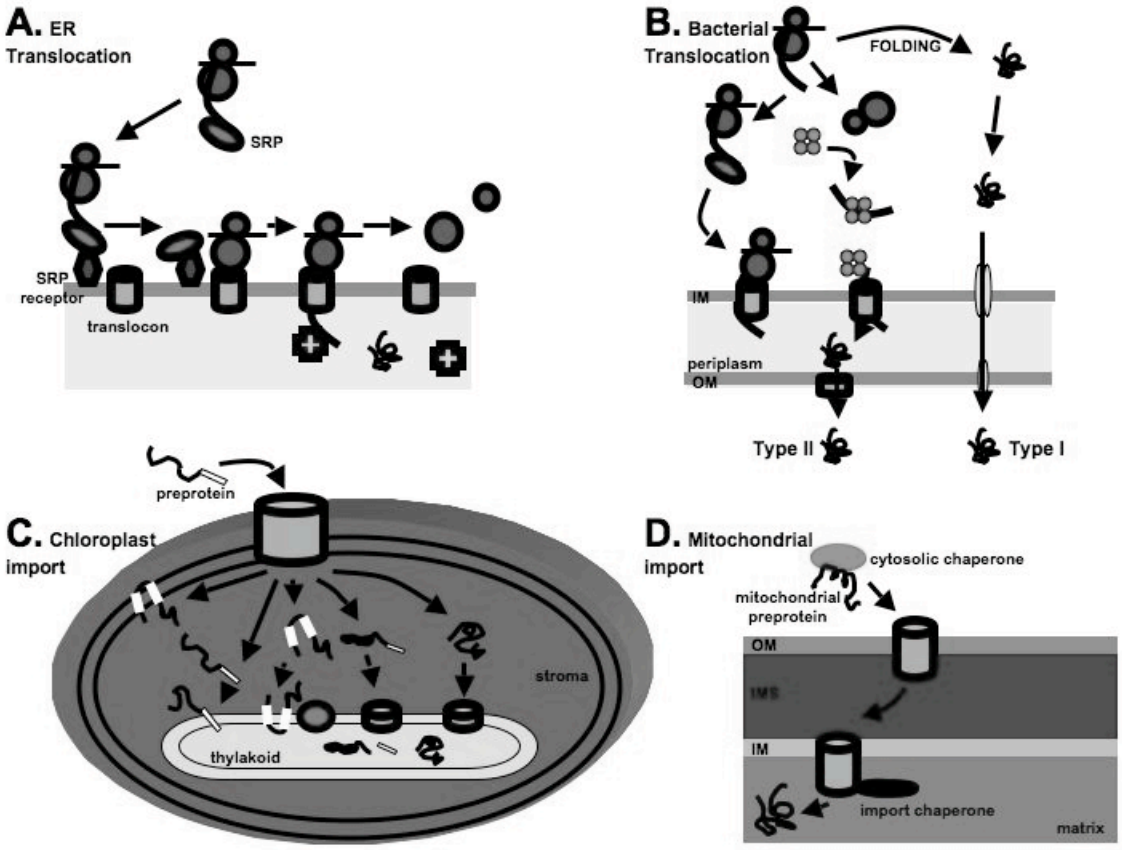

Figure 1.6. Conserved translocation schemes. A) Cotranslational translocation into the ER. B) Bacterial translocation pathways. C) Chloroplast protein translocation. D) Mitochondrial protein import. Illustrations adapted from Wickner and Schekman (2005).

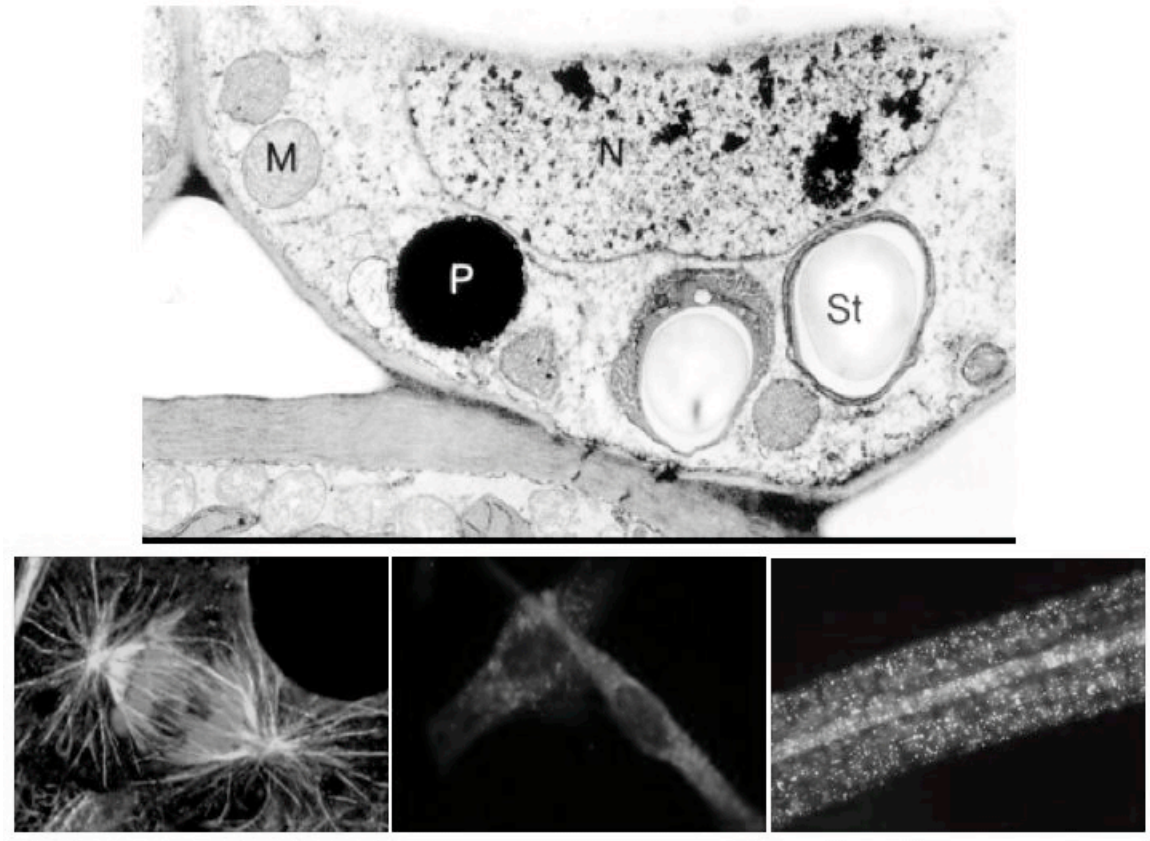

Figure 1.7. Intracellular representations of peroxisomes. The top panel is an electron micrograph showing the intracellular milieu of a mature cowpea nodule (Webb and Newcomb, 1987). M, mitochndria; N, nucleus; St, starch-containing plastid; P, peroxisome. **The bottom left panel** is a fluorescent micrograph of a eukaryotic cell undergoing mitosis (taken by T.J. Deerinck. Cold Spring Harbor Laboratories, NY) Peroxisomes are indicated in blue. **The bottom center panel** is a fluorescent microgrph peroxisomes located in human fibroblast skin cells stained with anti-catalase antibodies (taken by Antionette L. Williams, University of Michigan, Ann Arbor, MI). **The bottom right panel** is a fluorescent micrograph of peroxisomes located in the hypocotyl of an Arabidopsis plant (taken by Jianping Hu, Michigan State University, Lansing, MI).

Gene	Identified in Hs	At	Sc	Yl	Nc	Ce	Subcellular localization	Characteristics
PEX1	+	+	+	+	+	+	Cytosolic; peroxisomal	AAA protein; required for matrix protein import
PEX2	+	+	+	+	+	+	Integral PMP	RING zinc finger; matrix protein import downstream of receptor docking
PEX3	+	+	+	-	+	-	Integral PMP	Possible Pex19p docking factor; PMP import
PEX4	-	+	+	-	+	-	Peripheral PMP	E2 ubiquitin conjugating enzyme; matrix protein import
PEX5	+	+	+	+	+	+	Cytosolic; peroxisomal	TPR protein; PTS1 receptor
PEX6	+	+	+	+	+	+	Cytosolic; peroxisomal	AAA protein; matrix protein import
PEX7	+	+	+	-	+	-	Cytosolic; peroxisomal	WD40 protein; PTS2 receptor
PEX8	-	-	+	+	+	-	Lumenal PMP	Matrix protein import downstream of receptor docking
PEX9	-	-	-	+	-	-	Integral PMP	Matrix protein import
PEX10	+	+	+	+	+	-	Integral PMP	RING zinc finger; matrix protein import downstream of receptor docking
PEX11	+	+	+	+	+	-	Integral PMP	Organelle division and proliferatio; transport of medium chain fatty acids
PEX12	+	+	+	-	+	+	Integral PMP	RING zinc finger; matrix protein import downstream of receptor docking
PEX13	+	+	+	-	+	+	Integral PMP	SH3 protein; receptor docking
PEX14	+	+	+	+	+		PMP	Initial site of receptor docking
PEX15	-	-	+	-	-		Integral PMP	Memrane anchor; matrix protein import
PEX16	+	+	-	+	+		Integral PMP	PMP import
PEX17	-	-	+	-	-	-	Peripheral PMP	Matrix protein import
PEX18	-	-	+	-	-		Cytosolic; peroxisomal	PTS2 matrix protein import
PEX19	+	+	+	+	+	+	Cytosolic; peroxisomal	Cytosolic PMP receptor
PEX20	-	-	-	+	+	-	Cytosolic; peroxisomal	PTS2 matrix protein import
PEX21	-	-	+	-	-	-	Cytosolic	PTS2 matrix protein import
PEX22	-	-	+	-	-	-	Integral PMP	Matrix protein import
PEX23	-	-	-	+	+	-	Integral PMP	Matrix protein import
PEX24	-	-	-	+	-	-	Integral PMP	Peroxisome assembly
PEX25	-	-	+	-	-	-	Perpheral PMP	Peroxisome proliferation
PEX26	+	-	-	-	-	-	Integral PMP	Matrix protein import
PEX27	-	-	+	-	-	-	Peripheral PMP	Peroxisome proliferation
PEX28	-	-	-	+	-	-	Integral PMP	Peroxisome proliferation
PEX29	-	-	-	+	-	-	Integral PMP	Peroxisome proliferation
PEX30	-	-	+	-	-	-	Integral PMP	Peroxisome proliferation
PEX31	-	-	+	-	-	-	Integral PMP	Peroxisome proliferation
PEX32	-	-	+	-	-	-	Integral PMP	Peroxisome proliferation

Table 1.3. The PEX genes and characteristics of their protein products (peroxins). Information adapted from Wanders and Waterham (2005) and AraPerox (www.araperox. uni-goettingen.de), a database of putative Arabidopsis proteins from plant peroxisomes (Reumann, 2004). Hs, *Homo sapiens*; At, *Arabidopsis thaliana*; Sc, *Saccharomyces cerevisiae*; Yl, *Yarrowia lipolytica*; Nc, *Neurospora crassa*; Ce, *Caenorhabditis elegans*

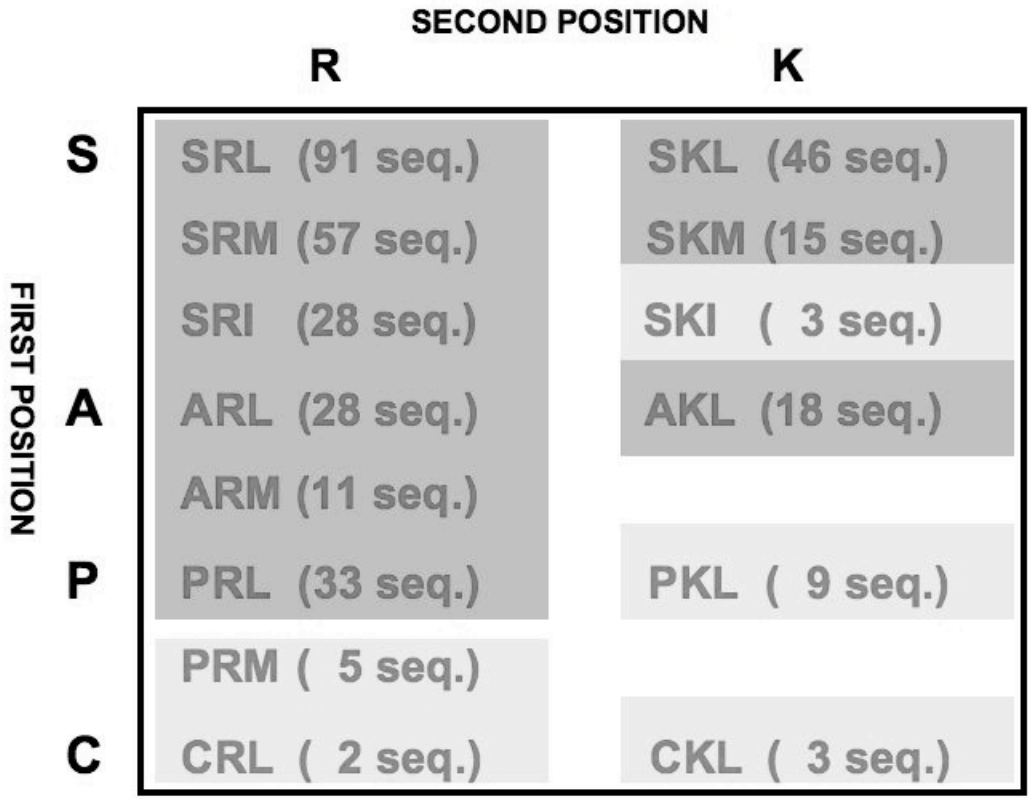

Figure 1.8. PTS1 tripeptides of peroxisomal matrix proteins from plants. Major PTS1 sequences (red, dark gray shade) are present in at least 10 sequences and 3 orthologous groups. Minor PTS1 sequences (blue, light gray shade) are present in at least 2 sequences. Other non-canonical PTS1 tripeptide sequences include: SRV, SNL, SNM, ANL, SML, SSM, and SHL.
Adapted from Reumann (2004).

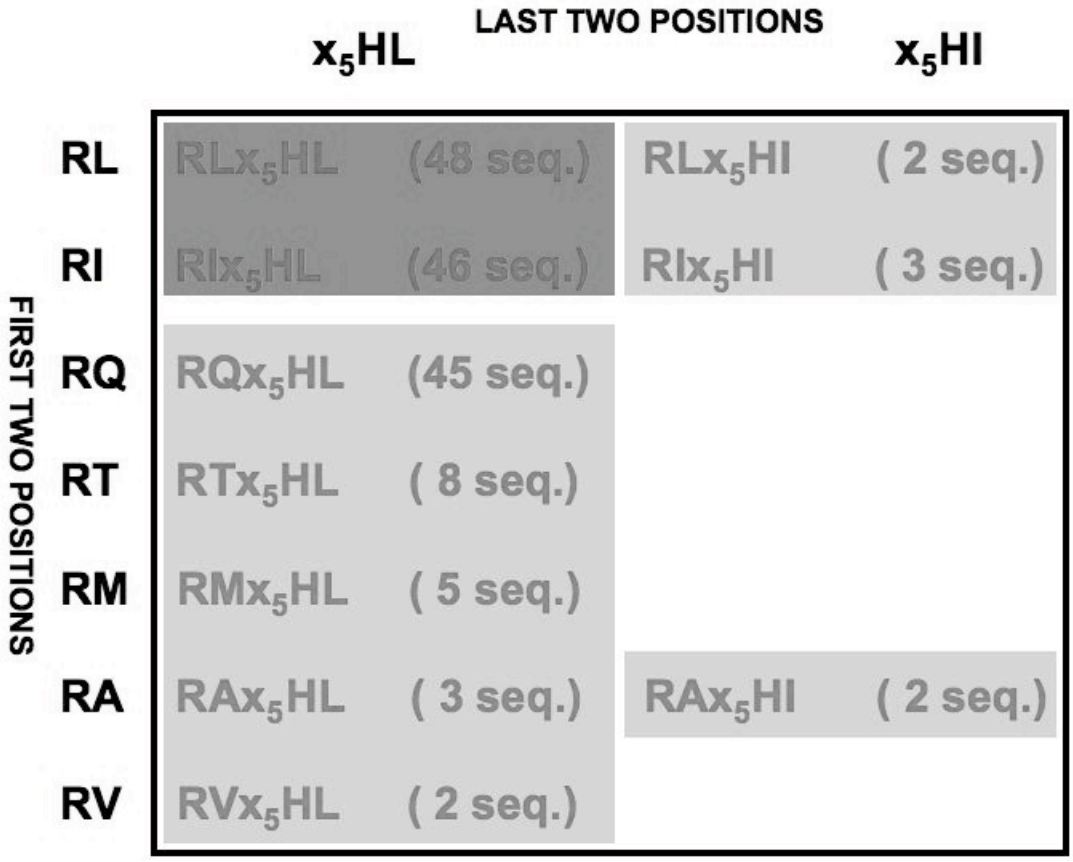

Figure 1.9. PTS2 nonapeptides of peroxisomal matrix proteins from plants. Major PTS2 sequences (red, dark gray shade) are present in at least 10 sequences and 3 orthologous groups. Minor PTS2 sequences (blue, light gray shade) are present in at least 2 sequences. Additional PTS2 nonapeptide sequences include the minor PTS2 RLx_5HF and the unique PTS2 RLx_5HV. Adapted from Reumann (2004).

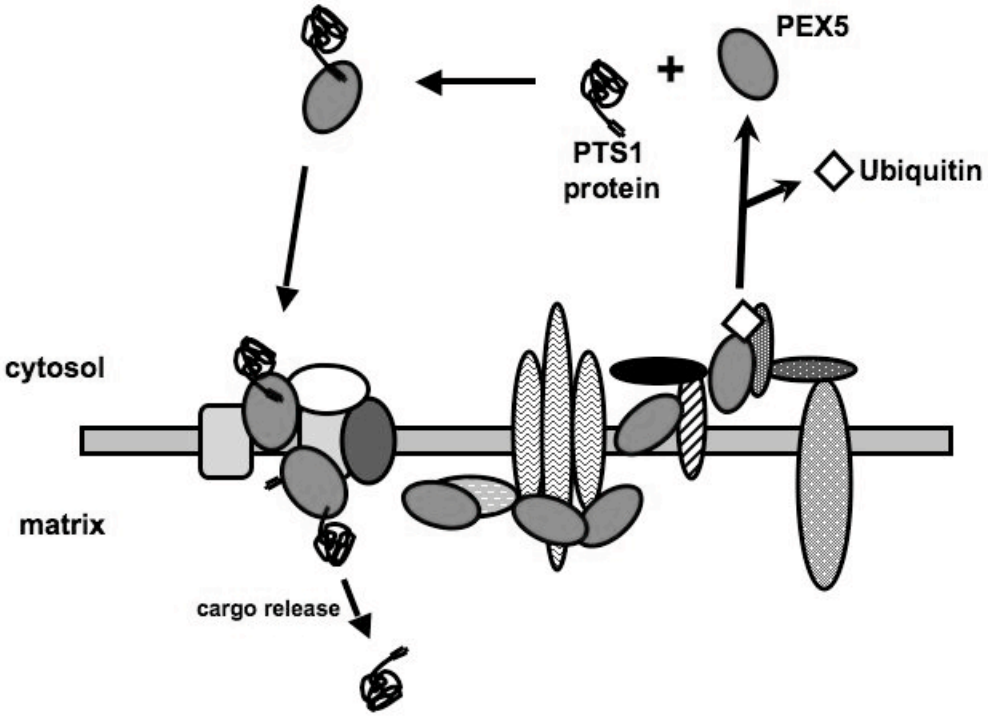

Figure 1.10. PTS1 protein import model (Receptor PEX5 cycle). Proteins harboring a PTS1 are recognized by the soluble receptor PEX5 (shown in blue). The receptor/cargo complex docks at the peroxisomal membrane After translocation, the receptor/cargo complex dissociates in the peroxisome matrix. Subsequently, PEX5 is monoubiquitinated (represented by the open diamond). Following membrane dissociation and removal of ubiquitin, PEX5 is recycled back to the cytosol for further rounds of cargo binding and import.

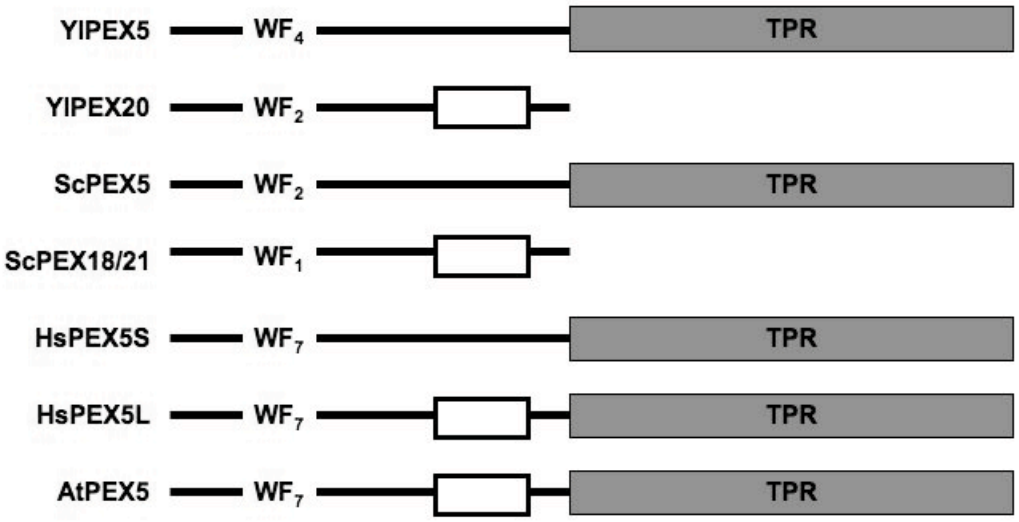

Figure 1.11. Sequence similarities among the PTS2 co-receptors. A) Schematic representation of conserved sequence regions. The number of WxxxF motifs (WF) is indicated by the subscript numbers. Clear white boxes represent the PEX7 binding domains. The large boxes in the carboxyl terminal halves of the PEX5 receptors correspond to the TPR motifs.

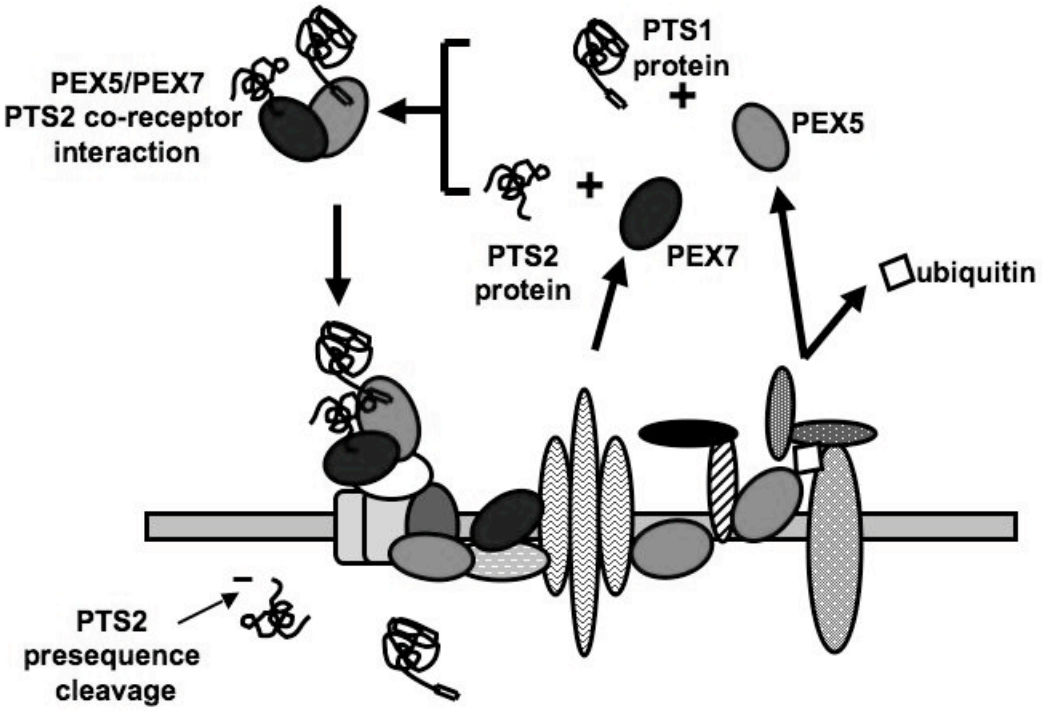

Figure 1.12. PTS2 protein import model (PEX7 receptor cycle). PEX7 (dark blue oval) recognizes and binds to PTS2 cargo in the cytosol, The PEX7-PTS2 receptor/cargo complex then interacts with PTS2 co-receptors; the interaction with receptor PEX5 (light blue oval) is represented here. The entire import complex formed in the cytosol docks at the peroxisomal membrane. Following translocation, PTS2 proteins are then unloaded into the peroxisome matrix. Finally, both PEX7 and its co-receptor PEX5 are recycled back to the cytosol for further rounds of import.

Plants and mammals

Enzyme Species	PTS2 sequence (cleavage recognition site*)	Mature subunit
Malate dehydrogenase		
Watermelon	Q**RIARISAHL**HPPKSQMEESSALRRAN**C**R*	AKGGAPGFKVAI
Pumpkin	E**RIARISAHL**PPKSQMEEGSVLRRAN**C**R*	AKGGAPGFRVAI
Alfalfa	S**RITRIASHL**NPPNLKMNEHGGSSLTNVH**C**R*	AKGGTPGFKVAI
Rice	R**RMERLASHL**RPPASQMEESPLLRGSN**C**R*	AKGAAPGFKVAI
Rapeseed	K**RIAMISAHL**QPSFTPQMEAKNSVMGLES**C**R*	AKGGNPGFKVAI
Arabidopsis (At5g09660)	Q**RIARISAHL**TPQMEAKNSVIGREN**C**R*	AKGGNPGFKVAI
Arabidopsis (At2g22780)	Q**RIARISAHL**NPPNLHNQIADGSGLNRVA**C**R*	AKGGSPGFKVAI
Citrate synthase		
Pumpkin	RH**RLAVLAAHL**SAASLEPPVMASSLEAH**C**V*	SAQTMVAPPEL
Arabidopsis (At2g42790)	RA**RLAVLSGHL**SEGKQDSPAIERW**C**T*	SADTSVAPLGS
Arabidopsis (At3g58740)	RA**RLAVLNAHL**TVSEPNQVLPAIEPW**C**T*	SAHITAAPHGS
Acyl CoA oxidase		
Pumpkin	R**RIERLSLHL**TPIPLDDSQGVEMET**C***	AAGKAKAKIEVD
Arabidopsis (At5g65110)	R**RIQRLSLHL**SPSLTLSPSLPLVQTET**C***	SARSKKLDVNGE
3-keto-acyl-CoA thiolase		
Cucumber	N**RQSILLHHL**RPSSSAYTNESSLSASV**C***	AAGDSASY
Pumpkin	N**RQSILLHHL**RPSSSAYSHESSLSASV**C***	AAGDSASY
Mango	N**RQSILLHHL**RPSNSSSHNYESALAASV**C***	AAGDSAAY
Rapeseed	E**RQRVLLEHL**RPSSSSSHSFEGSLSASA**C***	LAGDSAAY
Arabidopsis (At5g48880)	E**RQRVLLEHL**RPSSSSSHNYEASLSASA**C***	LAGDSAAY
Rat	H**RLQVVLGHL**AGRPESSSALQAAP**C***	SAGFPQAS
Human	Q**RLQVVLGHL**RGPADSGWMPQAAP**C***	LSGAPQAS

Table 1.4. Consensus sequences of known PTS2 matrix proteins in plants and mammals. PTS2 sequences are indicated in bold. The conserved Cys near the cleavage site for recognition by the peroxisomal processing peptidase is indicated in bold. Adapted from Helm, *et al.* (2007).

REFERENCES

1. **Aalto, M. K., S. Keranen, and H. Ronne.** 1992. A family of proteins involved in intracellular transport. Cell **68:**181-2.
2. **Agarraberes, F. A., and J. F. Dice.** 2001. Protein translocation across membranes. Biochim Biophys Acta **1513:**1-24.
3. **Aitchison, J. D., W. M. Nuttley, R. K. Szilard, A. M. Brade, J. R. Glover, and R. A. Rachubinski.** 1992. Peroxisome biogenesis in yeast. Mol Microbiol **6:**3455-60.
4. **Antonin, W., D. Fasshauer, S. Becker, R. Jahn, and T. R. Schneider.** 2002. Crystal structure of the endosomal SNARE complex reveals common structural principles of all SNAREs. Nat Struct Biol **9:**107-11.
5. **Aridor, M., and L. A. Hannan.** 2000. Traffic jam: a compendium of human diseases that affect intracellular transport processes. Traffic **1:**836-51.
6. **Aridor, M., and L. A. Hannan.** 2002. Traffic jams II: an update of diseases of intracellular transport. Traffic **3:**781-90.
7. **Authier, F., J. J. Bergeron, W. J. Ou, R. A. Rachubinski, B. I. Posner, and P. A. Walton.** 1995. Degradation of the cleaved leader peptide of thiolase by a peroxisomal proteinase. Proc Natl Acad Sci U S A **92:**3859-63.
8. **Baker, A.** 1996. In vitro systems in the study of peroxisomal protein import. Experientia **52:**1055-62.
9. **Baker, A., I. A. Graham, M. Holdsworth, S. M. Smith, and F. L. Theodoulou.** 2006. Chewing the fat: beta-oxidation in signalling and development. Trends Plant Sci **11:**124-32.
10. **Balfe, A., G. Hoefler, W. W. Chen, and P. A. Watkins.** 1990. Aberrant subcellular localization of peroxisomal 3-ketoacyl-CoA thiolase in the Zellweger syndrome and rhizomelic chondrodysplasia punctata. Pediatr Res **27:**304-10.
11. **Banjoko, A., and R. N. Trelease.** 1995. Development and application of an in vivo plant peroxisome import system. Plant Physiol **107:**1201-8.
12. **Barlowe, C.** 1998. COPII and selective export from the endoplasmic reticulum. Biochim Biophys Acta **1404:**67-76.
13. **Baudhuin, P., M. Mueller, B. Poole, and C. Deduve.** 1965. Non-Mitochondrial Oxidizing Particles (Microbodies) In Rat Liver And Kidney And In Tetrahymena Pyriformis. Biochem Biophys Res Commun **20:**53-9.
14. **Beevers, H.** 1979. Microbodies in higher plants. Annual Reviews in Plant Physiology **30:**159 - 193.
15. **Beevers, H., and R. W. Breidenbach.** 1974. Glyoxysomes. Methods Enzymol **31:**565-71.
16. **Betz, A., M. Okamoto, F. Benseler, and N. Brose.** 1997. Direct interaction of the rat unc-13 homologue Munc13-1 with the N terminus of syntaxin. J Biol Chem **272:**2520-6.
17. **Blobel, G.** 1980. Intracellular protein topogenesis. Proc Natl Acad Sci U S A **77:**1496-500.

18. **Blobel, G., and B. Dobberstein.** 1975. Transfer of proteins across membranes. I. Presence of proteolytically processed and unprocessed nascent immunoglobulin light chains on membrane-bound ribosomes of murine myeloma. J Cell Biol **67:**835-51.
19. **Blobel, G., and B. Dobberstein.** 1975. Transfer to proteins across membranes. II. Reconstitution of functional rough microsomes from heterologous components. J Cell Biol **67:**852-62.
20. **Block, M. R., B. S. Glick, C. A. Wilcox, F. T. Wieland, and J. E. Rothman.** 1988. Purification of an N-ethylmaleimide-sensitive protein catalyzing vesicular transport. Proc Natl Acad Sci U S A **85:**7852-6.
21. **Bock, J. B., H. T. Matern, A. A. Peden, and R. H. Scheller.** 2001. A genomic perspective on membrane compartment organization. Nature **409:**839-41.
22. **Bonifacino, J. S., and B. S. Glick.** 2004. The mechanisms of vesicle budding and fusion. Cell **116:**153-66.
23. **Bonsegna, S., S. P. Slocombe, L. De Bellis, and A. Baker.** 2005. AtLACS7 interacts with the TPR domains of the PTS1 receptor PEX5. Arch Biochem Biophys **443:**74-81.
24. **Bracher, A., and W. Weissenhorn.** 2004. Crystal structure of the Habc domain of neuronal syntaxin from the squid Loligo pealei reveals conformational plasticity at its C-terminus. BMC Struct Biol **4:**6.
25. **Bracher, A., and W. Weissenhorn.** 2002. Structural basis for the Golgi membrane recruitment of Sly1p by Sed5p. EMBO J **21:**6114-24.
26. **Braverman, N., G. Dodt, S. J. Gould, and D. Valle.** 1998. An isoform of pex5p, the human PTS1 receptor, is required for the import of PTS2 proteins into peroxisomes. Hum Mol Genet **7:**1195-205.
27. **Brickner, D. G., J. J. Harada, and L. J. Olsen.** 1997. Protein transport into higher plant peroxisomes. In vitro import assay provides evidence for receptor involvement. Plant Physiol **113:**1213-21.
28. **Brocard, C., and A. Hartig.** 2006. Peroxisome targeting signal 1: is it really a simple tripeptide? Biochim Biophys Acta **1763:**1565-73.
29. **Brose, N., C. Rosenmund, and J. Rettig.** 2000. Regulation of transmitter release by Unc-13 and its homologues. Curr Opin Neurobiol **10:**303-11.
30. **Brugger, B., W. Nickel, T. Weber, F. Parlati, J. A. McNew, J. E. Rothman, and T. Sollner.** 2000. Putative fusogenic activity of NSF is restricted to a lipid mixture whose coalescence is also triggered by other factors. EMBO J **19:**1272-8.
31. **Bryant, N. J., and D. E. James.** 2001. Vps45p stabilizes the syntaxin homologue Tlg2p and positively regulates SNARE complex formation. EMBO J **20:**3380-8.
32. **Carpp, L. N., L. F. Ciufo, S. G. Shanks, A. Boyd, and N. J. Bryant.** 2006. The Sec1p/Munc18 protein Vps45p binds its cognate SNARE proteins via two distinct modes. J Cell Biol **173:**927-36.
33. **Carr, C. M., E. Grote, M. Munson, F. M. Hughson, and P. J. Novick.** 1999. Sec1p binds to SNARE complexes and concentrates at sites of secretion. J Cell Biol **146:**333-44.

34. **Chen, Y. A., and R. H. Scheller.** 2001. SNARE-mediated membrane fusion. Nat Rev Mol Cell Biol **2:**98-106.
35. **Chua, N. H., and G. W. Schmidt.** 1978. Post-translational transport into intact chloroplasts of a precursor to the small subunit of ribulose-1,5-bisphosphate carboxylase. Proc Natl Acad Sci U S A **75:**6110-6114.
36. **Connell, E., F. Darios, K. Broersen, N. Gatsby, S. Y. Peak-Chew, C. Rickman, and B. Davletov.** 2007. Mechanism of arachidonic acid action on syntaxin-Munc18. EMBO Rep **8:**414-9.
37. **Crookes, W. J., and L. J. Olsen.** 1998. The effects of chaperones and the influence of protein assembly on peroxisomal protein import. J Biol Chem **273:**17236-42.
38. **Dammai, V., and S. Subramani.** 2001. The human peroxisomal targeting signal receptor, Pex5p, is translocated into the peroxisomal matrix and recycled to the cytosol. Cell **105:**187-96.
39. **De Duve, C., and P. Baudhuin.** 1966. Peroxisomes (microbodies and related particles). Physiol Rev **46:**323-57.
40. **de Hoop, M. J., and G. Ab.** 1992. Import of proteins into peroxisomes and other microbodies. Biochem J **286 (Pt 3):**657-69.
41. **Didion, T., and R. Roggenkamp.** 1992. Targeting signal of the peroxisomal catalase in the methylotrophic yeast Hansenula polymorpha. FEBS Lett **303:**113-6.
42. **Dietrich, L. E., C. Boeddinghaus, T. J. LaGrassa, and C. Ungermann.** 2003. Control of eukaryotic membrane fusion by N-terminal domains of SNARE proteins. Biochim Biophys Acta **1641:**111-9.
43. **Distel, B., S. J. Gould, T. Voorn-Brouwer, M. van der Berg, H. F. Tabak, and S. Subramani.** 1992. The carboxyl-terminal tripeptide serine-lysine-leucine of firefly luciferase is necessary but not sufficient for peroxisomal import in yeast. New Biol **4:**157-65.
44. **Dodt, G., D. Warren, E. Becker, P. Rehling, and S. J. Gould.** 2001. Domain mapping of human PEX5 reveals functional and structural similarities to Saccharomyces cerevisiae Pex18p and Pex21p. J Biol Chem **276:**41769-81.
45. **Dulubova, I., M. Khvotchev, S. Liu, I. Huryeva, T. C. Sudhof, and J. Rizo.** 2007. Munc18-1 binds directly to the neuronal SNARE complex. Proc Natl Acad Sci U S A **104:**2697-702.
46. **Dulubova, I., T. Yamaguchi, D. Arac, H. Li, I. Huryeva, S. W. Min, J. Rizo, and T. C. Sudhof.** 2003. Convergence and divergence in the mechanism of SNARE binding by Sec1/Munc18-like proteins. Proc Natl Acad Sci U S A **100:**32-7.
47. **Dulubova, I., T. Yamaguchi, Y. Wang, T. C. Sudhof, and J. Rizo.** 2001. Vam3p structure reveals conserved and divergent properties of syntaxins. Nat Struct Biol **8:**258-64.
48. **Einwachter, H., S. Sowinski, W. H. Kunau, and W. Schliebs.** 2001. Yarrowia lipolytica Pex20p, Saccharomyces cerevisiae Pex18p/Pex21p and mammalian Pex5pL fulfil a common function in the early steps of the peroxisomal PTS2 import pathway. EMBO Rep **2:**1035-9.

49. **Elazar, Z., R. Scherz-Shouval, and H. Shorer.** 2003. Involvement of LMA1 and GATE-16 family members in intracellular membrane dynamics. Biochim Biophys Acta **1641:**145-56.
50. **Elgersma, Y., M. Elgersma-Hooisma, T. Wenzel, J. M. McCaffery, M. G. Farquhar, and S. Subramani.** 1998. A mobile PTS2 receptor for peroxisomal protein import in Pichia pastoris. J Cell Biol **140:**807-20.
51. **Elgersma, Y., L. Kwast, A. Klein, T. Voorn-Brouwer, M. van den Berg, B. Metzig, T. America, H. F. Tabak, and B. Distel.** 1996. The SH3 domain of the Saccharomyces cerevisiae peroxisomal membrane protein Pex13p functions as a docking site for Pex5p, a mobile receptor for the import PTS1-containing proteins. J Cell Biol **135:**97-109.
52. **Erdmann, R., and G. Blobel.** 1996. Identification of Pex13p a peroxisomal membrane receptor for the PTS1 recognition factor. J Cell Biol **135:**111-21.
53. **Faber, K. N., P. Haima, C. Gietl, W. Harder, G. Ab, and M. Veenhuis.** 1994. The methylotrophic yeast Hansenula polymorpha contains an inducible import pathway for peroxisomal matrix proteins with an N-terminal targeting signal (PTS2 proteins). Proc Natl Acad Sci U S A **91:**12985-9.
54. **Fan, J., X. Yang, J. Lu, L. Chen, and P. Xu.** 2007. Role of H(abc) domain in membrane trafficking and targeting of syntaxin 1A. Biochem Biophys Res Commun **359:**245-50.
55. **Fasshauer, D., R. B. Sutton, A. T. Brunger, and R. Jahn.** 1998. Conserved structural features of the synaptic fusion complex: SNARE proteins reclassified as Q- and R-SNAREs. Proc Natl Acad Sci U S A **95:**15781-6.
56. **Fernandez-Chacon, R., A. Konigstorfer, S. H. Gerber, J. Garcia, M. F. Matos, C. F. Stevens, N. Brose, J. Rizo, C. Rosenmund, and T. C. Sudhof.** 2001. Synaptotagmin I functions as a calcium regulator of release probability. Nature **410:**41-9.
57. **Filippini, F., V. Rossi, T. Galli, A. Budillon, M. D'Urso, and M. D'Esposito.** 2001. Longins: a new evolutionary conserved VAMP family sharing a novel SNARE domain. Trends Biochem Sci **26:**407-9.
58. **Flynn, C. R., R. T. Mullen, and R. N. Trelease.** 1998. Mutational analyses of a type 2 peroxisomal targeting signal that is capable of directing oligomeric protein import into tobacco BY-2 glyoxysomes. Plant J **16:**709-20.
59. **Fries, E., and J. E. Rothman.** 1980. Transport of vesicular stomatitis virus glycoprotein in a cell-free extract. Proc Natl Acad Sci U S A **77:**3870-4.
60. **Fukasawa, M., O. Varlamov, W. S. Eng, T. H. Sollner, and J. E. Rothman.** 2004. Localization and activity of the SNARE Ykt6 determined by its regulatory domain and palmitoylation. Proc Natl Acad Sci U S A **101:**4815-20.

61. **Fukuda, R., J. A. McNew, T. Weber, F. Parlati, T. Engel, W. Nickel, J. E. Rothman, and T. H. Sollner.** 2000. Functional architecture of an intracellular membrane t-SNARE. Nature **407:**198-202.
62. **Fulda, M., J. Shockey, M. Werber, F. P. Wolter, and E. Heinz.** 2002. Two long-chain acyl-CoA synthetases from Arabidopsis thaliana involved in peroxisomal fatty acid beta-oxidation. Plant J **32:**93-103.
63. **Fung, K., and C. Clayton.** 1991. Recognition of a peroxisomal tripeptide entry signal by the glycosomes of Trypanosoma brucei. Mol Biochem Parasitol **45:**261-4.
64. **Gallwitz, D., and R. Jahn.** 2003. The riddle of the Sec1/Munc-18 proteins - new twists added to their interactions with SNAREs. Trends Biochem Sci **28:**113-6.
65. **Gatto, G. J., Jr., B. V. Geisbrecht, S. J. Gould, and J. M. Berg.** 2000. Peroxisomal targeting signal-1 recognition by the TPR domains of human PEX5. Nat Struct Biol **7:**1091-5.
66. **Gatto, G. J., Jr., E. L. Maynard, A. L. Guerrerio, B. V. Geisbrecht, S. J. Gould, and J. M. Berg.** 2003. Correlating structure and affinity for PEX5:PTS1 complexes. Biochemistry **42:**1660-6.
67. **Gerst, J. E.** 2003. SNARE regulators: matchmakers and matchbreakers. Biochim Biophys Acta **1641:**99-110.
68. **Gietl, C., B. Wimmer, J. Adamec, and F. Kalousek.** 1997. A cysteine endopeptidase isolated from castor bean endosperm microbodies processes the glyoxysomal malate dehydrogenase precursor protein. Plant Physiol **113:**863-71.
69. **Glover, J. R., D. W. Andrews, S. Subramani, and R. A. Rachubinski.** 1994. Mutagenesis of the amino targeting signal of Saccharomyces cerevisiae 3-ketoacyl-CoA thiolase reveals conserved amino acids required for import into peroxisomes in vivo. J Biol Chem **269:**7558-63.
70. **Gonzalez, L. C., Jr., W. I. Weis, and R. H. Scheller.** 2001. A novel snare N-terminal domain revealed by the crystal structure of Sec22b. J Biol Chem **276:**24203-11.
71. **Gorlich, D., and R. A. Laskey.** 1995. Roles of importin in nuclear protein import. Cold Spring Harb Symp Quant Biol **60:**695-9.
72. **Gould, S. G., G. A. Keller, and S. Subramani.** 1987. Identification of a peroxisomal targeting signal at the carboxy terminus of firefly luciferase. J Cell Biol **105:**2923-31.
73. **Gould, S. J., and C. S. Collins.** 2002. Opinion: peroxisomal-protein import: is it really that complex? Nat Rev Mol Cell Biol **3:**382-9.
74. **Gould, S. J., J. E. Kalish, J. C. Morrell, J. Bjorkman, A. J. Urquhart, and D. I. Crane.** 1996. Pex13p is an SH3 protein of the peroxisome membrane and a docking factor for the predominantly cytoplasmic PTs1 receptor. J Cell Biol **135:**85-95.
75. **Gould, S. J., G. A. Keller, N. Hosken, J. Wilkinson, and S. Subramani.** 1989. A conserved tripeptide sorts proteins to peroxisomes. J Cell Biol **108:**1657-64.

76. **Gouveia, A. M., C. P. Guimaraes, M. E. Oliveira, C. Reguenga, C. Sa-Miranda, and J. E. Azevedo.** 2003. Characterization of the peroxisomal cycling receptor Pex5p import pathway. Adv Exp Med Biol **544:**219-20.
77. **Gouveia, A. M., C. P. Guimaraes, M. E. Oliveira, C. Sa-Miranda, and J. E. Azevedo.** 2003. Insertion of Pex5p into the peroxisomal membrane is cargo protein-dependent. J Biol Chem **278:**4389-92.
78. **Gouveia, A. M., C. Reguenga, M. E. Oliveira, C. Sa-Miranda, and J. E. Azevedo.** 2000. Characterization of peroxisomal Pex5p from rat liver. Pex5p in the Pex5p-Pex14p membrane complex is a transmembrane protein. J Biol Chem **275:**32444-51.
79. **Guan, R., H. Dai, and J. Rizo.** 2008. Binding of the Munc13-1 MUN Domain to Membrane-Anchored SNARE Complexes. Biochemistry.
80. **Hanks, J. F., N. E. Tolbert, and K. R. Schubert.** 1981. Localization of Enzymes of Ureide Biosynthesis in Peroxisomes and Microsomes of Nodules. Plant Physiol **68:**65-69.
81. **Hanson, P. I., J. E. Heuser, and R. Jahn.** 1997. Neurotransmitter release - four years of SNARE complexes. Curr Opin Neurobiol **7:**310-5.
82. **Hasegawa, H., S. Zinsser, Y. Rhee, E. O. Vik-Mo, S. Davanger, and J. C. Hay.** 2003. Mammalian ykt6 is a neuronal SNARE targeted to a specialized compartment by its profilin-like amino terminal domain. Mol Biol Cell **14:**698-720.
83. **Hausler, T., Y. D. Stierhof, E. Wirtz, and C. Clayton.** 1996. Import of a DHFR hybrid protein into glycosomes in vivo is not inhibited by the folate-analogue aminopterin. J Cell Biol **132:**311-24.
84. **Hay, J. C.** 2001. SNARE complex structure and function. Exp Cell Res **271:**10-21.
85. **Hayashi, H., L. De Bellis, K. Yamaguchi, A. Kato, M. Hayashi, and M. Nishimura.** 1998. Molecular characterization of a glyoxysomal long chain acyl-CoA oxidase that is synthesized as a precursor of higher molecular mass in pumpkin. J Biol Chem **273:**8301-7.
86. **Hayashi, M., M. Aoki, A. Kato, M. Kondo, and M. Nishimura.** 1996. Transport of chimeric proteins that contain a carboxy-terminal targeting signal into plant microbodies. Plant J **10:**225-34.
87. **Hayashi, M., and M. Nishimura.** 2006. Arabidopsis thaliana--a model organism to study plant peroxisomes. Biochim Biophys Acta **1763:**1382-91.
88. **Hayashi, M., and M. Nishimura.** 2003. Entering a new era of research on plant peroxisomes. Curr Opin Plant Biol **6:**577-82.
89. **Hayashi, M., K. Toriyama, M. Kondo, A. Kato, S. Mano, L. De Bellis, Y. Hayashi-Ishimaru, K. Yamaguchi, H. Hayashi, and M. Nishimura.** 2000. Functional transformation of plant peroxisomes. Cell Biochem Biophys **32 Spring:**295-304.
90. **Helm, M., C. Luck, J. Prestele, G. Hierl, P. F. Huesgen, T. Frohlich, G. J. Arnold, I. Adamska, A. Gorg, F. Lottspeich, and C. Gietl.** 2007. Dual specificities of the glyoxysomal/peroxisomal processing protease Deg15 in higher plants. Proc Natl Acad Sci U S A **104:**11501-6.

91. **Holroyd, C., and R. Erdmann.** 2001. Protein translocation machineries of peroxisomes. FEBS Lett **501:**6-10.
92. **Hong, W.** 2005. SNAREs and traffic. Biochim Biophys Acta **1744:**120-44.
93. **Howell, G. J., Z. G. Holloway, C. Cobbold, A. P. Monaco, and S. Ponnambalam.** 2006. Cell biology of membrane trafficking in human disease. Int Rev Cytol **252:**1-69.
94. **Hu, K., and B. Davletov.** 2003. SNAREs and control of synaptic release probabilities. Faseb J **17:**130-5.
95. **Jahn, R., and P. I. Hanson.** 1998. Membrane fusion. SNAREs line up in new environment. Nature **393:**14-5.
96. **Jahn, R., T. Lang, and T. C. Sudhof.** 2003. Membrane fusion. Cell **112:**519-33.
97. **Jahn, R., and R. H. Scheller.** 2006. SNAREs--engines for membrane fusion. Nat Rev Mol Cell Biol **7:**631-43.
98. **Kamada, T., K. Nito, H. Hayashi, S. Mano, M. Hayashi, and M. Nishimura.** 2003. Functional differentiation of peroxisomes revealed by expression profiles of peroxisomal genes in Arabidopsis thaliana. Plant Cell Physiol **44:**1275-89.
99. **Karpichev, I. V., and G. M. Small.** 2000. Evidence for a novel pathway for the targeting of a Saccharomyces cerevisiae peroxisomal protein belonging to the isomerase/hydratase family. J Cell Sci **113 (Pt 3):**533-44.
100. **Kato, A., M. Hayashi, M. Kondo, and M. Nishimura.** 1996. Targeting and processing of a chimeric protein with the N-terminal presequence of the precursor to glyoxysomal citrate synthase. Plant Cell **8:**1601-11.
101. **Kato, A., Y. Takeda-Yoshikawa, M. Hayashi, M. Kondo, I. Hara-Nishimura, and M. Nishimura.** 1998. Glyoxysomal malate dehydrogenase in pumpkin: cloning of a cDNA and functional analysis of its presequence. Plant Cell Physiol **39:**186-95.
102. **Keller, G. A., S. Gould, M. Deluca, and S. Subramani.** 1987. Firefly luciferase is targeted to peroxisomes in mammalian cells. Proc Natl Acad Sci U S A **84:**3264-8.
103. **Khvotchev, M., I. Dulubova, J. Sun, H. Dai, J. Rizo, and T. C. Sudhof.** 2007. Dual modes of Munc18-1/SNARE interactions are coupled by functionally critical binding to syntaxin-1 N terminus. J Neurosci **27:**12147-55.
104. **Kikuchi, M., N. Hatano, S. Yokota, N. Shimozawa, T. Imanaka, and H. Taniguchi.** 2004. Proteomic analysis of rat liver peroxisome: presence of peroxisome-specific isozyme of Lon protease. J Biol Chem **279:**421-8.
105. **Klein, A. T., P. Barnett, G. Bottger, D. Konings, H. F. Tabak, and B. Distel.** 2001. Recognition of peroxisomal targeting signal type 1 by the import receptor Pex5p. J Biol Chem **276:**15034-41.
106. **Klein, A. T., M. van den Berg, G. Bottger, H. F. Tabak, and B. Distel.** 2002. Saccharomyces cerevisiae acyl-CoA oxidase follows a novel, non-PTS1, import pathway into peroxisomes that is dependent on Pex5p. J Biol Chem **277:**25011-9.

107. **Koehler, C. M., S. Merchant, and G. Schatz.** 1999. How membrane proteins travel across the mitochondrial intermembrane space. Trends Biochem Sci **24:**428-32.
108. **Kragler, F., G. Lametschwandtner, J. Christmann, A. Hartig, and J. J. Harada.** 1998. Identification and analysis of the plant peroxisomal targeting signal 1 receptor NtPEX5. Proc Natl Acad Sci U S A **95:**13336-41.
109. **Kragler, F., A. Langeder, J. Raupachova, M. Binder, and A. Hartig.** 1993. Two independent peroxisomal targeting signals in catalase A of Saccharomyces cerevisiae. J Cell Biol **120:**665-73.
110. **Kunau, W. H.** 2001. Peroxisomes: the extended shuttle to the peroxisome matrix. Curr Biol **11:**R659-62.
111. **Kunze, M., I. Pracharoenwattana, S. M. Smith, and A. Hartig.** 2006. A central role for the peroxisomal membrane in glyoxylate cycle function. Biochim Biophys Acta **1763:**1441-52.
112. **Kurochkin, I. V., Y. Mizuno, A. Konagaya, Y. Sakaki, C. Schonbach, and Y. Okazaki.** 2007. Novel peroxisomal protease Tysnd1 processes PTS1- and PTS2-containing enzymes involved in beta-oxidation of fatty acids. Embo J **26:**835-45.
113. **Laage, R., and C. Ungermann.** 2001. The N-terminal domain of the t-SNARE Vam3p coordinates priming and docking in yeast vacuole fusion. Mol Biol Cell **12:**3375-85.
114. **Lee, J. R., H. H. Jang, J. H. Park, J. H. Jung, S. S. Lee, S. K. Park, Y. H. Chi, J. C. Moon, Y. M. Lee, S. Y. Kim, J. Y. Kim, D. J. Yun, M. J. Cho, K. O. Lee, and S. Y. Lee.** 2006. Cloning of two splice variants of the rice PTS1 receptor, OsPex5pL and OsPex5pS, and their functional characterization using pex5-deficient yeast and Arabidopsis. Plant J **47:**457-66.
115. **Lee, M. S., R. T. Mullen, and R. N. Trelease.** 1997. Oilseed isocitrate lyases lacking their essential type 1 peroxisomal targeting signal are piggybacked to glyoxysomes. Plant Cell **9:**185-97.
116. **Leon, S., J. M. Goodman, and S. Subramani.** 2006. Uniqueness of the mechanism of protein import into the peroxisome matrix: transport of folded, co-factor-bound and oligomeric proteins by shuttling receptors. Biochim Biophys Acta **1763:**1552-64.
117. **Lin, R. C., and R. H. Scheller.** 1997. Structural organization of the synaptic exocytosis core complex. Neuron **19:**1087-94.
118. **Liu, Y., and C. Barlowe.** 2002. Analysis of Sec22p in endoplasmic reticulum/Golgi transport reveals cellular redundancy in SNARE protein function. Mol Biol Cell **13:**3314-24.
119. **Maccecchini, M. L., Y. Rudin, and G. Schatz.** 1979. Transport of proteins across the mitochondrial outer membrane. A precursor form of the cytoplasmically made intermembrane enzyme cytochrome c peroxidase. J Biol Chem **254:**7468-71.

120. **Mancias, J. D., and J. Goldberg.** 2007. The transport signal on Sec22 for packaging into COPII-coated vesicles is a conformational epitope. Mol Cell **26:**403-14.
121. **Margittai, M., D. Fasshauer, R. Jahn, and R. Langen.** 2003. The Habc domain and the SNARE core complex are connected by a highly flexible linker. Biochemistry **42:**4009-14.
122. **Martinez-Arca, S., R. Rudge, M. Vacca, G. Raposo, J. Camonis, V. Proux-Gillardeaux, L. Daviet, E. Formstecher, A. Hamburger, F. Filippini, M. D'Esposito, and T. Galli.** 2003. A dual mechanism controlling the localization and function of exocytic v-SNAREs. Proc Natl Acad Sci U S A **100:**9011-6.
123. **Matsumura, T., H. Otera, and Y. Fujiki.** 2000. Disruption of the interaction of the longer isoform of Pex5p, Pex5pL, with Pex7p abolishes peroxisome targeting signal type 2 protein import in mammals. Study with a novel Pex5-impaired Chinese hamster ovary cell mutant. J Biol Chem **275:**21715-21.
124. **May, T., and J. Soll.** 1999. Chloroplast precursor protein translocon. FEBS Lett **452:**52-6.
125. **Mayer, A., W. Wickner, and A. Haas.** 1996. Sec18p (NSF)-driven release of Sec17p (alpha-SNAP) can precede docking and fusion of yeast vacuoles. Cell **85:**83-94.
126. **McNew, J. A., and J. M. Goodman.** 1996. The targeting and assembly of peroxisomal proteins: some old rules do not apply. Trends Biochem Sci **21:**54-8.
127. **McNew, J. A., M. Sogaard, N. M. Lampen, S. Machida, R. R. Ye, L. Lacomis, P. Tempst, J. E. Rothman, and T. H. Sollner.** 1997. Ykt6p, a prenylated SNARE essential for endoplasmic reticulum-Golgi transport. J Biol Chem **272:**17776-83.
128. **McNew, J. A., T. Weber, F. Parlati, R. J. Johnston, T. J. Melia, T. H. Sollner, and J. E. Rothman.** 2000. Close is not enough: SNARE-dependent membrane fusion requires an active mechanism that transduces force to membrane anchors. J Cell Biol **150:**105-17.
129. **Michels, P. A., J. Moyersoen, H. Krazy, N. Galland, M. Herman, and V. Hannaert.** 2005. Peroxisomes, glyoxysomes and glycosomes (review). Mol Membr Biol **22:**133-45.
130. **Misura, K. M., R. H. Scheller, and W. I. Weis.** 2001. Self-association of the H3 region of syntaxin 1A. Implications for intermediates in SNARE complex assembly. J Biol Chem **276:**13273-82.
131. **Misura, K. M., R. H. Scheller, and W. I. Weis.** 2000. Three-dimensional structure of the neuronal-Sec1-syntaxin 1a complex. Nature **404:**355-62.
132. **Miura, S., I. Kasuya-Arai, H. Mori, S. Miyazawa, T. Osumi, T. Hashimoto, and Y. Fujiki.** 1992. Carboxyl-terminal consensus Ser-Lys-Leu-related tripeptide of peroxisomal proteins functions in vitro as a minimal peroxisome-targeting signal. J Biol Chem **267:**14405-11.

133. **Miyazawa, S., T. Osumi, T. Hashimoto, K. Ohno, S. Miura, and Y. Fujiki.** 1989. Peroxisome targeting signal of rat liver acyl-coenzyme A oxidase resides at the carboxy terminus. Mol Cell Biol **9:**83-91.
134. **Motley, A., M. J. Lumb, P. B. Oatey, P. R. Jennings, P. A. De Zoysa, R. J. Wanders, H. F. Tabak, and C. J. Danpure.** 1995. Mammalian alanine/glyoxylate aminotransferase 1 is imported into peroxisomes via the PTS1 translocation pathway. Increased degeneracy and context specificity of the mammalian PTS1 motif and implications for the peroxisome-to-mitochondrion mistargeting of AGT in primary hyperoxaluria type 1. J Cell Biol **131:**95-109.
135. **Mukai, S., K. Ghaedi, and Y. Fujiki.** 2002. Intracellular localization, function, and dysfunction of the peroxisome-targeting signal type 2 receptor, Pex7p, in mammalian cells. J Biol Chem **277:**9548-61.
136. **Mukhopadhyay, D., and H. Riezman.** 2007. Proteasome-independent functions of ubiquitin in endocytosis and signaling. Science **315:**201-5.
137. **Mullen, R. T.** 2002. Targeting and Import of Matrix Proteins into Peroxisomes. Kluwer Academic Publishers, Netherlands.
138. **Mullen, R. T., M. S. Lee, and R. N. Trelease.** 1997. Identification of the peroxisomal targeting signal for cottonseed catalase. Plant J **12:**313-22.
139. **Muller, M., and G. Blobel.** 1984. In vitro translocation of bacterial proteins across the plasma membrane of Escherichia coli. Proc Natl Acad Sci U S A **81:**7421-5.
140. **Muller, M., and G. Blobel.** 1984. Protein export in Escherichia coli requires a soluble activity. Proc Natl Acad Sci U S A **81:**7737-41.
141. **Muller, O., M. J. Bayer, C. Peters, J. S. Andersen, M. Mann, and A. Mayer.** 2002. The Vtc proteins in vacuole fusion: coupling NSF activity to V(0) trans-complex formation. Embo J **21:**259-69.
142. **Munson, M., X. Chen, A. E. Cocina, S. M. Schultz, and F. M. Hughson.** 2000. Interactions within the yeast t-SNARE Sso1p that control SNARE complex assembly. Nat Struct Biol **7:**894-902.
143. **Munson, M., and F. M. Hughson.** 2002. Conformational regulation of SNARE assembly and disassembly in vivo. J Biol Chem **277:**9375-81.
144. **Nair, D. M., P. E. Purdue, and P. B. Lazarow.** 2004. Pex7p translocates in and out of peroxisomes in Saccharomyces cerevisiae. J Cell Biol **167:**599-604.
145. **Neuberger, G., S. Maurer-Stroh, B. Eisenhaber, A. Hartig, and F. Eisenhaber.** 2003. Motif refinement of the peroxisomal targeting signal 1 and evaluation of taxon-specific differences. J Mol Biol **328:**567-79.
146. **Neupert, W.** 1997. Protein import into mitochondria. Annu Rev Biochem **66:**863-917.
147. **Nicholson, K. L., M. Munson, R. B. Miller, T. J. Filip, R. Fairman, and F. M. Hughson.** 1998. Regulation of SNARE complex assembly by an N-terminal domain of the t-SNARE Sso1p. Nat Struct Biol **5:**793-802.
148. **Nito, K., M. Hayashi, and M. Nishimura.** 2002. Direct interaction and determination of binding domains among peroxisomal import factors in Arabidopsis thaliana. Plant Cell Physiol **43:**355-66.

149. **Novick, P., and R. Schekman.** 1979. Secretion and cell-surface growth are blocked in a temperature-sensitive mutant of Saccharomyces cerevisiae. Proc Natl Acad Sci U S A **76:**1858-62.
150. **Olsen, L. J.** 1998. The surprising complexity of peroxisome biogenesis. Plant Mol Biol **38:**163-89.
151. **Olsen, L. J., W. F. Ettinger, B. Damsz, K. Matsudaira, M. A. Webb, and J. J. Harada.** 1993. Targeting of glyoxysomal proteins to peroxisomes in leaves and roots of a higher plant. Plant Cell **5:**941-52.
152. **Osumi, T., T. Tsukamoto, S. Hata, S. Yokota, S. Miura, Y. Fujiki, M. Hijikata, S. Miyazawa, and T. Hashimoto.** 1991. Amino-terminal presequence of the precursor of peroxisomal 3-ketoacyl-CoA thiolase is a cleavable signal peptide for peroxisomal targeting. Biochem Biophys Res Commun **181:**947-54.
153. **Otera, H., T. Harano, M. Honsho, K. Ghaedi, S. Mukai, A. Tanaka, A. Kawai, N. Shimizu, and Y. Fujiki.** 2000. The mammalian peroxin Pex5pL, the longer isoform of the mobile peroxisome targeting signal (PTS) type 1 transporter, translocates the Pex7p.PTS2 protein complex into peroxisomes via its initial docking site, Pex14p. J Biol Chem **275:**21703-14.
154. **Otera, H., K. Okumoto, K. Tateishi, Y. Ikoma, E. Matsuda, M. Nishimura, T. Tsukamoto, T. Osumi, K. Ohashi, O. Higuchi, and Y. Fujiki.** 1998. Peroxisome targeting signal type 1 (PTS1) receptor is involved in import of both PTS1 and PTS2: studies with PEX5-defective CHO cell mutants. Mol Cell Biol **18:**388-99.
155. **Otera, H., K. Setoguchi, M. Hamasaki, T. Kumashiro, N. Shimizu, and Y. Fujiki.** 2002. Peroxisomal targeting signal receptor Pex5p interacts with cargoes and import machinery components in a spatiotemporally differentiated manner: conserved Pex5p WXXXF/Y motifs are critical for matrix protein import. Mol Cell Biol **22:**1639-55.
156. **Palade, G.** 1975. Intracellular aspects of the process of protein synthesis. Science **189:**347-58.
157. **Parlati, F., O. Varlamov, K. Paz, J. A. McNew, D. Hurtado, T. H. Sollner, and J. E. Rothman.** 2002. Distinct SNARE complexes mediating membrane fusion in Golgi transport based on combinatorial specificity. Proc Natl Acad Sci U S A **99:**5424-9.
158. **Parlati, F., T. Weber, J. A. McNew, B. Westermann, T. H. Sollner, and J. E. Rothman.** 1999. Rapid and efficient fusion of phospholipid vesicles by the alpha-helical core of a SNARE complex in the absence of an N-terminal regulatory domain. Proc Natl Acad Sci U S A **96:**12565-70.
159. **Paumet, F., V. Rahimian, and J. E. Rothman.** 2004. The specificity of SNARE-dependent fusion is encoded in the SNARE motif. Proc Natl Acad Sci U S A **101:**3376-80.
160. **Peng, R., and D. Gallwitz.** 2004. Multiple SNARE interactions of an SM protein: Sed5p/Sly1p binding is dispensable for transport. Embo J **23:**3939-49.

161. **Peng, R., and D. Gallwitz.** 2002. Sly1 protein bound to Golgi syntaxin Sed5p allows assembly and contributes to specificity of SNARE fusion complexes. J Cell Biol **157:**645-55.
162. **Peng, R. W.** 2005. Decoding the interactions of SM proteins with SNAREs. ScientificWorldJournal **5:**471-7.
163. **Petriv, O. I., L. Tang, V. I. Titorenko, and R. A. Rachubinski.** 2004. A new definition for the consensus sequence of the peroxisome targeting signal type 2. J Mol Biol **341:**119-34.
164. **Platta, H. W., F. El Magraoui, D. Schlee, S. Grunau, W. Girzalsky, and R. Erdmann.** 2007. Ubiquitination of the peroxisomal import receptor Pex5p is required for its recycling. J Cell Biol **177:**197-204.
165. **Platta, H. W., W. Girzalsky, and R. Erdmann.** 2004. Ubiquitination of the peroxisomal import receptor Pex5p. Biochem J **384:**37-45.
166. **Purdue, P. E., S. M. Castro, V. Protopopov, and P. B. Lazarow.** 1996. Targeting of human catalase to peroxisomes is dependent upon a novel C-terminal peroxisomal targeting sequence. Ann N Y Acad Sci **804:**775-6.
167. **Purdue, P. E., and P. B. Lazarow.** 2001. Peroxisome biogenesis. Annu Rev Cell Dev Biol **17:**701-52.
168. **Purdue, P. E., X. Yang, and P. B. Lazarow.** 1998. Pex18p and Pex21p, a novel pair of related peroxins essential for peroxisomal targeting by the PTS2 pathway. J Cell Biol **143:**1859-69.
169. **Rachubinski, R. A., and S. Subramani.** 1995. How proteins penetrate peroxisomes. Cell **83:**525-8.
170. **Rehling, P., M. Marzioch, F. Niesen, E. Wittke, M. Veenhuis, and W. H. Kunau.** 1996. The import receptor for the peroxisomal targeting signal 2 (PTS2) in Saccharomyces cerevisiae is encoded by the PAS7 gene. Embo J **15:**2901-13.
171. **Rehling, P., A. Skaletz-Rorowski, W. Girzalsky, T. Voorn-Brouwer, M. M. Franse, B. Distel, M. Veenhuis, W. H. Kunau, and R. Erdmann.** 2000. Pex8p, an intraperoxisomal peroxin of Saccharomyces cerevisiae required for protein transport into peroxisomes binds the PTS1 receptor pex5p. J Biol Chem **275:**3593-602.
172. **Reim, K., M. Mansour, F. Varoqueaux, H. T. McMahon, T. C. Sudhof, N. Brose, and C. Rosenmund.** 2001. Complexins regulate a late step in Ca2+-dependent neurotransmitter release. Cell **104:**71-81.
173. **Reumann, S.** 2004. Specification of the peroxisome targeting signals type 1 and type 2 of plant peroxisomes by bioinformatics analyses. Plant Physiol **135:**783-800.
174. **Reumann, S., and A. P. Weber.** 2006. Plant peroxisomes respire in the light: some gaps of the photorespiratory C2 cycle have become filled--others remain. Biochim Biophys Acta **1763:**1496-510.
175. **Rhodin, J.** 1958. Electron microscopy of the kidney. Am J Med **24:**661-75.
176. **Rice, L. M., and A. T. Brunger.** 1999. Crystal structure of the vesicular transport protein Sec17: implications for SNAP function in SNARE complex disassembly. Mol Cell **4:**85-95.

177. **Richmond, J. E., W. S. Davis, and E. M. Jorgensen.** 1999. UNC-13 is required for synaptic vesicle fusion in C. elegans. Nat Neurosci **2:**959-64.
178. **Rickman, C., and B. Davletov.** 2005. Arachidonic acid allows SNARE complex formation in the presence of Munc18. Chem Biol **12:**545-53.
179. **Rickman, C., C. N. Medine, A. Bergmann, and R. R. Duncan.** 2007. Functionally and spatially distinct modes of munc18-syntaxin 1 interaction. J Biol Chem **282:**12097-103.
180. **Rizo, J., and T. C. Sudhof.** 2002. Snares and Munc18 in synaptic vesicle fusion. Nat Rev Neurosci **3:**641-53.
181. **Rosenmund, C., A. Sigler, I. Augustin, K. Reim, N. Brose, and J. S. Rhee.** 2002. Differential control of vesicle priming and short-term plasticity by Munc13 isoforms. Neuron **33:**411-24.
182. **Rossi, V., D. K. Banfield, M. Vacca, L. E. Dietrich, C. Ungermann, M. D'Esposito, T. Galli, and F. Filippini.** 2004. Longins and their longin domains: regulated SNAREs and multifunctional SNARE regulators. Trends Biochem Sci **29:**682-8.
183. **Rothman, J. E.** 1996. The protein machinery of vesicle budding and fusion. Protein Sci **5:**185-94.
184. **Rothman, J. E., and G. Warren.** 1994. Implications of the SNARE hypothesis for intracellular membrane topology and dynamics. Curr Biol **4:**220-33.
185. **Rottensteiner, H., and F. L. Theodoulou.** 2006. The ins and outs of peroxisomes: co-ordination of membrane transport and peroxisomal metabolism. Biochim Biophys Acta **1763:**1527-40.
186. **Rowe, T., C. Dascher, S. Bannykh, H. Plutner, and W. E. Balch.** 1998. Role of vesicle-associated syntaxin 5 in the assembly of pre-Golgi intermediates. Science **279:**696-700.
187. **Saidowsky, J., G. Dodt, K. Kirchberg, A. Wegner, W. Nastainczyk, W. H. Kunau, and W. Schliebs.** 2001. The di-aromatic pentapeptide repeats of the human peroxisome import receptor PEX5 are separate high affinity binding sites for the peroxisomal membrane protein PEX14. J Biol Chem **276:**34524-9.
188. **Sato, T. K., P. Rehling, M. R. Peterson, and S. D. Emr.** 2000. Class C Vps protein complex regulates vacuolar SNARE pairing and is required for vesicle docking/fusion. Mol Cell **6:**661-71.
189. **Schafer, A., D. Kerssen, M. Veenhuis, W. H. Kunau, and W. Schliebs.** 2004. Functional similarity between the peroxisomal PTS2 receptor binding protein Pex18p and the N-terminal half of the PTS1 receptor Pex5p. Mol Cell Biol **24:**8895-906.
190. **Scharf, K. D., M. Siddique, and E. Vierling.** 2001. The expanding family of Arabidopsis thaliana small heat stress proteins and a new family of proteins containing alpha-crystallin domains (Acd proteins). Cell Stress Chaperones **6:**225-37.
191. **Schekman, R., and L. Orci.** 1996. Coat proteins and vesicle budding. Science **271:**1526-33.

192. **Schliebs, W., and W. H. Kunau.** 2006. PTS2 co-receptors: diverse proteins with common features. Biochim Biophys Acta **1763:**1605-12.
193. **Schliebs, W., J. Saidowsky, B. Agianian, G. Dodt, F. W. Herberg, and W. H. Kunau.** 1999. Recombinant human peroxisomal targeting signal receptor PEX5. Structural basis for interaction of PEX5 with PEX14. J Biol Chem **274:**5666-73.
194. **Scott, B. L., J. S. Van Komen, H. Irshad, S. Liu, K. A. Wilson, and J. A. McNew.** 2004. Sec1p directly stimulates SNARE-mediated membrane fusion in vitro. J Cell Biol **167:**75-85.
195. **Shen, J., D. C. Tareste, F. Paumet, J. E. Rothman, and T. J. Melia.** 2007. Selective activation of cognate SNAREpins by Sec1/Munc18 proteins. Cell **128:**183-95.
196. **Shiozawa, K., N. Maita, K. Tomii, A. Seto, N. Goda, Y. Akiyama, T. Shimizu, M. Shirakawa, and H. Hiroaki.** 2004. Structure of the N-terminal domain of PEX1 AAA-ATPase. Characterization of a putative adaptor-binding domain. J Biol Chem **279:**50060-8.
197. **Smith, J. J., and R. A. Rachubinski.** 2001. A role for the peroxin Pex8p in Pex20p-dependent thiolase import into peroxisomes of the yeast Yarrowia lipolytica. J Biol Chem **276:**1618-25.
198. **Sollner, T., S. W. Whiteheart, M. Brunner, H. Erdjument-Bromage, S. Geromanos, P. Tempst, and J. E. Rothman.** 1993. SNAP receptors implicated in vesicle targeting and fusion. Nature **362:**318-24.
199. **Sommer, J. M., Q. L. Cheng, G. A. Keller, and C. C. Wang.** 1992. In vivo import of firefly luciferase into the glycosomes of Trypanosoma brucei and mutational analysis of the C-terminal targeting signal. Mol Biol Cell **3:**749-59.
200. **Sommer, J. M., G. Peterson, G. A. Keller, M. Parsons, and C. C. Wang.** 1993. The C-terminal tripeptide of glycosomal phosphoglycerate kinase is both necessary and sufficient for import into the glycosomes of Trypanosoma brucei. FEBS Lett **316:**53-8.
201. **Stanley, W. A., and M. Wilmanns.** 2006. Dynamic architecture of the peroxisomal import receptor Pex5p. Biochim Biophys Acta **1763:**1592-8.
202. **Stein, K., A. Schell-Steven, R. Erdmann, and H. Rottensteiner.** 2002. Interactions of Pex7p and Pex18p/Pex21p with the peroxisomal docking machinery: implications for the first steps in PTS2 protein import. Mol Cell Biol **22:**6056-69.
203. **Steinberg, S. J., G. Dodt, G. V. Raymond, N. E. Braverman, A. B. Moser, and H. W. Moser.** 2006. Peroxisome biogenesis disorders. Biochim Biophys Acta **1763:**1733-48.
204. **Subramani, S.** 1998. Components involved in peroxisome import, biogenesis, proliferation, turnover, and movement. Physiol Rev **78:**171-88.
205. **Subramani, S.** 1993. Protein import into peroxisomes and biogenesis of the organelle. Annu Rev Cell Biol **9:**445-78.
206. **Subramani, S.** 1996. Protein translocation into peroxisomes. J Biol Chem **271:**32483-6.

207. **Subramani, S.** 1992. Targeting of proteins into the peroxisomal matrix. J Membr Biol **125:**99-106.
208. **Subramani, S., A. Koller, and W. B. Snyder.** 2000. Import of peroxisomal matrix and membrane proteins. Annu Rev Biochem **69:**399-418.
209. **Sugita, S., W. Han, S. Butz, X. Liu, R. Fernandez-Chacon, Y. Lao, and T. C. Sudhof.** 2001. Synaptotagmin VII as a plasma membrane Ca(2+) sensor in exocytosis. Neuron **30:**459-73.
210. **Sutton, R. B., D. Fasshauer, R. Jahn, and A. T. Brunger.** 1998. Crystal structure of a SNARE complex involved in synaptic exocytosis at 2.4 A resolution. Nature **395:**347-53.
211. **Swinkels, B. W., S. J. Gould, A. G. Bodnar, R. A. Rachubinski, and S. Subramani.** 1991. A novel, cleavable peroxisomal targeting signal at the amino-terminus of the rat 3-ketoacyl-CoA thiolase. Embo J **10:**3255-62.
212. **Titorenko, V. I., and R. A. Rachubinski.** 2004. The peroxisome: orchestrating important developmental decisions from inside the cell. J Cell Biol **164:**641-5.
213. **Titus, D. E., and W. M. Becker.** 1985. Investigation of the glyoxysome-peroxisome transition in germinating cucumber cotyledons using double-label immunoelectron microscopy. J Cell Biol **101:**1288-99.
214. **Tochio, H., M. M. Tsui, D. K. Banfield, and M. Zhang.** 2001. An autoinhibitory mechanism for nonsyntaxin SNARE proteins revealed by the structure of Ykt6p. Science **293:**698-702.
215. **Toonen, R. F., and M. Verhage.** 2003. Vesicle trafficking: pleasure and pain from SM genes. Trends Cell Biol **13:**177-86.
216. **Tsukamoto, T., S. Hata, S. Yokota, S. Miura, Y. Fujiki, M. Hijikata, S. Miyazawa, T. Hashimoto, and T. Osumi.** 1994. Characterization of the signal peptide at the amino terminus of the rat peroxisomal 3-ketoacyl-CoA thiolase precursor. J Biol Chem **269:**6001-10.
217. **van der Klei, I. J., and M. Veenhuis.** 2006. PTS1-independent sorting of peroxisomal matrix proteins by Pex5p. Biochim Biophys Acta **1763:**1794-800.
218. **Van Komen, J. S., X. Bai, B. L. Scott, and J. A. McNew.** 2006. An intramolecular t-SNARE complex functions in vivo without the syntaxin NH2-terminal regulatory domain. J Cell Biol **172:**295-307.
219. **Verhage, M., A. S. Maia, J. J. Plomp, A. B. Brussaard, J. H. Heeroma, H. Vermeer, R. F. Toonen, R. E. Hammer, T. K. van den Berg, M. Missler, H. J. Geuze, and T. C. Sudhof.** 2000. Synaptic assembly of the brain in the absence of neurotransmitter secretion. Science **287:**864-9.
220. **Volokita, M.** 1991. The carboxy-terminal end of glycolate oxidase directs a foreign protein into tobacco leaf peroxisomes. Plant J **1:**361-6.
221. **Walton, P. A.** 1996. Import of stably-folded proteins into peroxisomes. Ann N Y Acad Sci **804:**76-85.
222. **Walton, P. A., S. J. Gould, J. R. Feramisco, and S. Subramani.** 1992. Transport of microinjected proteins into peroxisomes of mammalian cells:

inability of Zellweger cell lines to import proteins with the SKL tripeptide peroxisomal targeting signal. Mol Cell Biol **12:**531-41.
223. **Walton, P. A., P. E. Hill, and S. Subramani.** 1995. Import of stably folded proteins into peroxisomes. Mol Biol Cell **6:**675-83.
224. **Wanders, R. J., and J. M. Tager.** 1998. Lipid metabolism in peroxisomes in relation to human disease. Mol Aspects Med **19:**69-154.
225. **Wanders, R. J., and H. R. Waterham.** 2005. Peroxisomal disorders I: biochemistry and genetics of peroxisome biogenesis disorders. Clin Genet **67:**107-33.
226. **Wanders, R. J., and H. R. Waterham.** 2006. Peroxisomal disorders: the single peroxisomal enzyme deficiencies. Biochim Biophys Acta **1763:**1707-20.
227. **Wang, X., M. A. McMahon, S. N. Shelton, M. Nampaisansuk, J. L. Ballard, and J. M. Goodman.** 2004. Multiple targeting modules on peroxisomal proteins are not redundant: discrete functions of targeting signals within Pmp47 and Pex8p. Mol Biol Cell **15:**1702-10.
228. **Wang, Y., I. Dulubova, J. Rizo, and T. C. Sudhof.** 2001. Functional analysis of conserved structural elements in yeast syntaxin Vam3p. J Biol Chem **276:**28598-605.
229. **Waterham, H. R., V. I. Titorenko, P. Haima, J. M. Cregg, W. Harder, and M. Veenhuis.** 1994. The Hansenula polymorpha PER1 gene is essential for peroxisome biogenesis and encodes a peroxisomal matrix protein with both carboxy- and amino-terminal targeting signals. J Cell Biol **127:**737-49.
230. **Weber, T., B. V. Zemelman, J. A. McNew, B. Westermann, M. Gmachl, F. Parlati, T. H. Sollner, and J. E. Rothman.** 1998. SNAREpins: minimal machinery for membrane fusion. Cell **92:**759-72.
231. **Wendland, M., and S. Subramani.** 1993. Cytosol-dependent peroxisomal protein import in a permeabilized cell system. J Cell Biol **120:**675-85.
232. **Wickner, W., and R. Schekman.** 2005. Protein translocation across biological membranes. Science **310:**1452-6.
233. **Woodward, A. W., and B. Bartel.** 2005. The Arabidopsis peroxisomal targeting signal type 2 receptor PEX7 is necessary for peroxisome function and dependent on PEX5. Mol Biol Cell **16:**573-83.
234. **Xu, D., and J. C. Hay.** 2004. Reconstitution of COPII vesicle fusion to generate a pre-Golgi intermediate compartment. J Cell Biol **167:**997-1003.
235. **Xu, D., A. P. Joglekar, A. L. Williams, and J. C. Hay.** 2000. Subunit structure of a mammalian ER/Golgi SNARE complex. J Biol Chem **275:**39631-9.
236. **Xu, Z., K. Sato, and W. Wickner.** 1998. LMA1 binds to vacuoles at Sec18p (NSF), transfers upon ATP hydrolysis to a t-SNARE (Vam3p) complex, and is released during fusion. Cell **93:**1125-34.
237. **Yamaguchi, T., I. Dulubova, S. W. Min, X. Chen, J. Rizo, and T. C. Sudhof.** 2002. Sly1 binds to Golgi and ER syntaxins via a conserved N-terminal peptide motif. Dev Cell **2:**295-305.

238. **Yang, X., P. E. Purdue, and P. B. Lazarow.** 2001. Eci1p uses a PTS1 to enter peroxisomes: either its own or that of a partner, Dci1p. Eur J Cell Biol **80:**126-38.
239. **Zhang, J. W., X. Cai, and P. B. Lazarow.** 1996. Peb1p (Pas7p) is an intra-peroxisomal receptor for the N-terminal, type 2, peroxisomal targeting signal of thiolase. Ann N Y Acad Sci **804:**654-5.
240. **Zhang, L., S. Leon, and S. Subramani.** 2006. Two independent pathways traffic the intraperoxisomal peroxin PpPex8p into peroxisomes: mechanism and evolutionary implications. Mol Biol Cell **17:**690-9.
241. **Zilly, F. E., J. B. Sorensen, R. Jahn, and T. Lang.** 2006. Munc18-bound syntaxin readily forms SNARE complexes with synaptobrevin in native plasma membranes. PLoS Biol **4:**e330.
242. **Zwilling, D., A. Cypionka, W. H. Pohl, D. Fasshauer, P. J. Walla, M. C. Wahl, and R. Jahn.** 2007. Early endosomal SNAREs form a structurally conserved SNARE complex and fuse liposomes with multiple topologies. EMBO J **26:**9-18.

CHAPTER TWO

ER to Golgi Transport: rsly1/Syntaxin 5 Interactions

ABSTRACT

Although some of the principles of SNAP receptor (SNARE) function are well understood, remarkably little detail is known about sec1/munc18 (SM) protein function and its relationship to SNAREs. Popular models of SM protein function hold that these proteins promote or maintain an open and/or monomeric pool of syntaxin molecules available for SNARE complex formation. To address the functional relationship of the mammalian ER/Golgi SM protein rsly1 and its SNARE binding partner syntaxin 5, we produced a conformation-specific monoclonal antibody that binds only the available, but not the cis-SNARE complexed nor intramolecularly closed form of syntaxin 5. Immunostaining experiments demonstrated that syntaxin 5 SNARE motif availability is non-uniformly distributed and focally regulated. In vitro ER to Golgi transport assays revealed that rsly1 was acutely required for transport, and that binding to syntaxin 5 was absolutely required for its function. Finally, manipulation of rsly1-syntaxin 5 interactions in vivo revealed that they had remarkably little impact on

the pool of available syntaxin 5 SNARE motif. Our results argue that although rsly1 does not appear to regulate the availability of syntaxin 5, its function is intimately associated with syntaxin binding, perhaps promoting a later step in SNARE complex formation or function.

INTRODUCTION

N-ethylmaleimide-sensitive factor attachment protein receptor (SNARE) proteins are widely accepted to be important constituents of the cellular membrane fusion machinery (13, 26, 28). SNARE complexes are composed of stable four-helix bundles of amphipathic helices known as SNARE motifs. When SNAREs in opposing membranes participate in membrane-bridging SNARE complexes, the two membranes are brought into very close proximity, a process which, at least in vitro, is sufficient to initiate bilayer merger and luminal contents mixing (20). Relatively little is known about the regulation of SNARE protein interactions with each other and other membrane trafficking proteins.

SNARE complex formation can be regulated by SNARE amino-terminal domains (NTDs). Of the several types of SNARE NTDs, the Habc domains of the syntaxin family are the best characterized. These domains consist of three-helix bundles that, in the case of exocytic syntaxins, can fold back to pack against the SNARE motif and inhibit its entry into SNARE complexes (7, 8, 18, 19). In support of a conserved autoinhibitory function for Habc domains, the ER/Golgi syntaxin 5 Habc domain potently retards SNARE complex assembly in vitro (29). On the other hand, there is also evidence against a conserved autoinhibitory role for Habc domains. For example, structural studies of several other SNAREs indicated that they did not adopt closed conformations in vitro (6). In addition, the Sso1p Habc domain, although autoinhibitory, is *required* for

SNARE function; constitutively open mutants are tolerated but removal of the domain is lethal (19). Thus, syntaxin Habc domains may have multiple roles.

Another potential regulator of SNARE complex formation is the sec1/munc18 (SM) protein family. These peripheral membrane proteins are universally required for all physiological membrane fusion steps, and, like SNAREs, comprise a multi-gene family with transport step-specific members (10, 27). The most salient feature of SM proteins is their specific interaction with syntaxins. One general hypothesis of SM protein function is that these proteins represent conformational regulators of syntaxins. Initially, the predominant model was as negative regulators that bind to the closed SNARE, reinforcing the autoinhibitory role of the Habc domains (23). This may be part of the role of N-sec1 in synaptic transmission, however, in most systems, SM proteins seem to play predominantly required, *positive* roles, rather than inhibitory ones (10, 27). This has led to the suggestion that SM proteins may somehow facilitate SNARE complex formation. In support of a SNARE complex-promoting role, depletion of Vps45p or Vps33p causes a reduced level of the endosomal and vacuolar SNARE complexes, respectively (3, 24). In addition, recombinant Sly1p promoted immunoprecipitation of ER/Golgi SNARE complexes in vitro (16). How might SM proteins favor SNARE complex assembly? A leading conjecture has been that SM proteins may promote SNARE complex formation by favoring the open, or otherwise trans-interaction-available, conformation of syntaxins (27). In support of this, the structure of the syntaxin 1A/N-sec1 binary complex indicates that N-sec1may put strain on the closed conformation of the SNARE, perhaps

exposing a SNAP-25 binding site and/or favoring the transition to an open conformation (17). Furthermore, in Golgi-to-endosome transport in yeast, the SM protein Vps45p was required for formation of the Tlg2p-containing SNARE complex, however, this requirement could be bipassed by removal of the Tlg2p Habc domain (3). This data supports a model where Vps45p either directly favors the open conformation, or otherwise maintains Tlg2p in a SNARE-receptive state.

The possibility that SM proteins possess a general, conserved role in SNARE complex formation is, however, cast into doubt by recent demonstrations of diverse modes of interaction between SM proteins and syntaxins. In the neuronal system, N-sec1 binds only the closed syntaxin (31). In contrast, yeast exocytic Sec1p is found only in a complex with the fully assembled SNARE complex (4). Yeast vacuolar Vps33p on the other hand, associates with its syntaxin, Vam3p, indirectly through several other proteins (24). And to deepen the complexity, the intracellular SM proteins Sly1p/rsly1 and Vps45p bind to their syntaxins, Sed5p/syntaxin 5 and Tlg2p, respectively, via a short N-terminal peptide (1, 5, 30). The diversity in binding mechanisms could indicate diverse functions for SM proteins at different transport steps. It could also suggest that the interactions with SNAREs are relevant to SM protein function only in that they concentrate the SM protein to the site of membrane fusion, where they perform a function unrelated to SNAREs, perhaps in controlling fusion pore dynamics (9). In fact, there is still no convincing evidence that syntaxin binding, per se, is even critical to the essential function of SM proteins in membrane fusion. A promising

beginning was the demonstration that the blocking of rsly1 binding to syntaxin 5 caused a morphological disruption of Golgi structure in vero cells (30).

On the other hand, the diversity in binding mechanisms could also be reconciled with a conserved role in SNARE complex formation if one postulated that the various types of interactions represent different stages in a *series* of distinct interactions that SM proteins undergo with syntaxins. Intriguingly, Vps45p appeared to be recruited to the cis-SNARE complex containing Tlg2p, remain bound through Sec18p-dependent SNARE dissociation, and then dissociate from Tlg2p during a late stage of trans-SNARE complex formation or fusion (2). Likewise, Sly1p pre-bound to Sed5p remained bound during SNARE complex formation in vitro (22). These reports are consistent with a given SM protein binding to its syntaxin in multiple conformation states, perhaps employing multiple interaction surfaces.

Production of a conformation-specific monoclonal antibody against the syntaxin 5 SNARE motif allowed us to monitor the availability of the SNARE motif and examine its relationship to the SM protein rsly1. We found that available syntaxin 5 is focally regulated relative to total syntaxin 5, indicating that precise spatial control of SNARE motif availability is a bona fide feature of cells. Endogenous rsly1 largely colocalized with syntaxin 5 and required its association with syntaxin 5 to maintain this distribution. However, the amount of available syntaxin 5 did not influence the distribution of rsly1, suggesting that rsly1 is bound to both available and unavailable syntaxin 5 in cells. rsly1 was acutely required for transport between the ER and Golgi in permeabilized cells.

Furthermore, rsly1 binding to the syntaxin 5 N-terminus was absolutely required for its direct role in transport. Finally, we tested the hypothesis that rsly1 binding to syntaxin 5 promotes or maintains the available syntaxin 5 pool in intact cells, by competing off rsly1 and monitoring the conformation of syntaxin 5. Interestingly, we observed remarkably little change in the availability of syntaxin 5, even when interactions with rsly1 were largely removed. Hence, our data are inconsistent with opener models of rsly1 function and suggest an essential function at a later stage in the SNARE cycle.

MATERIALS AND METHODS

DNA constructs. Bacterial constructs encoding GST-syntaxin 5 (55-333), GST-syntaxin 5 (251-333), GST-rbet1 cytoplasmic domain, GST-membrin full-length and His_6-sec22b cytoplasmic domain were described previously (29). DNA inserts for new bacterial constructs, including GST-rsly1 full-length (amino acids 1-648), GST-Habc (including the first 195 residues of the 34 kD isoform), and GST-syntaxin 5 (1-43) were amplified by PCR and subcloned into vector pGEX-KG (11) with an amino-terminal GST. Myc-tagged mammalian expression constructs, myc-Habc (including the first 195 residues of the 34 kD isoform), myc-rsly1 (amino acids 1-648) were prepared by PCR and subcloning into pCMV-tag3 (Stratagene; La Jolla, CA) with an amino-terminal myc tag, while syntaxin 5 (1-43)-GFP was amplified by PCR and subcloned into pEGFP (Clontech; Palo Alto, CA) giving it a carboxy-terminal GFP. All DNA constructs were confirmed by DNA sequencing.

Antibody production and functional evaluation. GST-syntaxin 5 residues 251-333 was produced and purified by glutathione-Sepharose chromatography as described previously (29). Following cleavage with thrombin, the liberated 9.5 kD SNARE motif (residues 251-333) was purified further by preparative SDS-PAGE and electroelution. After extensive dialysis against 50 mM NH_4CO_3, the protein solution was completely dried in a Speed Vac and resuspended in PBS. Mice were injected intraperitoneally with 200 μl of Ribi adjuvant (Corixa;

Hamilton, MT) containing 30 μg of SNARE motif. Mice were injected a total of six times over a period of seven months, after which a strong anti-syntaxin 5 antibody response was detected in immunoblots of liver membranes. Mice were then maintained for seven months without injections to allow antibody titers to go down. Antigen for final intravenous boosts was purified free of SDS using reversed phase chromatography instead of preparative PAGE. Briefly, glutathione-Sepharose-purified, thrombin-cleaved GST-syntaxin 5 (251-333) was mixed 1:1 with water containing 0.05% trifluoroacetic acid (TFA) and loaded on a 3 ml Resource RPC column (Pharmacia; Piscataway, NJ) equilibrated in water/0.05% TFA. The column was eluted with increasing acetonitrile containing 0.065% TFA. Fractions containing SNARE motif that were free of GST and other contaminants were dried, resuspended in PBS, and 200 μl containing ~40 μg of homogeneous SNARE motif was injected intravenously into an immune mouse. Later that day, the mouse was injected with another ~40 μg of SNARE motif intraperitoneally with Ribi adjuvant as described above. After three days, the mouse was sacrificed, the spleen removed and dissociated and hybridomas were produced using standard methods (12). Only clones that were strongly positive for ELISA and decorated syntaxin 5 bands in immunoblots of crude membranes were subcloned and re-screened..

Monoclonal antibodies were purified from tissue culture supernatants using protein A- and protein G-Sepharose (Pharmacia; Piscataway, NJ), and tested for efficiency of immunoprecipitation of dilute, purified syntaxin 5 SNARE motif (not shown). All of the antibodies positive for immunoprecipitation were

tested for ability to disrupt ternary SNARE complex formation (18C8 and 9D8 are shown in Figure 2). These binding assays employed purified recombinant glutathione-Sepharose-immobilized GST-membrin, soluble syntaxin5 and rbet1, prepared and assembled as described in a previous publication (29). Under these conditions, syntaxin5 binds only in the presence of soluble rbet1 (29). After the binding incubation and buffer washes, bead pellets were analyzed for bound syntaxin5 by immunoblotting. Purified syntaxin5 SNARE motif was incubated with soluble membrin, sec22b and rbet1, and a quaternary complex containing these four proteins was isolated by gel filtration as described in Xu et al. The high molecular weight gel-filtered complex, or the original, cleaved syntaxin5 preparation in the absence of other SNAREs, was employed in immunoprecipitations using protein A-purified 18C8. Syntaxin5 in the immunoprecipitated pellets was detected by immunoblotting.

Bead binding studies to examine syntaxin5 intramolecular interactions (Figure 3) were conducted using a GST-Habc construct encoding the first 195 amino acids of the short syntaxin5 isoform (or amino acids 55-251 of the long isoform) in conjunction with purified syntaxin5 SNARE motif. Binding reactions were conducted in 400 μl of Buffer A (20 mM Hepes, pH 7.2, 0.15 M KCl, 2 mM EDTA, 5% glycerol) containing 0.1 % Triton X-100, 2 mg/ml BSA, 10 μl (packed volume) of glutathione-Sepharose beads pre-loaded with ~200 pmoles of GST or GST-Habc, and varying amounts of syntaxin5 (252-333) and protein A/G-purified monoclonal antibodies. After binding at 4 °C for 30 minutes, beads were washed

three times with Buffer A containing 0.1% Triton X-100, and the bound syntaxin5 (252-333) was determined by immunoblotting.

To produce polyclonal anti-rsly1 antibodies, full-length GST-rsly1 was expressed in bacteria, purified by glutathione-Sepharose and preparative SDS PAGE, and employed to immunize a rabbit subcutaneously in Freund's adjuvant. Anti-rsly1 antibodies were later affinity purified from immune rabbit serum on a column of GST-rsly1 conjugated to cyanogen bromide-activated Sepharose, following pre-depletion on a similar column of GST.

Antibody Fab fragments were produced by papain cleavage of the intact, purified IgG in the presence of cysteine as described (12). Our conditions resulted in complete elimination of intact IgG, as monitored by non-reducing SDS-PAGE with Coomassie staining and by an immunoprecipitation assay (not shown). We did not attempt to isolate the Fab fragments free of Fc fragments.

Cell culture and transfections. NRK cells were maintained in DMEM containing 4.5 g/L glucose, 10% fetal calf serum, 100 units/ml penicillin and 100 μg/ml streptomycin in a 5% CO_2 incubator at 37 °C. For NRK cell transfections, plasmid DNA was freed of excess salts and exchanged into PBS using Microcon YM-100 centrifugal concentrators. Trypsinized, suspended NRK cells were washed twice with ice-cold PBS and resuspended at a concentration of 3×10^7 cells/ml; 0.2 ml of cells was mixed with 15 μg of plasmid DNA and incubated on ice 10 min in a pre-chilled 4 mm gap electroporation cuvette. The cells were pulsed three times for 4 ms at 1 sec intervals and 250 V using a BTX ECM 830

square-wave electroporator. Cells were then diluted with cold medium containing 20% serum, plated on polylysine-treated coverslips in three wells of a six-well plate, and returned to 37 °C for 24 hours prior to immunofluorescence microscopy. In some experiments, NRK cells were washed twice with warm DMEM lacking serum, covered with the same medium containing 50 μM NEM, and placed in the incubator for 5 minutes prior to processing for immunofluorescence.

Immunofluorescence microscopy. For normal immunofluorescence on fixed, intact cells, the cells were fixed for 30 minutes at room temperature with 4% paraformaldehyde in 0.1 M sodium phosphate, pH 7.0, then quenched twice for 10 min with 0.1 M glycine in PBS. Cell permeabilization was then carried out for 15 minutes at room temperature using Permeabilization Solution (0.4% saponin, 1% BSA, 2% normal goat serum in PBS), followed by incubation in primary antibody in Permeabilization Solution for 1 hour. After three washes with Permeabilization Solution, cells were incubated with secondary antibody in the same buffer for 30 minutes. Secondary antibodies were usually FITC- and Texas Red-conjugated and purchased from Jackson Immunoresearch (West Grove, PA, USA). For triple-label experiments, we used intrinsic GFP fluorescence, anti-mouse cy3 and anti-rabbit cy5 secondary antibodies (Jackson). After the secondary antibody incubation, coverslips were washed with Permeabilization Solution three further times and mounted using Vectashield mounting medium (Vector Laboratories, Burlingame, CA, USA) and sealed with nail polish. Slides

were analyzed using a Nikon E800 microscope employing a 60X CFI Plan Apo objective. Optics included standard FITC, Texas Red and cy5 excitation/emission filter sets that allowed negligible cross-talk. Images were collected using a Hamamatsu ORCA 2 digital camera and Improvision Openlab 2 software. For deconvolution, we used separate excitation and emission filter wheels equipped with GFP and dsRed-optimized filters, and captured images every 0.2 μm from the top to bottom of the cells (about 30 z-sections). We then deconvolved the stack of images using the Openlab 3D Restoration algorithm. We present single optical sections of deconvolved image stacks.

For staining of cells with selectively permeabilized plasma membranes (Figure 9A), NRK cells grown on round poly-lysine-treated coverslips in 24-well dishes were either NEM treated (see cell culture section) or not, then chilled on ice and rinsed several times with ice-cold 50 mM Hepes, pH 7.2, 90 mM potassium acetate, 2 mM magnesium acetate, followed by incubation for five minutes on ice in the same buffer containing 50 μg/ml digitonin. The digitonin was removed and replaced with the same buffer lacking digitonin (control) or lacking digitonin and containing purified NSF, α-SNAP, and the ATP-regenerating system for ER-to-Golgi transport incubations (see below) and incubated a further 30 minutes on ice. After the 30 minutes with or without NSF/α-SNAP, cells were fixed on ice for 30 minutes with 4% paraformaldehyde in 0.1 M sodium phosphate, pH 7.0, then quenched twice for 10 minutes each at room temperature with 0.1 M glycine in PBS. Blocking was accomplished with 1% BSA and 2% normal goat serum in PBS for 15 minutes at room temperature,

followed by primary antibody in the same solution for one hour. After washing with PBS, secondary antibody incubations were carried out in blocking solution for 30 minutes at room temperature. Following washing with PBS, coverslips were mounted and analyzed as above.

Quantitation of 18C8 staining. Openlab images were converted to 8-bit TIFF files and quantified using NIH Image 1.63 software. The intense Golgi region 18C8 staining in each cell was selected, and the mean pixel intensity for the selection was determined for 18C8 staining, after background subtraction (where background was the mean pixel intensity of a region lacking cells in the same image). This number was divided by the background-subtracted mean pixel intensity of the precisely corresponding pixels in the syntaxin5- or rsly1-counterstained paired image. The log of this staining ratio was calculated for each cell in each experimental group, the mean of these values and standard errors were calculated for each experimental group, and then these values were converted back into staining ratios for presentation purposes. Each of the bars in Figure 9A represents the mean staining ratios for 4 representative fields of cells (containing an average of 30 cells per field) where every cell was quantified. In Figure 9B, each pair of bars represents 4-5 fields of cells, where all cells in each field were distinguished as being transfected or untransfected by inspection of the GFP image, and then the staining ratio for each cell and the mean value for each of the four conditions was determined. The number of cells (N) counted for each of the four bars was 29, 16, 54 and 34, respectively. T-testing determined

that the logs of the staining ratios for transfected versus untransfected cells was significantly different for both 18C8:rsly1 ($p = 2.25 \times 10^{-14}$) and 18C8:syntaxin5 ($p = 0.0046$).

Partial purification of rsly1 from rat liver. A freshly dissected rat liver (~15 g) was homogenized in a Potter-Elvejem device in Homo Buffer (20 mM Hepes, pH 7.0, 0.25 M sucrose, 2 mM EGTA, 2 mM EDTA) supplemented with 1 mM DTT, 2 μg /ml leupeptin , 4 μg/ml aprotinin, 1 μg/ml pepstatin A, 1mM phenylmethylsulfonyl fluoride, and centrifuged for 15 minutes at 1000 x g to obtain a postnuclear supernatant (PNS). PNS fractions were then centrifuged at 100,000 x g for 40 minutes to separate membranes from the cytosol. Membranes were re-homogenized in 20 mM Hepes, pH 7.2, 1 M KCl and 2 mM EDTA plus protease inhibitors and DTT, and agitated at 3 °C for 90 minutes prior to a second 100,000 x g centrifugation. The supernatant of this centrifugation appeared to contain a majority of the total liver rsly1, when compared to the cytosol and stripped membrane fractions by immunoblotting (not shown). The high-salt fraction was then desalted on Sephadex G-25 (Pharmacia; Piscataway, NJ), and loaded onto a 30 ml Q-Sepharose (Pharmacia; Piscataway, NJ) column equilibrated in 20 mM Tris, pH 7.6, 2 mM EGTA. After gradient elution to 1 M KCl in the same buffer, immunoblotting revealed that rsly1 had completely bound to the column and eluted in a sharp peak at about 0.28 M KCl. These fractions were pooled, concentrated to 2 ml using a YM-10 membrane in a stirred cell concentrator (Millipore, Bedford, MA) and gel-filtered on a 100 ml Superose 12

column (Pharmacia; Piscataway, NJ) equilibrated in 25/125 Buffer (25 mM Hepes, pH 7.2, 125 mM potassium acetate). Immunoblotting revealed that rsly1 eluted sharply at approximately its expected monomer size. These fractions were concentrated in a Centricon 10 (Millipore) centrifugal concentrator and stored at –80 °C until use in transport experiments.

ER-to-Golgi transport assay. Transport experiments were based closely upon the original published protocol (25), with modifications. A 10 cm plate of NRK cells were infected with vesicular stomatitus virus strain ts045 at 32 °C for 45 minutes, followed by a post-infection incubation at the same temperature for four hours. Cells were then transferred to a 40 °C water bath, washed with cysteine/methionine-free RPMI medium lacking serum and starved for five minutes in the same medium. The medium was replaced with 1.5 ml of the same medium containing 100 μCi of ^{35}S-cysteine and-methionine (ICN Trans-Label; Irvine, CA) and incubated 10 minutes at 40 °C. The medium was then supplemented with 5 mM each of unlabeled cysteine and methionine for an additional 2 minutes at 40 °C prior to transfer to ice. The labeled cells were then washed several times with ice-cold 50/90 Buffer (50 mM Hepes, pH 7.2, 90 mM potassium acetate), and gently scraped from the plate in 3 ml of the same buffer using a rubber policeman. Scrape-permeabilized cells were washed and resuspended in ~200 μl of 50/90 Buffer. An ATP-regenerating system was prepared by mixing 100 μl of 0.2 M creatine phosphate in water with 8 μl of 0.5 M sodium ATP (neutralized, in water), 20 μl of 1000 U/ml creatine phosphokinase in

25/125 Buffer, and 72 μl water. Transport incubations contained a total of 40 μl made up from the following additions: 2.4 μl water, 1 μl 0.1 M magnesium acetate in water, 2 μl of ATP regenerating system (see above), 0.6 μl 1 M Hepes in water, pH 7.2, 4 μl of a solution of 50 mM EGTA, 18 mM $CaCl_2$ and 20 mM Hepes, pH 7.2, 10 μl of dialyzed or G-25-desalted rat liver cytosol prepared without protease inhibitors or DTT in 25/125 Buffer, 2 μl of 25 mM UDP-N-acetylglucosamine in water, 2 μl of 25 mM UTP in water, 11 μl of 25/125 Buffer or antibodies/peptides dissolved in this buffer, and 5 μl of permeabilized cells in 50/90 Buffer. For experiments to examine the effects of antibodies in transport, the assembled reactions including antibodies were incubated on ice for 30 minutes prior to transport, which takes place during a 90-minute incubation at 32 °C. For experiments where cells are pre-incubated with antibodies prior to removal of unbound antibodies (Figure 11C), the preincubation was assembled on ice identically to a transport reaction containing antibody, however, after 30 minutes on ice the cells were gently pelleted and washed twice with 50/90 Buffer containing 1 mg/ml BSA. After the third centrifugation, the cell pellets were resuspended in full transport cocktail with or without additions and then incubated 90 minutes at 32 °C for transport. Following 90-minute transport incubations, cells were centrifuged at 15,000 x g for one minute, the supernatant discarded, and the pellet dissolved in 20 μl 0.1 M sodium acetate, pH 5.6, containing 0.3% SDS, boiled 5 minutes, then diluted to 0.1% SDS with 0.1 M sodium acetate, pH 5.6. A 30 μl portion of each sample was then supplemented with 2.5 mU endoglycosidase H (Roche; Indianapolis, CA), incubated overnight at 37 °C, and

analyzed by 10% SDS PAGE, gel drying and phosphorimaging and/or autoradiography.

Other reagents. Recombinant rsly1 used in the experiments of Figure 11 was expressed as a GST-rsly1 fusion protein (see constructs section), purified by glutathione-Sepharose, and then cleaved with thrombin to liberate rsly1 from the GST tag. This preparation was then dialyzed into 25/125 Buffer and stored at -80 °C until use in transport experiments. No attempt was made to eliminate contaminating GST. HPLC-purified synthetic peptides with the sequences MSCRDRTQEFLSACKSLQSRQNGIQTNK and MSCRDRAQEALSACKSLQSRQNGIQTNK were purchased from Genemed Synthesis (S. San Francisco, CA). Purified, recombinant, active NSF and α-SNAP were a kind gift from Dr. Phyllis Hanson (Washington University, St. Louis, MO). Anti-GM130 polyclonal antisera was a kind gift of Dr. Martin Lowe (University of Manchester, Great Britain).

RESULTS

A monoclonal antibody to the syntaxin5 SNARE motif that binds mutually exclusively with other SNAREs and the Habc domain. Seeking a reagent that could report the status of the SNARE motif in vivo or in vitro, we immunized mice with purified bacterially expressed syntaxin5 SNARE motif, residues 251-333. We then produced hybridomas, which were culled by screening sequentially by ELISA, Western blot and immunoprecipitation to yield 17 high-affinity antibody-producing hybridomas. Figure 1 shows Western blots of crude rat brain membranes using several of the purified monoclonal antibodies. Diversity in the epitopes recognized is apparent since the antibodies differentially recognized a syntaxin5 degradation product of ~32 kD. Monoclonal antibodies were then functionally tested for their ability to block formation of a ternary SNARE complex assembled from immobilized GST-membrin and soluble syntaxin5 and rbet1 (29). Formation of this ternary complex, which likely represents the t-SNARE for ER-to-Golgi transport (15), is indicated by the rbet1-potentiated binding of syntaxin5 to GST-membrin-coated glutathione beads (29). Only one antibody, 18C8, significantly inhibited ternary complex assembly. Inhibition of SNARE complex formation by 18C8, but not by an equal concentration of 9D8, is demonstrated in Figure 2A. Thus, it appeared that 18C8 binding to the SNARE motif prevented the SNARE motif from engaging other SNAREs. We wondered whether the converse was also true, i.e., would the assembly of syntaxin5 with SNAREs prevent 18C8 binding to its epitope? As shown in Figure 2C and quantified in

Figure 2B, isolated syntaxin5 SNARE motif was very efficiently precipitated by 18C8, however, the same protein, when assembled into an ER/Golgi quaternary complex containing syntaxin5, membrin, sec22b and rbet1, was not efficiently precipitated, even when present at a much higher concentration. Thus, it appears that 18C8 binds to the syntaxin5 SNARE motif mutually exclusively with other SNAREs.

Our previous work demonstrated that removal of the syntaxin5 Habc domain resulted in vastly greater SNARE complex formation in vitro (29). This is consistent with the Habc domain playing an autoinhibitory role *in vivo*, a feature which has been well-documented for exocytic yeast syntaxins (19). We wondered whether the inhibitory effect of the syntaxin5 Habc domain could be due to formation of a closed conformation, and if so, whether 18C8 binding would be mutually exclusive with the closed conformation. We performed a protein binding experiment employing a GST fusion of the syntaxin5 Habc domain immobilized on glutathione beads and free syntaxin5 SNARE motif in solution. As shown in Figure 3B and quantified in Figure 3A, there was indeed a strong and specific interaction between the GST-Habc construct and the SNARE motif, with significant binding above control. The intramolecular interaction represented by this binding event would presumably be much more efficient and likely explains the previously observed inhibitory effect of Habc on SNARE complex formation (29). As shown in Figure 3E and quantified in Figure 3D, 18C8, but not 10A1, potently inhibited this interaction. This establishes that the 18C8 epitope is required for Habc binding to the SNARE motif, making it also very likely that a

tightly closed Habc domain would preclude 18C8 binding, just as it inhibits SNARE complex formation. In summary, Figures 2 and 3 demonstrate that 18C8 has binding properties that make it a very good candidate for a probe to report the status of the syntaxin5 SNARE motif in vitro or in vivo.

18C8 immunostains only the available syntaxin5 in NRK cells. 18C8 immunostaining in fixed NRK cells resembled that of a polyclonal anti-syntaxin5 antibody (Figure 4A vs. B). This particular polyclonal antibody has been employed to isolate multiple overlapping protein complexes containing syntaxin5, rsly1, GOS-28, membrin, sec22b, and rbet1 (14). This antiserum also efficiently immunoprecipitates the isolated syntaxin5 molecule in vitro and completely inhibits ER-to-Golgi transport in permeabilized NRK cells (not shown). Thus, it seems very likely that this antibody recognizes multiple conformations of syntaxin5. On the other hand, based upon Figures 2 and 3, we predicted that 18C8 would only stain the pool of syntaxin5 molecules with available, unengaged, SNARE motifs. To test this prediction, we inhibited N-ethylmaleimide-sensitive factor (NSF) in living cells at 37 °C using N-ethylmaleimide (NEM). As evident in Figure 4C vs. D, NEM treatment completely abrogates 18C8 staining without altering anti-syntaxin5 staining intensity. The loss of 18C8 staining was not due to destruction of the 18C8 epitope, since 18C8 recognized syntaxin5 in Western blots of control as well as NEM-treated cells (Figure 4G). In addition, the effect on 18C8 staining did not appear to result from any direct action of NEM on the cells or preparation, since treatment of cells with

NEM at low temperatures that prohibit vesicle transport, followed by washout of NEM in the cold, did not effect the staining, however, subsequent warming of the cells after NEM washout led to a loss of 18C8 staining within 5 minutes (Figure 4E and F). The results demonstrate that 18C8 staining disappears as a downstream metabolic consequence of NEM treatment and likely results from inaccessibility of the SNARE motif as SNARE complexes accumulate. A complimentary result was that addition of purified NSF, α-SNAP, and MgATP to permeabilized cells increased 18C8 staining intensity (see below, Figure 9A). Thus, 18C8 is a useful probe of SNARE motif accessibility in intact cells.

Syntaxin 5 availability is spatially regulated in cells. Although 18C8 epifluorescent staining was very similar overall to polyclonal anti-syntaxin 5 staining, we noticed differences in staining emphasis within the Golgi area. This prompted us to examine their precise spatial co-distribution by deconvolution microscopy. In the single optical sections shown in Figure5, 18C8 was often brightest in small focal areas containing relatively little anti-syntaxin 5 staining (arrows). Most areas contained both types of staining, but there were also regions that contained intense anti-syntaxin 5 staining and little 18C8 (arrowheads). The overall pattern on merged images suggests that syntaxin 5 distributed throughout the Golgi area is regularly punctuated by focal regions containing little total but primarily available syntaxin 5. This result is quite different from what would be expected if a constant fraction of syntaxin 5 were available wherever syntaxin 5 were present, and strongly suggests that

mechanisms exist to actively promote and/or discourage the availability of syntaxin 5 in a spatially defined manner. We do not know what factor(s) determine 18C8 staining hotspots, but speculate that these may represent receptive sites for VTC fusion with the Golgi or with other VTCs. These results further validate 18C8 as a probe of syntaxin 5 availability because they demonstrate that the variance in availability of syntaxin 5 at steady state is well within the capacity of 18C8 to report.

Persistent rsly1 localization to the Golgi area requires syntaxin 5 binding but is not influenced by syntaxin 5 availability. We produced a polyclonal antibody to rsly1. As shown in Figure 6A, the epifluorescence staining pattern for anti-rsly1 includes some presumably diffuse cytosolic staining as well as intense membrane staining in the Golgi area. The staining pattern is specific as it was blocked by recombinant rsly1 (Figure 6B). We wondered whether the immunostained rsly1 was bound to syntaxin 5 in the Golgi and if so, which pool of syntaxin 5, available or sequestered, it was bound to. Since NEM treatment was shown to shift all of the 18C8-available syntaxin 5 SNARE-motif into a sequestered state (Figure 4), we treated NRK cells with NEM under identical conditions and tested whether the rsly1 staining intensity or distribution changed. If rsly1 were bound primarily to the open syntaxin 5 but not when in a cis-SNARE complex, then rsly1 staining would be expected to dramatically decrease as with 18C8. If it were bound primarily to the SNARE complex, as is the case with Sec1p (4), then we would expect the increased number of rsly1 binding sites

upon NEM treatment to recruit soluble rsly1 to the membrane and intensify the Golgi staining. As shown in Figure 6C & D, there was no noticeable change in rsly1 staining upon an NEM treatment shown to cause massive sequestration of the SNARE motif. This indicates that either rsly1 localization was independent of syntaxin 5 binding altogether, or was dependent upon syntaxin 5 but not influenced by the oligomeric state of syntaxin 5. The results are consistent with the persistence of VPS45p-Tlg2p interactions in sec18 yeast strains at the restrictive temperature (2).

To address whether binding to syntaxin 5 was in fact important for rsly1 retention in the Golgi area, we transfected cells with the first 105 residues of the 34 kD syntaxin 5 isoform containing an N-terminal myc epitope (myc-Habc). Since this construct included the binding site for rsly1, it should compete with endogenous membrane-bound syntaxin 5 for rsly1 binding. We found that cells expressing myc-Habc had dramatically reduced rsly1 staining in the Golgi area (not shown). In general there appeared to be a decrease in total cellular anti-rsly1 staining intensity. rsly1 binds to an N-terminal sequence of syntaxin 5 (30) whose disposition could change during syntaxin 5 opening, closing, or complex formation. We next expressed a construct containing GFP fused to the first 43 amino acids of the syntaxin 5 N-terminus (syn 5 (1-43)-GFP), including the necessary and sufficient rsly1 binding site. A very similar construct was previously employed to examine morphological consequences of rsly1-syntaxin 5 interactions in vero cells (30). As shown in triple-label images in Figure 7A and C, cells expressing syn 5 (1-43)-GFP (arrows) displayed dramatically less rsly1

Golgi area staining than nontransfected cells (arrowheads), similar to that described above for myc-Habc transfectants. In contrast to results published in vero cells (30), we found mostly minor consequences on Golgi morphology as indicated by GM130 staining (Figure 7G and I), even in highly expressing cells. Note that we cannot say for sure whether rsly1 in transfected cells was merely redistributed, presumably to a less-concentrated cytosolic pool, or whether the protein was destabilized and degraded when its syntaxin 5 binding function was blocked. We did not observe an effect of the proteasome inhibitors MG-132 and lactacystin on the change in rsly1 staining (not shown). Whether due to mistargeting or to degradation, the effects of myc-Habc and syn 5 (1-43)-GFP expression on rsly1 staining indicate that syntaxin 5 interactions are required for the Golgi retention of rsly1. Taken together with the NEM results of Figure 6 and previous immunoprecipitations (14), our results favor the hypothesis that rsly1 in the Golgi is bound to syntaxin 5 whether available or sequestered in cis-SNARE complexes.

Inhibition of rsly1-syntaxin 5 interactions results in a modest increase in syntaxin 5 availability. We noticed that Golgi 18C8 staining was present, albeit often at reduced levels, in cells expressing syn 5 (1-43)-GFP, even when rsly1 staining almost entirely disappeared (Figure 7A-F). This is made clear in the merge of 18C8 and rsly1 staining in Figure 7F, where transfected cells have green Golgi staining but untransfected cells have yellow Golgis. This seemed to indicate that some available syntaxin 5 persisted in the absence of rsly1 binding,

however, did not distinguish whether the reduction in 18C8 staining was due to a reduction in SNARE motif availability versus a decrease in the total amount of syntaxin 5 in those cells. Several syntaxins have been demonstrated to be unstable in the absence of their SM binding partner (27). We therefore performed triple label experiments to examine the relationship between syn 5 (1-43)-GFP expression, 18C8 staining, and total syntaxin 5 staining using the polyclonal syntaxin 5 antisera described above. As evident in Figure 8A-E, transfected cells (arrows) generally, but not always, displayed less 18C8 and anti-syntaxin 5 staining than untransfected cells (arrowheads), consistent with a moderate destabilization of syntaxin 5 in the absence of rsly1 binding. Although the destabilization of Tlg2p in the absence of Vps45p could be reversed by proteasome inactivation (3), we were unable to affect the loss of syntaxin 5 staining in transfected cells with MG-132 and lactacystin (not shown). Despite the trend toward lower total syntaxin 5 staining in transfected cells, there was sufficient high quality staining to compare the relative 18C8 and anti-syntaxin 5 staining in transfected versus untransfected cells. Figure 8A-E demonstrates that the relationship between 18C8 staining intensity and anti-syntaxin 5 intensity is qualitatively equivalent in untransfected cells (arrowheads), low to moderately expressing cells (short arrows), and high expressing cells (long arrows). This seemed to indicate that the loss of rsly1-syntaxin 5 interactions did not significantly alter the relative pool of available syntaxin 5 SNARE motif. Note that rsly1 readily and efficiently co-immunoprecipitates with syntaxin 5 using 18C8, indicating that rsly1 and 18C8 do not bind syntaxin 5 mutually exclusively (A.

Joglekar and J. Hay, unpublished observations). This eliminates the possibility that removal of rsly1 from syntaxin 5 would have any direct effect on 18C8 staining intensity per se.

To validate the above impressions quantitatively, we used a ratiometric 18C8 staining intensity relative to colocalizing markers. To calculate the relative 18C8 staining intensity, the bright area of 18C8 Golgi staining was quantified for each cell in a field, along with the precisely corresponding area in the same cells co-stained for either rsly1 or anti-syntaxin 5. For each Golgi, the relative 18C8 staining intensity was calculated and averaged over many cells (see Materials and Methods for details). To test whether this method was sensitive enough to detect changes in syntaxin 5 conformation, we performed an experiment using NRK cells whose plasma membranes had been selectively permeabilized with digitonin. As shown in Figure 9A (open bars), the 18C8:rsly1 staining ratio in control NRK cells had a value of ~1:1.55 and the 18C8:syntaxin 5 staining ratio had a value of ~1:1.15. Note that these baseline values arbitrarily vary between experiments depending upon day-to-day variations in staining intensity and camera exposure times. Within each staining series, however, ratios should be quantitatively comparable. When the permeabilized cells were incubated on ice with purified, recombinant NSF, α-SNAP, and MgATP prior to fixation and staining, a significant increase above control for both 18C8:rsly1 and 18C8:syntaxin 5 staining ratios was detected (Figure 9A, gray bars), as expected if NSF activity were to favor available syntaxin 5. On the other hand, a strong decrease in the relative18C8 staining intensity was found in cells preincubated

with NEM at 37 °C prior to permeabilization and fixation (Figure 9A, black bars). The experiment in Figure 9A demonstrates that both increases and decreases in available syntaxin 5 are possible in NRK cells and quantifiable using 18C8 staining ratios.

We next quantitated the syn 5 (1-43)-GFP transfection experiments discussed above. As shown in Figure 9B (left-hand open bar), the 18C8:rsly1 staining ratio for nontransfected cells had a value of about 1:1. Cells that had been transfected with syn 5 (1-43)-GFP, however, had a dramatically higher value of 1.8:1 (Figure 9B, left-hand solid bar), confirming the impression from Figure 7 that the 18C8-positive Golgi syntaxin 5 was substantially depleted of rsly1. Nontransfected cells had an 18C8:syntaxin 5 ratio of about 1.1:1 (Figure 9B, right-hand open bar). If rsly1 binding favored an open or monomeric conformation of syntaxin 5 or in any other way maintained an available pool of syntaxin 5, a significantly lower 18C8:syntaxin 5 staining ratio would be expected in syn 5 (1-43)-GFP-transfected cells. However, as seen in Figure 9B (right-hand solid bar), the 18C8:syntaxin 5 ratio slightly *increased* in the transfected cells. Thus, our results are inconsistent with opener models of rsly1 function. The modest increase in 18C8:syntaxin 5 ratio was statistically significant ($p = 0.0047$; Student's T-test). There are several potential explanations for this effect, including the possibility that rsly1 favors SNARE complex formation or stabilizes SNARE complexes by a later or more direct mechanism than by altering SNARE motif availability (see Discussion).

For a further test of conformational effects of rsly1 on syntaxin 5, we overexpressed full-length, myc-tagged rsly1 in NRK cells. As shown in Figure 10A & B, the transfected myc-rsly1 presumably saturated Golgi binding sites and filled up the cytoplasm. Based upon the α-rsly1 staining in transfected and untransfected cells such as in Figure 10B, we estimate that the exogenous expression was at least 10-fold over endogenous. As shown in Figure 10C-F, the 18C8 staining in cells overexpressing myc-rsly1 (arrows) appeared similar in nature and intensity to surrounding nontransfected cells (arrowheads). This observation is consistent with the modest changes in syntaxin 5 availability caused by dramatic reduction in rsly1-syntaxin 5 interactions (Figures 7-9). Taken together, these sets of experiments argue against rsly1 playing a major role in promoting or maintaining syntaxin 5 availability, the most commonly invoked model of conserved SM protein function (27).

rsly1-syntaxin 5 interactions are directly required for ER to Golgi transport in permeabilized cells. SM proteins are essential for transport in many systems, however, it is not clear whether their interaction with syntaxins is part of their essential function. We addressed this issue using an in vitro assay that reconstitutes ER to Golgi transport of temperature-sensitive vesicular stomatitus virus glycoprotein (VSVG) in scrape-permeabilized NRK cells (25). As shown in Figure 11A and quantified in Figure 11B, addition of either anti-rsly1 or 18C8 Fab fragments to transport reactions potently and specifically inhibited transport relative to control antibodies. Supplementation of a partially inhibitory dose of α-

rsly1 antibody with a ~100-fold excess of purified, recombinant rsly1 significantly protected against inhibition by the antibody, demonstrating that it was rsly1-reactive antibody molecules that caused the inhibition (Figure 11B, right). The results of Figure 11A&B establish that rsly1 is directly involved in ER to Golgi transport, since abrupt neutralization of rsly1 with the Fab blocks transport. Furthermore, that 18C8 inhibits transport implies that functionally relevant syntaxin 5 SNARE motif is available during at least part of the transport incubation. This is in agreement with the microscopy figures and argues that the pool of syntaxin 5 immunostained by 18C8 is in fact functionally important.

Since rsly1 is a hydrophilic protein that can be added exogenously to permeabilized cells, we had the opportunity to test whether soluble rsly1 could complement the function of antibody-neutralized membrane-bound rsly1. If rsly1 need not be bound to syntaxin 5 to perform its essential function, for example if it bound to syntaxin 5 only to concentrate at the site of membrane fusion where it performed a non-SNARE-related function, then pre-neutralization of the membrane-bound rsly1 pool at low temperature followed by washout of unbound antibody should be complemented by addition of excess soluble rsly1 during a transport incubation. On the other hand, if only the syntaxin-bound rsly1 can perform its essential function, then pre-neutralization of the membrane-bound pool would prevent the function of even a large excess of exogenous rsly1 added later (assuming essentially irreversible rsly1 and antibody binding). The anti-rsly1 pre-neutralization incubation was carried out on ice to inhibit transport-related events that might, in the absence of rsly1 function, result in irreversible

dead-end intermediates. As shown in Figure 11C, 6th bar, inclusion of anti-rsly1 during both the pre-neutralization as well as the transport incubation resulted in virtually complete inhibition of transport. The 7th bar demonstrates, strikingly, that inclusion of anti-rsly1 only during the pre-neutralization step still resulted in almost complete inhibition of transport, even though fresh transport cocktail containing the regular amount of cytosolic rsly1 was provided during the transport reaction. This indicated that soluble rsly1 at the regular concentration could not function in transport nor readily replace the membrane-bound inactivated pool. To test whether a higher concentration of fresh soluble rsly1 could restore at least some rsly1 function, we prepared purified soluble recombinant rsly1 and partially purified native rat liver rsly1. As shown in Figure 11D, regular transport reactions contain about one-third soluble and two-thirds membrane-bound rsly1. Supplementation of transport cocktails with recombinant rsly1 increased the total rsly1 in transport reactions by about 100-fold, whereas the liver rsly1 represented about a 10-fold excess over normal levels. Figure 11C, 8th and 9th bars demonstrate that the addition of the ~100-fold excess of soluble recombinant rsly1, or the 10-fold excess of partially purified native rat liver rsly1, respectively, did not significantly restore transport after pre-neutralization with anti-rsly1. Thus, it appears that rsly1 requires interaction with its membrane receptor, presumably syntaxin 5, to provide its essential function. The first 4 bars demonstrate that neither the recombinant nor liver rsly1 preparations contain major inhibitors of transport, and the 5th bar shows that the preincubation on ice and washing steps themselves do not account for the irreversible loss of

transport activity. The possibility that residual anti-rsly1 antibody in the permeabilized cells inhibited the function of the fresh soluble rsly1 is rendered very unlikely by the excess of rsly1 additions, as this was shown to neutralize the antibody inhibition (Figure 11B). Together, the experiments of Figure 11 suggest that rsly1 function can only be provided when stoichiometrically bound to a particular membrane receptor present in limiting quantities. Although the transfection experiments of Figures 7-9 and previous immunoprecipitation results (14) suggest that syntaxin 5 is the membrane receptor, other critical membrane site(s) are also consistent with Figure 11.

To further address whether syntaxin 5 binding, per se, was critical for the direct function of rsly1 in ER to Golgi transport, we added competitor peptides corresponding to the rsly1 binding site on syntaxin 5. Syntaxin 5 residues 1-43 were expressed as a GST fusion protein in bacteria, cleaved free of GST, and tested in transport incubations relative to GST as a control. As shown in Figure 12A, the preparation containing the peptide specifically inhibited ER to Golgi transport, albeit not to as great an extent as anti-rsly1 antibodies had in Figure 11. We speculate that complete removal of all rsly1 from its syntaxin 5 binding site may require very high local concentrations of peptide, perhaps implying the existence of two functional pools of rsly1, one easier to compete off than the other. To evaluate whether the inhibition we observed was in fact a result of blocked rsly1-syntaxin 5 interactions, we further correlated the inhibition with known requirements for rsly1 binding. As shown in Figure 12B, a synthetic peptide, UM-1, representing the minimal 27 amino acids for rsly1 binding

identified by Yamaguchi et al, inhibited transport as well, although requiring even higher concentrations. That this inhibition is due to its rsly1 binding rather than general biophysical properties is supported by the observation that a control peptide, UM-2, mutated at two amino acids found to be important for rsly1 binding (30), caused significantly less inhibition of transport. In conclusion, the results of Figure 11 and 12 together form a strong argument that rsly1 binding to syntaxin 5 is in fact an active and critical feature of its required role in transport. Thus, although our 18C8 microscopy work argues that rsly1 functions downstream of the production or maintenance of SNARE motif accessibility, our in vitro transport experiments indicate that rsly1 function is intimately intertwined with that of SNAREs.

DISCUSSION

Despite ten years of scrutiny, the mechanism of action of SM proteins continues to elude cell biologists. Several potential positive mechanisms of action of rsly1 are summarized schematically in Figure 13. These potential roles can be grouped into those that act early in the SNARE cycle to provide or protect available syntaxin 5 ("opener roles", Figure 13A), and those that act late to promote trans-SNARE associations, four-helix bundle zippering or multi-complex organization ("late-stage roles", Figure 13B). We have exploited a conformation-specific antibody to examine the relationship between rsly1-syntaxin 5 protein interactions and syntaxin 5 conformation. Our results argue strongly against opener models of rsly1 function whereby this SM protein promotes or maintains an available population of syntaxin 5 molecules. Instead, our results are consistent with rsly1-syntaxin 5 interactions being critical at a later stage of SNARE complex formation or function such as trans complex formation, helix bundle zippering, or the organization of multipe SNARE complexes around a fusion site (see Figure 13 legend for more explanation).

A difficulty in the interpretation of our data stems from not knowing precisely which conformational states exist for syntaxin 5 in vivo, and which of those states are available to 18C8. For example, we cannot be certain that an Habc-closed state exists for syntaxin 5 in vivo, or that 18C8 can discriminate that state from an open state under our immunostaining conditions. We have demonstrated that the syntaxin 5 Habc domain interacts robustly with the

syntaxin 5 SNARE motif (Figure 3), and that the presence of Habc in the syntaxin 5 molecule hinders the rate of ER/Golgi SNARE complex formation by at least an order of magnitude (29). Thus, it seems likely that syntaxin 5, like exocytic syntaxins, forms a closed conformation that plays an autoinhibitory role in vivo. However, although 18C8 binding is incompatible with a closed conformation (Figure 3), it is still possible that the four-helix bundle formed during a closed conformation is more dynamic, even in aldehyde-fixed cells, than a SNARE motif four-helix bundle, and therefore less able to exclude 18C8 from binding during staining experiments. Nonetheless, even lacking these conformational details, our 18C8 immunostaining assay provides at least an operational measure of SNARE motif availability for experiments in fixed cells. And since, based upon the NEM experiments, it seems quite certain that 18C8 immunostains the monomeric but not cis-SNARE complexed syntaxin 5, our data would at least seem to exclude models where rsly1 promotes new SNARE complex formation by preventing newly-available syntaxin 5 from falling back into cis-SNARE complexes (see Figure 13A). Although it has been possible in the past to quantify total immunoprecipitable SNARE complexes in cell extracts, our experiments represent the first opportunity to directly assess the level of *free* syntaxin in cells.

Another potential limitation in our interpretations is the nonspecific nature of NEM inhibition as a means of shifting the balance of free and SNARE-complexed syntaxin 5. We cannot eliminate the possibility that NEM treatment may have effected syntaxin 5 staining in ways other then inhibiting NSF activity.

In support of a somewhat more complex explanation, we were unable to restore 18C8 staining to NEM-inhibited permeabilized cells merely by addition of purified NSF, α-SNAP and MgATP on ice (not shown). However, several observations argue that the effect was due to a bona fide change in syntaxin 5 conformation and not a trivial or direct affect of NEM on immunostaining. First, the SNARE motif is not a substrate for NEM, as it lacks a cysteine. Second, the 18C8 epitope was fully reactive by Western blot after NEM treatment (Figure 4G), indicating that it was only its availability that was altered by NEM. Third, NEM treatment at low temperature did not alter 18C8 staining; however, after removal of NEM, 18C8 staining decreased in a time-dependent fashion on incubation of cells at 37 °C (Figure 4E and F). This is consistent with a requirement for ongoing vesicle docking and fusion reactions to consume free syntaxin 5 before the effect on 18C8 staining occurs. Finally, we found that in permeabilized cells, purified NSF, α-SNAP and MgATP caused a significant increase in the 18C8 staining intensity (Figure 9A). All of these observations are consistent with 18C8 staining being dependent upon free syntaxin 5 molecules.

A striking finding of this study was that available syntaxin 5 was non-uniformly distributed in the Golgi region, and was present in foci of high concentration relative to total syntaxin 5. At this time we do not know what these syntaxin 5 “hotspots” represent and what factors and signals initiate them. Functionally, they could represent active sites for membrane fusion between incoming VTCs and the Golgi. One possibility is that microtubules pass through the Golgi area near these sites, causing nearby Golgi membranes to sustain a

higher load of membrane fusion and consequent recruitment of SNARE regulatory factors. They could also represent Golgi cisternal rims, where intra-Golgi transport vesicles may be tethered on string-like attachments that restrain their diffusion and fusion to within a fixed distance (21). What regulatory machinery maintains the available syntaxin 5? NSF is responsible for dissociating used SNARE complexes, but little is known about factors that maintain SNAREs in an active state once dissociated, if such factors are indeed necessary. Our study does not shed light upon the identity of those factors other than to argue strongly that rsly1 is not one of them. If rsly1 binding to syntaxin 5 were required for maintenance of a free population of syntaxin 5, then a significant decrease in 18C8-availailable syntaxin 5 would have been expected to result from disruption of rsly1-syntaxin 5 interactions (Figure 9B). The mechanisms underlying the available syntaxin 5 foci, as well as their precise ultrastructure, are interesting topics for future studies.

Significant disruption of rsly1-syntaxin 5 interactions caused unexpectedly little change in the 18C8:syntaxin 5 staining ratio, however, it did result in a small but statistically significant increase in this ratio (Figure 9B). There are several ways that this effect could be interpreted: Firstly, since the effect is relatively small, it is possible that the effect was due to a change in the degree of co-localization of 18C8 and anti-syntaxin 5 staining, rather than to a change in the staining intensities. This effect is possible since we used 18C8 staining to select the precise regions of the cell to include for quantification of both color channels. Hence, if a manipulation were to cause a slight decrease in colocalization of the

two staining patterns, this could cause a slight increase in the 18C8 staining index. We did not notice such a change by eye, however, this does not exclude the possibility. Secondly, since disruption of rsly1-syntaxin 5 interactions caused a significant decrease in total syntaxin 5 molecules in the cell (Figures 7 and 8, arrowheads vs. arrows), it is possible that a compensatory regulatory mechanism resulted in a higher proportion of syntaxin 5 molecules residing in an available state, and thus an increase in the 18C8:syntaxin 5 staining ratio. Thirdly, the slight increase in the 18C8:syntaxin 5 staining ratio could have been caused by an indirect effect on SNARE complex formation or stability resulting from a later block in membrane fusion—assuming that SNARE complex formation is a readily reversible process when full membrane fusion, and hence full SNARE zippering, is inhibited. Fourthly and finally, the simplest interpretation is that rsly1 is in fact positively involved in syntaxin 5 SNARE complex formation. However, it would have to promote SNARE complex formation via a mechanism that does not increase available SNARE motif. For example, it could act to stabilize intermediates in the trans-complex assembly process, the completion of zippering or the supra-molecular arrangement of multiple forming SNARE complexes around a fusion site (see schematic, Figure 13B). Although the slight staining ratio increase is also compatible with rsly1 stabilizing the closed, rather than the open, conformation of syntaxin 5, this interpretation seems very unlikely since it would not predict the potent inhibition of transport by anti-rsly1 antibodies, nor would it be compatible with previous work that found a Sly1p-

dependent increase in Sed5p-containing SNARE complexes by immunoprecipitation (16).

FUTURE DIRECTIONS

At the time of this manuscript the prevailing theme revolved around a lack of understanding of the precise mechanism of action of SM proteins in terms of their potential regulation of SNAREs. Past models of SM protein function held that these proteins assume a regulatory role responsible for maintaining an available open and/or monomeric pool of syntaxin molecules for SNARE complex formation. But the exploration of the interactions of SM proteins with syntaxins and their functional consequences *in vivo* within several eukaryotes has led to a reconsideration of the long-standing assumption that SM proteins fulfill their regulatory role by binding to syntaxins.

By addressing the functional relationship of the mammalian ER/Golgi SM protein rsly1 and its SNARE binding partner syntaxin5, we were able to demonstrate that rsly1-syntaxin5 interactions are critical at a later stage of SNARE complex formation or function such as *trans* complex formation, helix bundle zippering, or the organization of multiple SNARE complexes around a fusion site (see Figure 13 legend for more explanation). These results are consistent with the emerging picture unifying connections between individual SM/syntaxin interactions and one complete functional model for SM/SNARE protein-protein interactions, whereby each of the interactions observed *in vitro* represent intermediate stages of a SM protein-controlled molecular pathway of specific SNARE complex assembly that results in membrane fusion. However, much still remains uncovered. First, why does Munc18-1 bind syntaxin1A in a

closed conformation? Second, if this closed conformation is the first step in a series of SM protein-mediated steps toward SNARE complex formation, how and when does the SM/closed syntaxin dimer transit to the SM protein/SNARE complex: does it truly involve an intermediate where the SM protein is bound to the amino-terminus of syntaxin or is the association of the SM protein to SNARE complexes preceded by complete dissociation of the SM protein followed by re-binding? Third, do all SM proteins undergo all three modes of binding? Finally, is there another uncovered SM/syntaxin binding mode?

Current research aimed at addressing these questions have employed Fluorescence Resonance Energy Transfer (FRET) microscopy to take a deeper look at the protein-protein interactions involved in SM protein/SNARE-mediated vesicle fusion. The use of this technique permits an analysis of the interactions between native participating proteins in single living or fixed cells. In this way false results, positive or negative, that could be produced by the interference of outside elements are eliminated. Using confocal microscopy, FRET is able to capture weak and transient interactions through fluorescent signals that indicate direct interactions. *In vivo* FRET analysis of SM protein/syntaxin interactions should promote further understanding of the precise timing at which these complexes assemble and function within the seretory pathway and how these interactions coordinate eventual membrane fusion.

ACKNOWLEDGMENTS

This work was supported by NIH grant GM59378 to J. C. H. and by a fellowship from the Rackham Graduate School, University of Michigan, to A. L. W. The authors thank Kaustuv Datta (University of Michigan) for preparation of anti-rsly1 antisera. We also wish to thank Dr. Phyllis Hanson (Washington University) for generously sharing reagents.

FOOTNOTES

This chapter was published as:

Antionette L. Williams, Sebastian Ehm, Noëlle C. Jacobson, Dalu Xu, and Jesse C. Hay. 2004. rsly1 Binding to Syntaxin 5 is Required for ER to Golgi Transport but Does Not Promote SNARE Motif Accessibility. Molecular Biology of the Cell 15(1):162-75.

I performed experiments described in figures 2.1, 2.2, 2.3, 2.4, 2.5, 2.6, 2.7,2.8, 2.9 and 2.10

A discussion of future directions for this work was written in fulfillment of dissertation requirements and was not included as part of the original published manuscript.

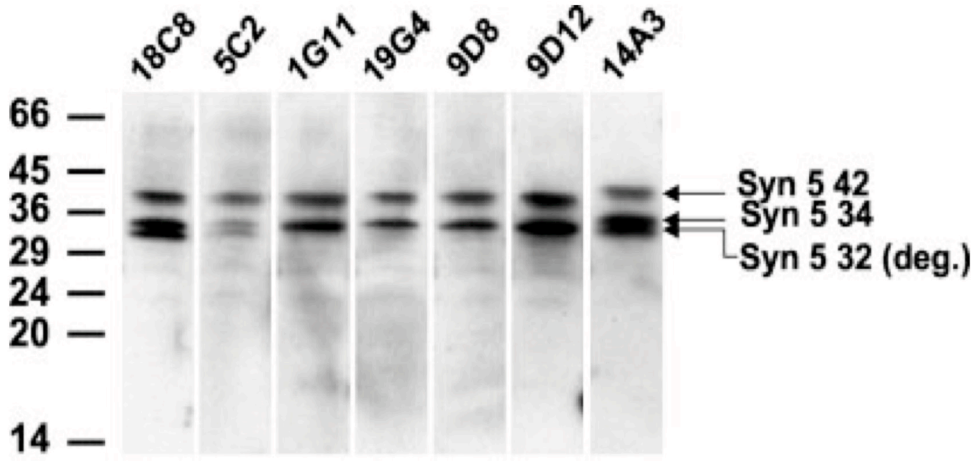

Figure 2.1. A set of monoclonal antibodies directed against the syntaxin 5 SNARE motif. Antibodies from tissue culture supernatants from the indicated hybridomas (*above*) were purified by protein A or protein G-Sepharose and utilized to immunoblot identical lanes of crude rat brain membranes separated by SDS-PAGE and transferred to nitrocellulose. The migration of molecular weight marker proteins are shown (*left*), as are the positions of the 42 kD (*syn 5 42*) and 34 kD (*syn 5 34*) endogenous syntaxin 5 isoforms and a commonly seen syntaxin 5 degradation fragment at 32 kD (*syn 5 32 (deg.)*).

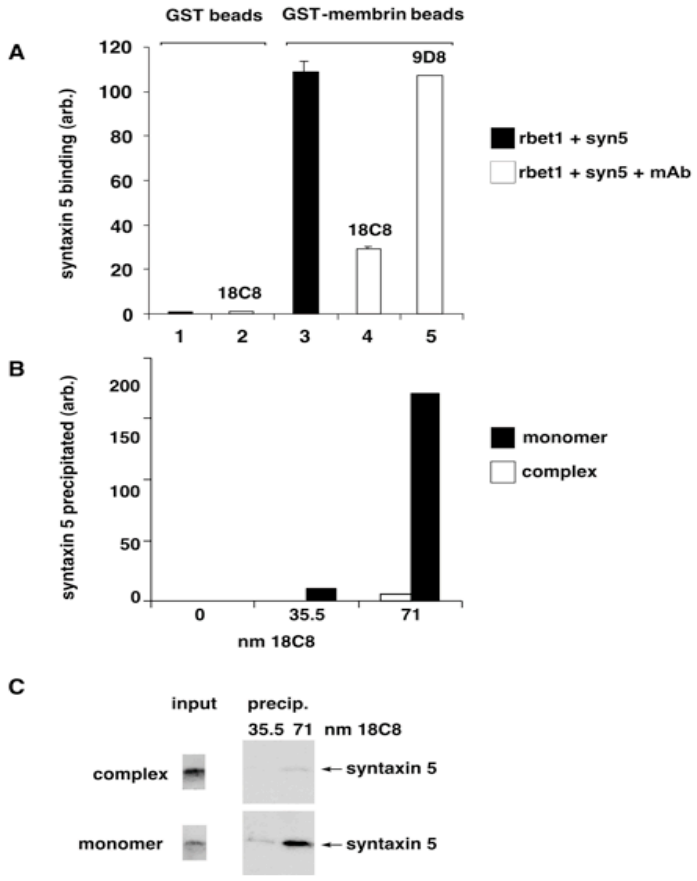

Figure 2.2. 18C8 binds to the syntaxin 5 SNARE motif mutually exclusively with ER/Golgi SNAREs. ***A,*** Purified bacterially expressed GST or GST-membrin was immobilized on glutathione beads and mixed with soluble syntaxin 5 SNARE motif and rbet1 cytoplasmic domain. Shown is a quantification of syntaxin 5 bound to the GST and GST-membrin beads after washing with buffer and immunoblotting. GST and GST-membrin beads were reacted either in the absence of monoclonal antibody (*filled bars*) or the presence of equal concentrations of the indicated monoclonal antibody (*open bars*). ***B,*** ER/Golgi quaternary complexes were formed from syntaxin 5 SNARE motif, membrin, rbet1 and sec22b in solution and purified by gel filtration as described previously (29). Purified ER/Golgi quaternary complex (*open bars*), or a lesser amount of syntaxin 5 SNARE motif in isolation (*filled bars*), were subjected to immunoprecipitation with 18C8 and protein A-Sepharose beads at the indicated antibody concentrations, and syntaxin 5 in the immunoprecipitated pellets was quantified by immunoblotting following SDS-PAGE and transfer to nitrocellulose. ***C***, Autoradiogram of the blot that was quantified to produce part B. Shown are the immunoprecipitation input lanes (*left*) and the immunoprecipitated pellets (*right*).

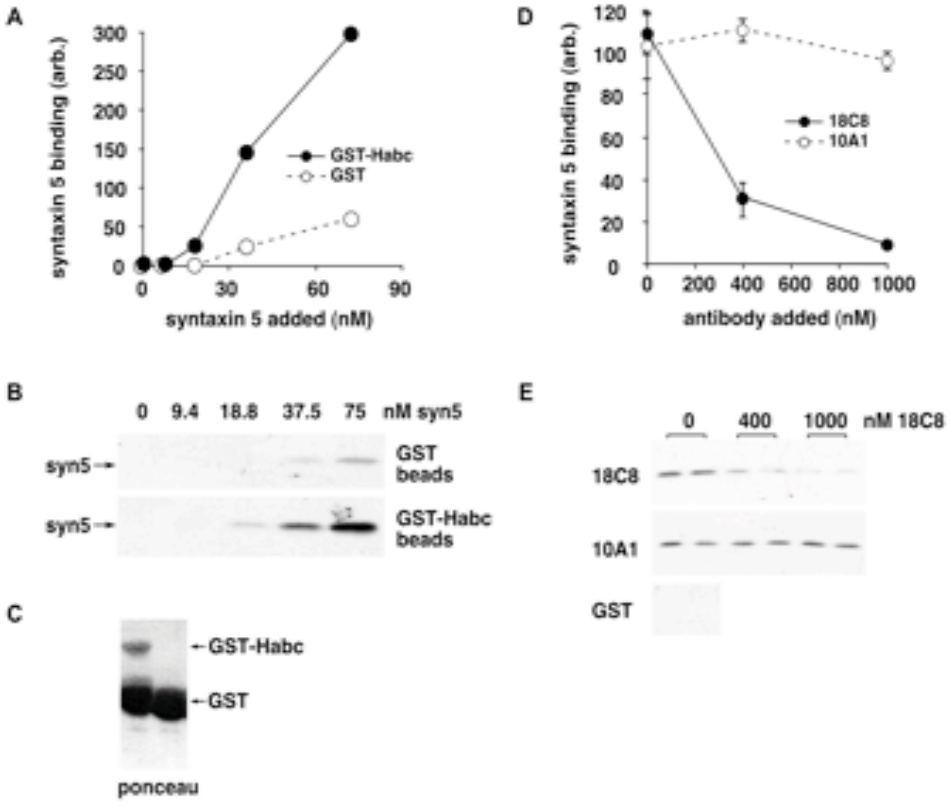

Figure 2.3. 18C8 inhibits binding between the syntaxin 5 SNARE motif and Habc domain. ***A*****,** Purified bacterially expressed GST (open symbols) or GST-syntaxin 5 Habc domain (filled symbols) was immobilized on glutathione beads and mixed with soluble syntaxin 5 SNARE motif at the indicated concentrations. SNARE motif bound to the beads after buffer washes was quantified by immunoblotting. ***B*****,** Autoradiogram of the blot that was quantified to produce part A. **C,** Ponceau stain of the immunoblot lanes to which no soluble SNARE motif was added; a high proportion of the protein in the GST-Habc preparation was GST. ***D*****,** Purified bacterially expressed GST-syntaxin 5 Habc domain was immobilized on glutathione beads and mixed with soluble syntaxin 5 SNARE motif at the highest concentration on the curve in part A, in the presence of increasing concentrations of purified 18C8 (open symbols) or 10A1 (closed symbols). SNARE motif bound to the beads after buffer washes was quantified by immunoblotting following SDS-PAGE and transfer to nitrocellulose. ***E*****,** Autoradiogram of the blot that was quantified to produce part D.

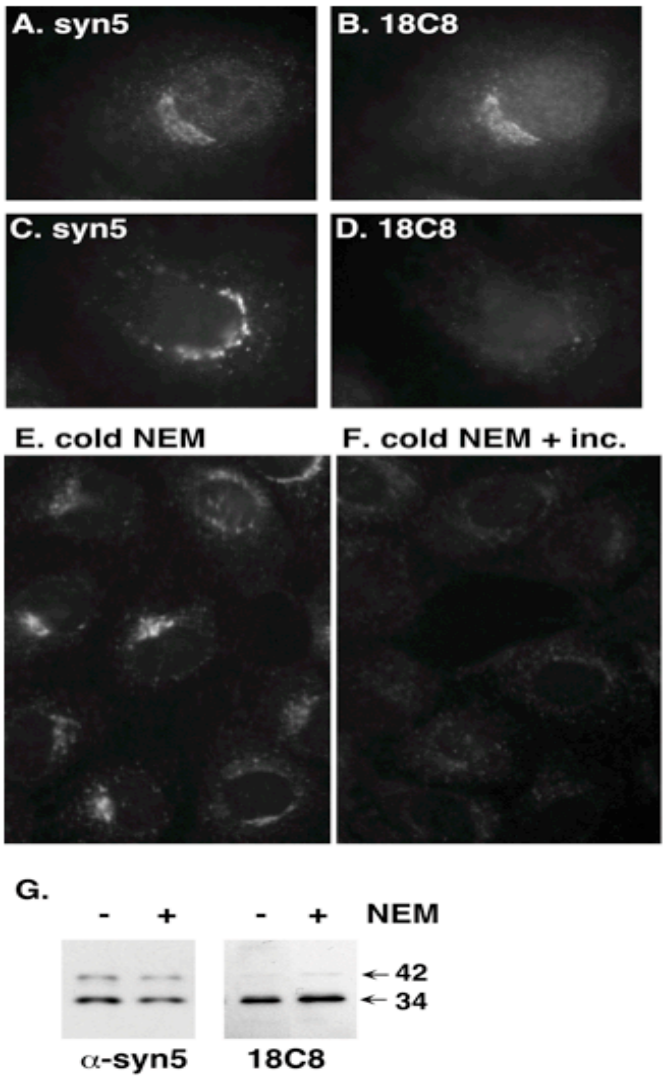

Figure 2.4. 18C8 stains only free, uncomplexed syntaxin 5 in fixed NRK cells. ***A-D***, NRK cells were either incubated in control medium (*A, B*) or in medium containing 50 μM NEM (*C*, *D*) for 5 minutes at 37 °C in a CO_2 incubator prior to fixation with paraformaldehyde and immunostaining with 18C8 and polyclonal anti-syntaxin 5 as described in the methods section. ***E, F,*** NRK cells were incubated in medium containing 100 μM NEM for 5 minutes on ice, then washed several times with NEM-free medium and either fixed on ice (*E*), or incubated at 37 °C for 5 min and then fixed on ice (*F*). After fixation, the cells were immunostained with purified 18C8. ***G***, Cells that had undergone control or NEM incubations were placed on ice, lysed, separated by SDS-PAGE and immunoblotted using 18C8 or polyclonal anti-syntaxin 5 antisera.

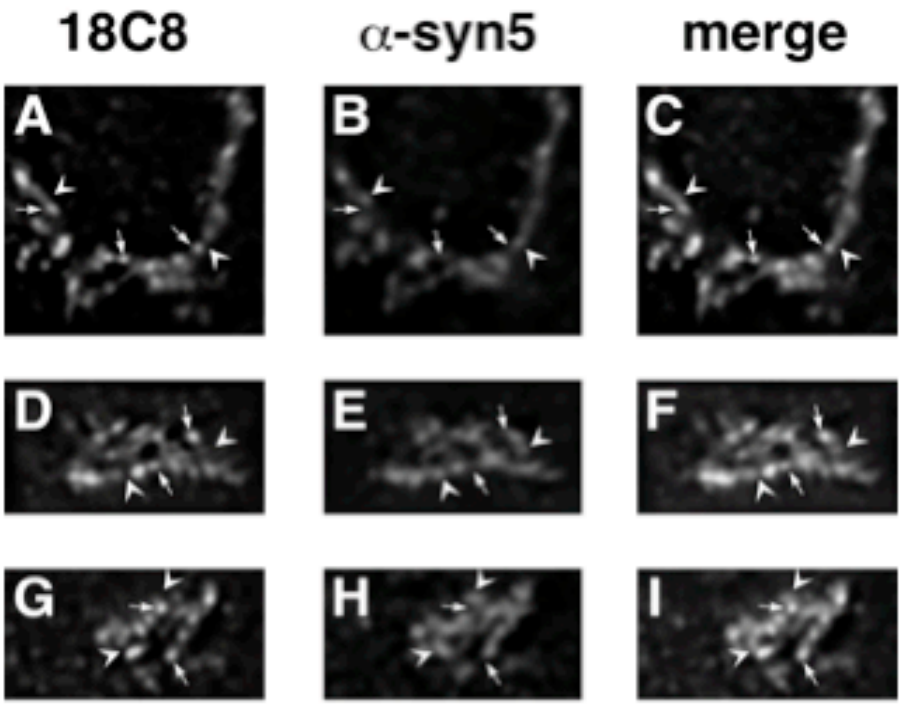

Figure 2.5. 18C8-available syntaxin 5 is nonuniformly and focally localized. Fixed NRK cells were double-stained with 18C8 and polyclonal anti-syntaxin 5 antibodies using FITC- and Texas Red-labeled secondary antibodies, respectively. Images were collected for both filter sets every 0.2 microns through the cell, and the image stacks were optically deconvolved using an algorithm that removes no light from the stack and involves no arbitrary user inputs. Single optical sections of three Golgi regions, from three different cells are shown for the FITC channel (*A, D, G*), the Texas Red channel (*B, E, H*) and merged images (*C, F, I*).

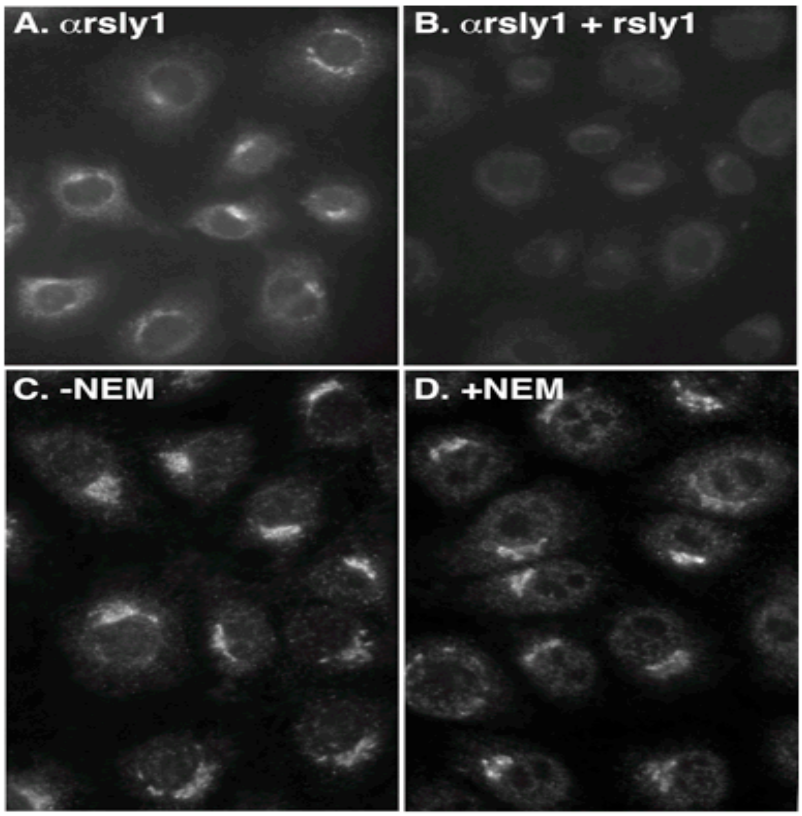

Figure 2.6. rsly1 is localized to the Golgi region independently of the oligomeric state of syntaxin 5. Fixed NRK cells were immunostained using an affinity-purified anti-rsly1 antiserum under control conditions (*A, C*), after 50 μM NEM treatment as in Figure 4 (*D*), or in the presence of an excess of purified bacterially produced GST-rsly1 (*B*). A and B are from a separate experiment from C and D.

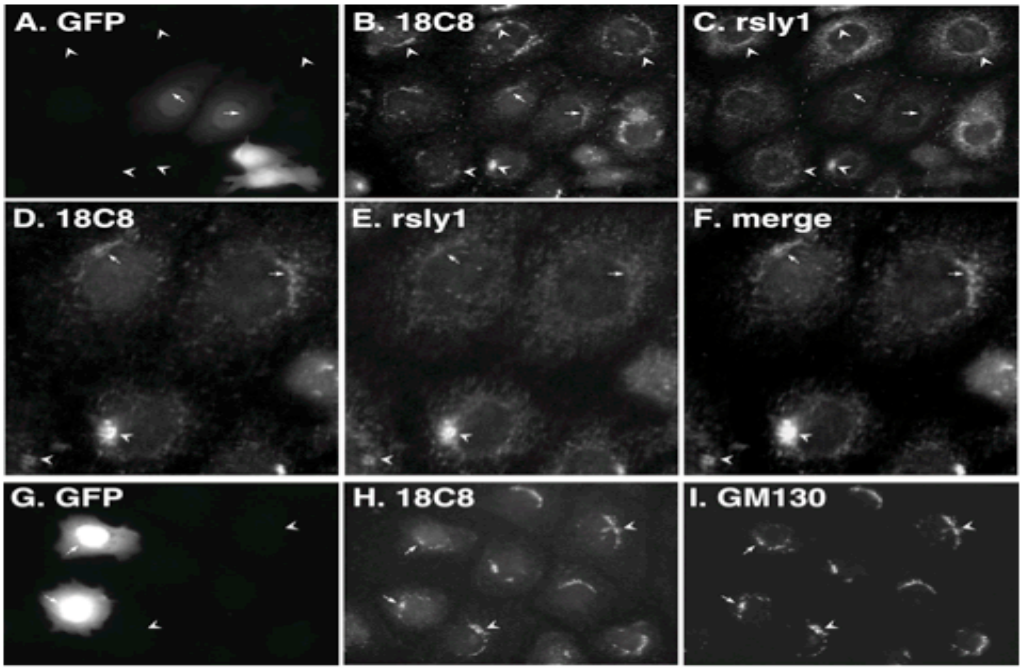

Figure 2.7. Expression of syntaxin 5 (1-43)-GFP dissociates Golgi rsly1 staining from that of 18C8. NRK cells were transfected with syntaxin 5 (1-43)-GFP, fixed, and immunostained with the indicated primary antibodies followed by cy3- and cy5-labeled secondary antibodies. Images shown employed filter sets for GFP *(A, G*), cy3 (*B, D, H*) and cy5 (*C, E, I*) or a merge of cy3 and cy5 (*F*). Panel D, E, and F are magnified views of the boxed region in B and C. *Arrowheads* mark staining in nontransfected cells, and *arrows* mark staining in transfected cells.

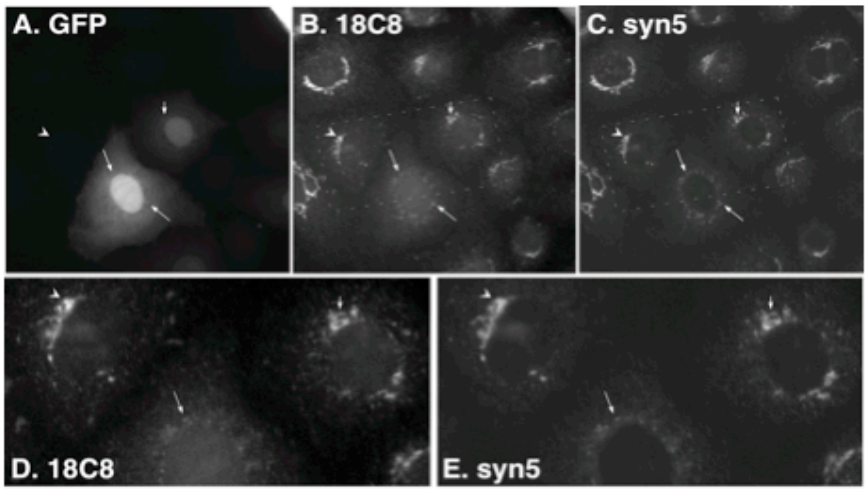

Figure 2.8. Expression of syntaxin 5 (1-43)-GFP does not significantly alter 18C8 staining intensity relative to polyclonal anti-syntaxin 5 staining. NRK cells were transfected with -syntaxin 5 (1-43)-GFP, fixed, and immunostained with 18C8 or polyclonal anti-syntaxin 5 antibodies followed by cy3- and cy5 -labeled secondary antibodies, respectively. Images shown employed filter sets for GFP *(A*), cy3 (*B, D*) and cy5 (*C, E*). Panels D and E are magnified views of the boxed region in B and C. *Arrowheads* demonstrate staining in nontransfected cells, *short arrows* demonstrate staining in low expressing cells and *long arrows* demonstrate staining in moderate to highly expressing cells.

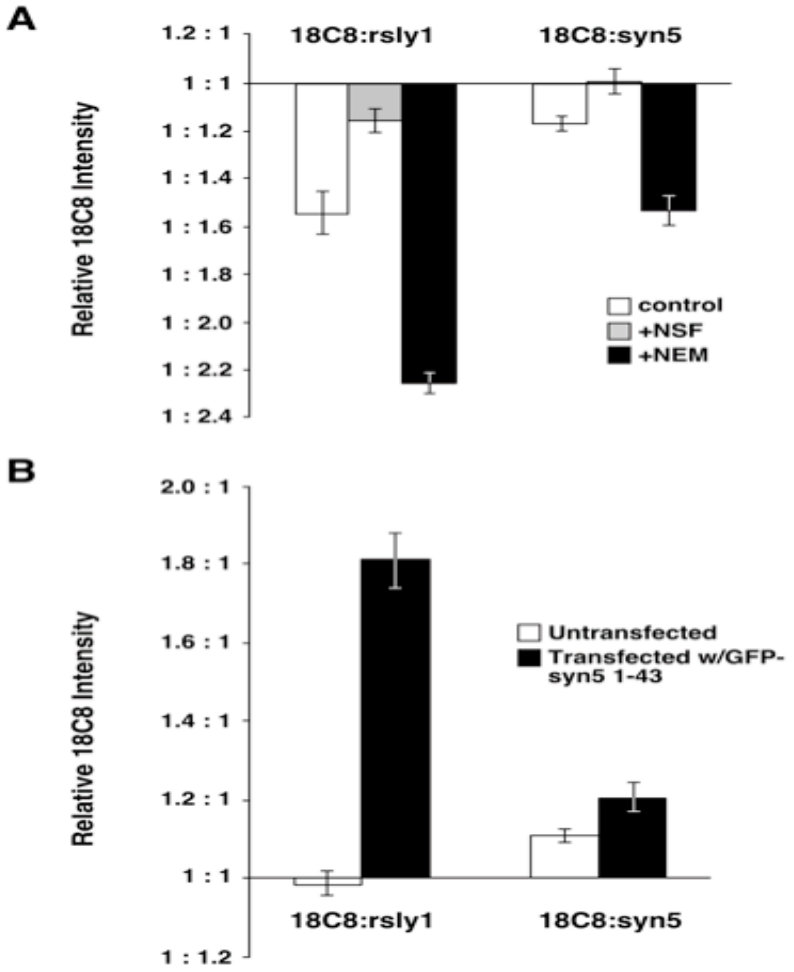

Figure 2.9. Quantitation of 18C8 staining intensities reveals that dissociation of rsly1-syntaxin 5 interactions causes a modest increase in 18C8 accessibility. ***A***, Demonstration of ratiometric quantitation of 18C8 staining intensity relative to rsly1 staining (left) and polyclonal anti-syntaxin 5 staining (right). Digitonin-permeabilized cells were fixed and stained after incubation on ice with buffer (open bars), with buffer containing purified NSF, α-SNAP and MgATP (gray bars), or following a 37 °C NEM treatment as in Figure 4 (filled bars). Plotted is the ratio of Golgi-area 18C8 staining intensity to that of anti-rsly1 or anti-syntaxin 5, averaged over approximately 120 cells per condition as described in the Materials and Methods section. ***B***, Ratiometric quantitation of 18C8 staining intensity relative to rsly1 staining (left) and polyclonal anti-syntaxin 5 staining (right) in untransfected (open bars) and syntaxin 5 (1-43)-GFP-transfected cells (solid bars). Nontransfected and transfected cells were from the same coverslips. For both panels A and B, the means are plotted plus or minus standard error.

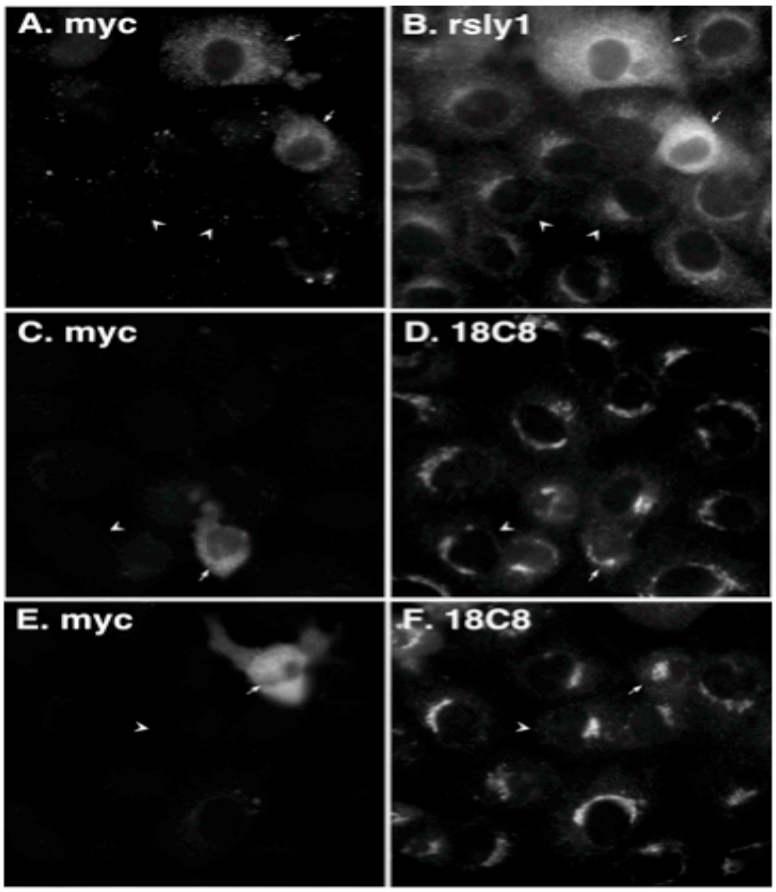

Figure 2.10. Overexpression of myc-rsly1 does not significantly change 18C8 accessibility of syntaxin 5. NRK cells were transfected with myc-rsly1, fixed and immunostained with anti-myc (*A, C, E*), anti-rsly1 (*B*), or 18C8 (*D, F*) antibodies. Overexpressing cells (*arrows*) displayed similar 18C8 staining to that of surrounding nontransfected cells (*arrowheads*).

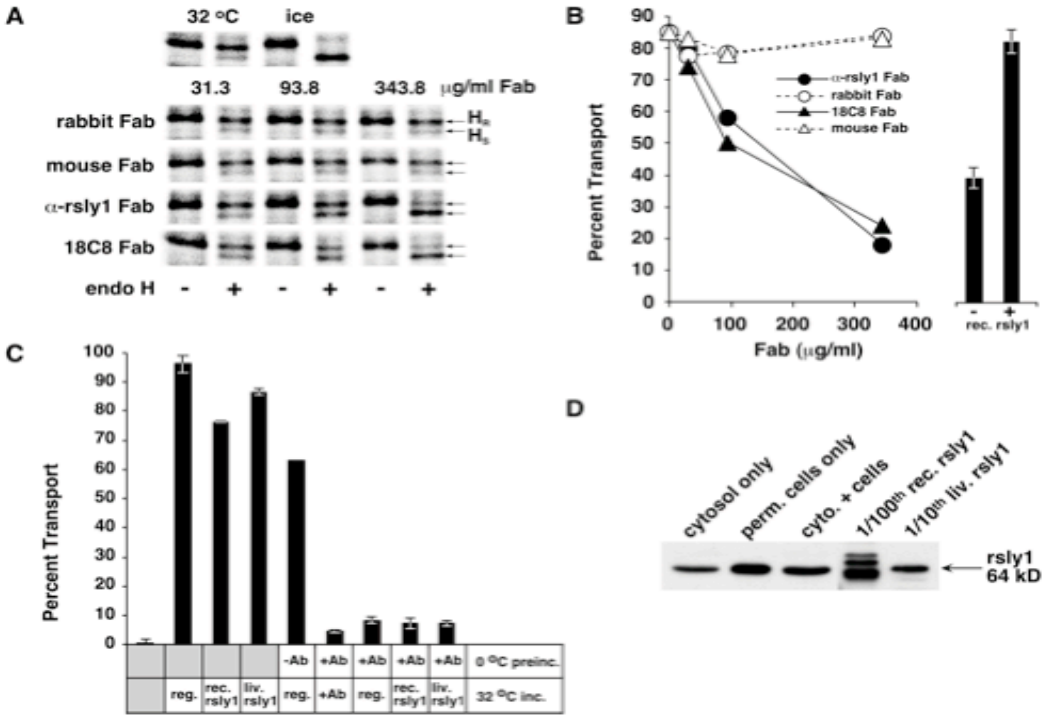

Figure 2.11. rsly1 must bind stoichiometrically to a fillable membrane site to function in ER to Golgi transport. ***A***, Endoglycosidase H analysis of VSVG ts045 protein in permeabilized NRK cells after transport incubations containing the indicated concentrations of the indicated control *(mouse, rabbit)* or immune *(α-rsly1, 18C8)* Fab fragments. Endo H-resistant *(H_R)* and –sensitive *(H_S)* bands are indicated *(arrows)*. Control reactions lacking any Fabs are shown *above*. ***B***, Quantitation of the experiment from part A *(main axis)* and also a separate experiment *(histogram)* in which a partially inhibitory concentration of α-rsly1 intact IgG was tested in the absence *(left bar)* or presence *(right bar)* of excess purified GST and rsly1. ***C,*** Permeabilized NRK cells were either preincubated on ice with or without anti-rsly1 antibodies *(bars 5-9)* or else incubated at 32 °C immediately *(bars 2-4)* with regular transport cocktail *(reg.)* or cocktail supplemented with a 100-fold excess of soluble purified recombinant rsly1 *(rec. rsly1)* or a 10-fold excess of partially purified native liver rsly1 *(liv. rsly1)*. The preincubated cells *(bars 5-9)* were subsequently washed twice and resuspended in regular transport cocktail *(reg.)* or cocktail supplemented with α-rsly1 antibodies *(+Ab)* or excess rsly1-containing cocktails *(rec. rsly1 & liv. rsly1)*. VSV G transport was quantified after 90 minutes at 32 °C as in part B. Plotted values are means of duplicate reactions plus or minus standard error. ***D***, Immunoblots demonstrating the quantity of rsly1 present in washed, permeabilized NRK cells used for transport, the normal rat liver cytosol used for transport, and the indicated dilutions of the purified recombinant and partially purified cytosolic rsly1 used in part B.

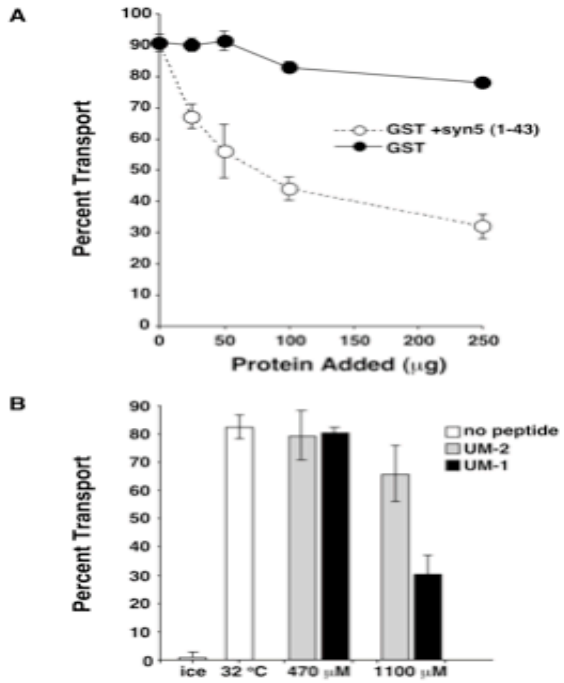

Figure 2.12. Syntaxin 5 binding is essential for rsly1 function in ER to Golgi transport. ***A***, VSVG transport was monitored in the presence of the indicated concentrations of GST (*filled circles*) or thrombin-cleaved GST-syntaxin 5 (1-43) (*open circles*). ***B***, Transport was monitored under control conditions *(open bars)* or in the presence of the indicated concentrations of synthetic peptides corresponding to syntaxin 5 amino acids 1-27 (*UM-1, solid bars*) or the same peptide containing T7A and F10A mutations (*UM-2, gray bars*). Plotted are the mean transport values after 90 minutes of incubation at 32 °C, plus or minus standard error.

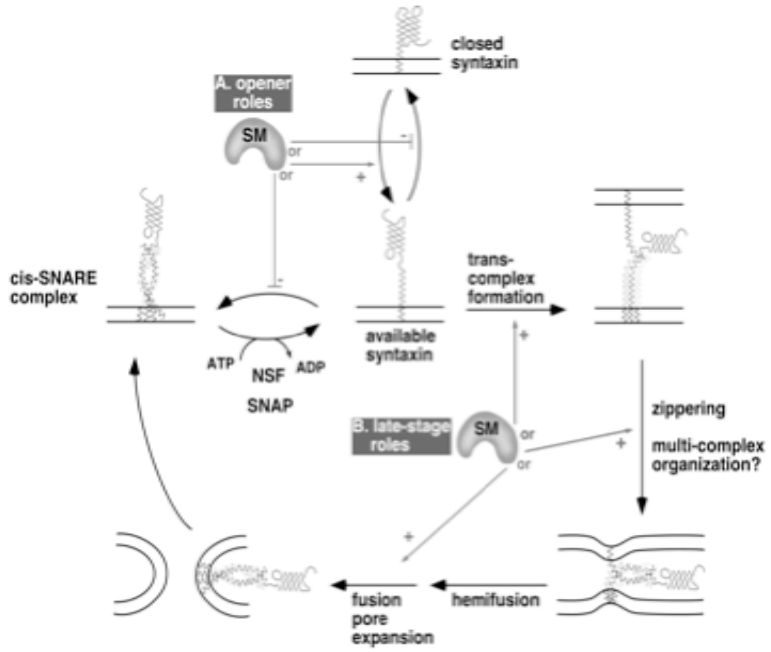

Figure 2.13. Schematic of possible mechanisms of action of SM proteins in the SNARE cycle and membrane fusion. Known or hypothetical steps in the SNARE cycle are represented with *black arrows*. Potential SM protein roles that are consistent with our data are indicated with *red arrows* and roles that are inconsistent or less consistent with our data are indicated with *gray arrows*. Potential SM protein roles are grouped for illustration purposes into Opener Roles ***(A),*** and Late Stage Roles ***(B)***. The opener roles are inconsistent with our staining experiments (e.g. Figures 9 and 10), since they would predict a decrease in available syntaxin 5 SNARE motif when syntaxin 5/rsly1 interactions were blocked, and an increase when rsly1 was overexpressed. Among the potential late-stage roles, a role in promotion of fusion pore expansion or other lipidic events is less consistent with our data than the other illustrated roles, since they would not necessarily require syntaxin 5/rsly1 interactions, whereas our transport experiments (Figures 11 and 12) demonstrated this requirement for rsly1 function. The role indicated by "multi-complex organization" is not explicitly illustrated since very little is known about what this may entail; one suggestion would be arrangement of multiple SNARE complexes around a central fusion site. We illustrate only potentially required, *positive* roles. Negative roles such as stabilization of closed syntaxin would not predict the strict requirement for rsly1 in ER/Golgi transport (Figure 11). Note that rsly1 could potentially perform more than one of the indicated functions.

REFERENCES

1. **Bracher, A., and W. Weissenhorn.** 2002. Structural basis for the Golgi membrane recruitment of Sly1p by Sed5p. EMBO J **21:**6114-24.
2. **Bryant, N. J., and D. E. James.** 2003. The Sec1p/Munc18 (SM) protein, Vps45p, cycles on and off membranes during vesicle transport. J Cell Biol **161:**691-6.
3. **Bryant, N. J., and D. E. James.** 2001. Vps45p stabilizes the syntaxin homologue Tlg2p and positively regulates SNARE complex formation. EMBO J **20:**3380-8.
4. **Carr, C. M., E. Grote, M. Munson, F. M. Hughson, and P. J. Novick.** 1999. Sec1p binds to SNARE complexes and concentrates at sites of secretion. J Cell Biol **146:**333-44.
5. **Dulubova, I., T. Yamaguchi, Y. Gao, S. W. Min, I. Huryeva, T. C. Sudhof, and J. Rizo.** 2002. How Tlg2p/syntaxin 16 'snares' Vps45. Embo J **21:**3620-31.
6. **Dulubova, I., T. Yamaguchi, Y. Wang, T. C. Sudhof, and J. Rizo.** 2001. Vam3p structure reveals conserved and divergent properties of syntaxins. Nat Struct Biol **8:**258-64.
7. **Fernandez, I., J. Ubach, I. Dulubova, X. Zhang, T. C. Sudhof, and J. Rizo.** 1998. Three-dimensional structure of an evolutionarily conserved N-terminal domain of syntaxin 1A. Cell **94:**841-9.
8. **Fiebig, K. M., L. M. Rice, E. Pollock, and A. T. Brunger.** 1999. Folding intermediates of SNARE complex assembly. Nat Struct Biol **6:**117-23.
9. **Fisher, R. J., J. Pevsner, and R. D. Burgoyne.** 2001. Control of fusion pore dynamics during exocytosis by Munc18. Science **291:**875-8.
10. **Gallwitz, D., and R. Jahn.** 2003. The riddle of the Sec1/Munc-18 proteins - new twists added to their interactions with SNAREs. Trends Biochem Sci **28:**113-6.
11. **Guan, K. L., and J. E. Dixon.** 1991. Eukaryotic proteins expressed in Escherichia coli: an improved thrombin cleavage and purification procedure of fusion proteins with glutathione S-transferase. Anal Biochem **192:**262-7.
12. **Harlow, E. a. L., D.** 1988. Antibodies: A Laboratory Manual. Cold Spring Harbor Laboratory Press, Plainview, NY.
13. **Hay, J. C.** 2001. SNARE complex structure and function. Exp Cell Res **271:**10-21.
14. **Hay, J. C., D. S. Chao, C. S. Kuo, and R. H. Scheller.** 1997. Protein interactions regulating vesicle transport between the endoplasmic reticulum and Golgi apparatus in mammalian cells. Cell **89:**149-58.
15. **Joglekar, A. P., D. Xu, D. J. Rigotti, R. Fairman, and J. C. Hay.** 2003. The SNARE motif contributes to rbet1 intracellular targeting and dynamics independently of SNARE interactions. J Biol Chem **278:**14121-33.
16. **Kosodo, Y., Y. Noda, H. Adachi, and K. Yoda.** 2002. Binding of Sly1 to Sed5 enhances formation of the yeast early Golgi SNARE complex. J Cell Sci **115:**3683-91.

17. **Misura, K. M., R. H. Scheller, and W. I. Weis.** 2000. Three-dimensional structure of the neuronal-Sec1-syntaxin 1a complex. Nature **404:**355-62.
18. **Munson, M., X. Chen, A. E. Cocina, S. M. Schultz, and F. M. Hughson.** 2000. Interactions within the yeast t-SNARE Sso1p that control SNARE complex assembly. Nat Struct Biol **7:**894-902.
19. **Munson, M., and F. M. Hughson.** 2002. Conformational regulation of SNARE assembly and disassembly in vivo. J Biol Chem **277:**9375-81.
20. **Nickel, W., T. Weber, J. A. McNew, F. Parlati, T. H. Sollner, and J. E. Rothman.** 1999. Content mixing and membrane integrity during membrane fusion driven by pairing of isolated v-SNAREs and t-SNAREs. Proc Natl Acad Sci U S A **96:**12571-6.
21. **Orci, L., A. Perrelet, and J. E. Rothman.** 1998. Vesicles on strings: morphological evidence for processive transport within the Golgi stack. Proc Natl Acad Sci U S A **95:**2279-83.
22. **Peng, R., and D. Gallwitz.** 2002. Sly1 protein bound to Golgi syntaxin Sed5p allows assembly and contributes to specificity of SNARE fusion complexes. J Cell Biol **157:**645-55.
23. **Pevsner, J., S. C. Hsu, J. E. Braun, N. Calakos, A. E. Ting, M. K. Bennett, and R. H. Scheller.** 1994. Specificity and regulation of a synaptic vesicle docking complex. Neuron **13:**353-61.
24. **Sato, T. K., P. Rehling, M. R. Peterson, and S. D. Emr.** 2000. Class C Vps protein complex regulates vacuolar SNARE pairing and is required for vesicle docking/fusion. Mol Cell **6:**661-71.
25. **Schwaninger, R., H. Plutner, H. W. Davidson, S. Pind, and W. E. Balch.** 1992. Transport of protein between endoplasmic reticulum and Golgi compartments in semiintact cells. Methods Enzymol **219:**110-24.
26. **Sollner, T., S. W. Whiteheart, M. Brunner, H. Erdjument-Bromage, S. Geromanos, P. Tempst, and J. E. Rothman.** 1993. SNAP receptors implicated in vesicle targeting and fusion. Nature **362:**318-24.
27. **Toonen, R. F., and M. Verhage.** 2003. Vesicle trafficking: pleasure and pain from SM genes. Trends Cell Biol **13:**177-86.
28. **Ungar, D., and F. M. Hughson.** 2003. SNARE protein structure and function. Annu Rev Cell Dev Biol **19:**493-517.
29. **Xu, D., A. P. Joglekar, A. L. Williams, and J. C. Hay.** 2000. Subunit structure of a mammalian ER/Golgi SNARE complex. J Biol Chem **275:**39631-9.
30. **Yamaguchi, T., I. Dulubova, S. W. Min, X. Chen, J. Rizo, and T. C. Sudhof.** 2002. Sly1 binds to Golgi and ER syntaxins via a conserved N-terminal peptide motif. Dev Cell **2:**295-305.
31. **Yang, B., M. Steegmaier, L. C. Gonzalez, Jr., and R. H. Scheller.** 2000. nSec1 binds a closed conformation of syntaxin1A. J Cell Biol **148:**247-52.

CHAPTER THREE

The Peroxisomal Targeting Signal 2 Processing Protease

ABSTRACT

A few peroxisomal matrix enzymes contain a PTS2 nonapeptide sequence with the consensus R-(L/V/I/Q)-X_5-(H/Q)-(L/A), located within the amino terminus of the protein. In plants and mammals, these enzymes are imported as precursor proteins that are processed to their mature forms subsequent to matrix entry. Bioinformatic analysis of the Arabidopsis genome revealed nine candidate proteases predicted to be in peroxisomes; among them was a 76 kDa DEG protease**.** Seeds from plants with a T-DNA insertion in *AtDEG15*, the Deg15 protease homolog in Arabidopsis (At1g28320), required sucrose for germination. Western blot analysis of whole plant extracts from these *atdeg15* knockout mutants reveals that only the unprocessed precursor form of the PTS2 protein thiolase (THL) was present. *In vitro* peroxisome import assays show that AtDEG15 imported into the peroxisome matrix. Purified recombinant AtDEG15 specifically processed the PTS2 proteins THL and aspartate aminotransferase 3 (ASP3) *in vitro*; the PTS1 proteins glycolate oxidase (GLO) and isocitrate lyase (IL) were not cleaved. In plants and mammals, a cysteine located downstream of

PTS2 sequences is required for processing of precursor forms of all PTS2 proteins identified so far. An engineered mutation to glycine prevented AtDEG15-mediated cleavage of THL, although its *in vitro* import was not impeded. Moreover, mutations of the PTS2 signal that resulted in decreased import of THL and ASP3 did not prevent the proteolytic processing of their precursor forms by AtDEG15. Taken together, these results indicate that AtDEG15 is a novel, PTS2-specific processing protease.

INTRODUCTION

Though the mechanisms of PTS2 protein import appear to be conserved among most species, one difference concerns the fate of PTS2 proteins following import into the matrix of peroxisomes in plants and mammals. In these eukaryotes, the PTS2 import signal is cleaved off subsequent to matrix protein import (11, 12, 15, 18, 20, 31, 33, 41). A completely conserved cysteine residue 35 to 45 amino acids downstream of the PTS2 has been suggested for the cleavage site of PTS2-containing precursor proteins (11, 12, 15, 18) (Table 1).

Although many attempts have been made to establish its identity, little is known about the enzyme responsible for PTS2 processing. Likely candidates must fulfill certain criteria: 1) since PTS1 import defects result in a lack of processing of PTS2 proteins and mutations that result in a lack of PTS2 import result in the accumulation of precursor protein in the cytosol, potential proteases must possess a PTS1 signal for peroxisome matrix localization (2, 15); 2) because yeast do not have proteolytically processed PTS2 proteins, potential candidates are not expected to have functional homologs in yeast (28); and 3) finally, the candidate protein must contain a proteolytic domain within its amino acid structure.

An insulin-degrading enzyme of the metalloproteinase family was localized to peroxisomes in mammalian fibroblasts cells (1). Although this protease, renamed PP110 for peroxisomal protease of 110kDa, was capable of degrading a synthetic presequence of thiolase, it failed to process full-length thiolase *in vitro*

(1). In plants, a 35kDa cysteine endopeptidase was isolated from the glyoxysomes of germinating castor bean endosperm via its capacity to specifically process the precursor form of the PTS2 protein malate dehydrogenase *in vivo*; the same endopetidase was unable to cleave thiolase at the proper processing site *in vitro* (9). Moreover, the castor bean protease was not peroxisomally localized, but rather it was localized to ricinosomes, which are ER-derived organelles that develop in senescing endosperm cells of plants, concomitant with nuclear DNA fragmentation (10). An ATP-dependent Lon protease, distinct from the mitochondrial isoform, was identified in rat liver peroxisomes (19). Like its bacterial and mitochondrial homologs, however, this protease is likely to function as a chaperone, degrading unfolded proteins (19).

Recently, more promising candidates for processing the PTS2-containing propeptide have been recognized. A novel PTS1-targeted protein called Tysnd1 (trypsin-domain-containing protein 1) was identified in mammalian peroxisomes. This protein was demonstrated to be responsible for both the removal of PTS2-containing leader peptide from prethiolase and for processing of PTS1 proteins involved in the peroxisomal β-oxidation pathway of fatty acids in mammals (20). Using a cell-based assay, these authors show that Tysnd1 overexpression led to the *in vitro* processing of the peroxisomal enzymes to fragments identical to the sizes described for their endogenous forms (20). Moreover, Tysnd1 itself is reported to undergo processing in a cysteine-dependent manner similar to its substrates, perhaps as an auto-activating mechanism (20).

The plant Tysnd1 homolog belongs to a group of ATP-independent trypsin-like serine proteases (12). This protease, referred to as Deg15, has been partially purified from the fat-storing cotyledons of watermelon (*Citrullus vulgaris*) and examined for its ability to act as a glyoxysomal processing protease (GPP) (12). In watermelon, Deg15 functions in two forms, a 72 kDa monomer and a 144 kDa dimer, whose equilibrium can be shifted in the presence of Ca^{2+} in favor of the dimeric GPP/Deg15 form, reportedly responsible for cleavage of the PTS2 presequence of malate dehydrogenase at the proper, cysteine-containing location (12). The monomer, on the other hand, acts as a general peptidase that cleaves denatured peroxisome matrix proteins (12).

In Arabidopsis, a knockout mutation in *DEG15* prevents processing of glyoxysomal malate dehydrogenase (gMDH) to its mature form (12). Although the presence of unprocessed malate dehydrogenase in *deg15* mutants provides evidence that DEG15 may be the PTS2-processing protease in plants, its peroxisomal localization and specific cleavage of PTS2 proteins *in vitro* have not yet been experimentally defined.

Using RT-PCR we isolated and cloned *DEG15* (At1g28320) from wild-type Arabidopsis plants. Only the unprocessed, precursor form of the PTS2 protein thiolase (THL) was present in *atdeg15* knockout mutants, consistent with the lack of processing of malate dehydrogenase previously described (12). Our results from *in vitro* peroxisome import, protease assays and mutagenic analysis indicate that AtDEG15 is a peroxisomal protease that specifically processes PTS2 proteins in Arabidopsis.

MATERIALS AND METHODS

DNA constructs. Plasmids containing the full-length cDNA inserts for isocitrate lyase (IL) from *Brassica napus,* spinach (*Spinacia oleracea*) glycolate oxidase (GLO), and thiolase (THL) from Arabidopsis were previously described (3, 4, 14). The plasmid (pASP3) containing the full-length cDNA insert coding for aspartate aminotransferase 3, in the pZL1 expression vector, was obtained from the Arabidopsis Biological Resource Center at Ohio State University (Columbus; EST stock 136A4T7; GenBank accession no. P46644; Arabidopsis Genome Initiative locus At5g11520). Mutants for THL and ASP3 constructs in the pZL1 expression vector were obtained using the Site-Directed Mutagenesis (SDM) kit (Statagene); mutations and primers are shown in Table 2.

To obtain the full-length cDNA of *AtDEG15* (At1g28320), the cDNA product from RT-PCR using RNA extracted from the leaves of wild-type plants was cloned into the *in vitro* expression vector pCRII-TOPO (Invitrogen). Additionallly, a bacterial expression construct encoding an amino-terminal maltose binding protein (MBP) fused to AtDEG15 was prepared by subcloning the full-length *AtDEG15* gene into the pMalC2 vector (New England Biolabs). Transformants were screened by PCR amplification using *AtDEG15* gene-specific primers (forward: 5’ GTC GAC ATG GAT GTG TCT AAA GTT GTC 3’ and reverse: 5’ CTC GAG GGC ACA AAT TAT GCA AAG AAG 3’) and a primer specific to the MalE gene located within the vector pMalC2 (5’ GCG GTC GTC

AGA CTG TCG ATG AAG CC 3'). DNA sequencing confirmed all DNA constructs.

Protein expression and purification. To synthesize radiolabeled GLO, IL, THL, ASP3, and AtDEG15 proteins all DNA templates were linearized with an appropriate restriction enzyme such that a single cleavage occurred 3' (RNA sense) to the coding region to be transcribed/translated (GLO, HindIII; IL, SphI; THL and ASP3, NotI or XbaI; AtDEG15, SacI). Transcription of the linearized DNA with SP6 RNA polymerase for pGLO and IL, T7 RNA polymerase for all others, was performed as described previously (24, 32). Radiolabeled proteins were synthesized in a cell-free wheat germ lysate system in the presence of [^{35}S]- L- methionine, (specific activity 43.3 TBq/mmol) purchased from MP Biomedicals, Inc. (Irvine, CA). The efficiency of translation was assessed by trichloroacetic acid precipitation onto glass fiber filters, followed by ethanol washes and quantitation in a liquid scintillation counter (model LS 6800, Beckman Coulter, Fullerton, CA). Radiolabeled THL and ASP3 were synthesized in their full-length precursor protein forms.

Full-length MBP-AtDEG15 was expressed in *E. coli* BL21 induced with isopropyl β-D-1-thiogalactopyranoside (IPTG) to a final concentration of 0.3 mM at 37°C for 4 hours. MBP-AtDEG15 was purified by affinity chromatography on amylose resin as described in the manufacturer's instructions (New England Biolabs). Following purification, protein concentration was determined by the Bradford protein assay (BioRad). Purified recombinant MBP-AtDEG15 was

resolved by 10% SDS-PAGE and assayed by Western blotting with anti-MBP (New England Biolabs) and anti-SKL antibodies (see below).

Isolation of pumpkin glyoxysomes. Pumpkin seeds (*Cucurbita pepo* var Connecticut Fields) purchased from Siegers Seed Co. (Zeeland, MI) seedlings were grown in moist vermiculite for 5 to 7 days in the dark at 25°C. Approximately 25-40 g cotyledons were harvested manually in dim light and glyoxysomes were isolated by slight modification of the procedure described previously (3). Initial homogenization occurred with three 3-second bursts using a Waring blender. Filtration was performed through one layer of Miracloth (Calbiochem). The final glyoxysomal pellet was resuspended in isolation buffer to a final concentration of 20 mg/ml total protein.

***In vitro* import assays.** Standard *in vitro* import reactions were initiated by the addition of 200 μg glyoxysomes to 500,000 cpm trichloroacetic-acid-precipitable, radiolabeled protein in the presence of import buffer (25 mm MES-KOH, pH 6, 500 mM sucrose, 10 mM KCl, 1 mM $MgCl_2$ and 5 mM MgATP) in a final volume of 200 μl. All import reactions were performed at 26°C for 1 hour unless otherwise noted. Following incubation, the import reactions were treated with thermolysin (freshly dissolved in import buffer containing 5 mM $CaCl_2$) using the following concentrations: GLO, 100 μg/ml; THL, 250 μg/ml; ASP3, 500 μg/ml; DEG15 100 μg/ml, to completely digest proteins that were not imported. Protease treatments were incubated for 30 min. on ice; reactions were stopped by the

addition of EDTA (25 mM final concentration) to inhibit the thermolysin. After protease treatment, the glyoxysomes were repurified on a 0.7 M sucrose cushion, solubilized in 1X (Laemmli) sample buffer, subjected to 10% SDS-PAGE and visualized by autoradiography after 12-16 hour overnight exposure at -70°C. Some samples (indicated in the figures) were incubated at either 4°C or -20°C during import to provide negative import controls. Note that the protein from these samples was fully digested after treatment with thermolysin and no longer detectable subsequent to repurification of glyoxysomes on sucrose. Each of the proteins used in these experiments contain roughly the same number of methionine residues (GLO, 13 Met residues; precursor THL and ASP3, as well as all associated SDM mutants have 12 Met residues). Therefore, equal counts of radioactive protein represent nearly equal amounts of protein presented for import.

Genotypic analysis. Seeds for the T-DNA insertion line Salk_007184, with a potential mutation in *AtDEG15,* were purchased from the Arabidopsis Biological Resource Center at Ohio State University. Seedlings were germinated on Murashige-Skoog media (Sigma-Aldrich) supplemented with 1% sucrose under 16-hour light/ 8-hour dark conditions at 22°C. DNA was extracted from the leaves of 2-week old seedlings. Leaf tissue was homogenized (200 mM Tris-HCl, pH 7.5, 250 mM NaCl, 25 mM EDTA and 0.5% SDS), vortexed, and immediately placed on ice. Following centrifugation in a microcentrifuge at maximum speed for 5 min., the supernatant was transferred to fresh tubes and the DNA was

precipitated with an equal volume of isopropanol for 2 min. at room temperature. The resulting DNA pellet was washed in 70% ethanol, air-dried and dissolved in 15-20 μl glass-distilled water. T-DNA insertions were detected by PCR with gene-specific primers (forward- 5' CGC TAG TGT AGC CAT AAT TCA CCT G 3'; reverse- 5' TGC GTA TTC TTT TCA GGG TCA GC 3') and the LBc1 primer (5' GCC GAT TTC GGA AGG AGG ATC 3') using conditions of 52°C annealing for 30 seconds and 1 minute 72°C extension for 25 cycles.

At 4 weeks, plants were transferred to fertilized soil and maintained under 16-hour light/ 8-hour dark conditions at 22°C for subsequent phenotypic analysis.

RT-PCR. Total RNA was extracted from the leaves of 2-week old wild-type and *deg15* mutant seedlings using the RNeasy Plant Mini kit (Qiagen) with column DNase I digestion, according to the manufacturer's directions. RNA was eluted with 30μl RNase-free water and quantitated by spectrophotometry at 260 nm. RT-PCR was performed using the Access RT-PCR System (Promega); PCR conditions of 52°C annealing for 30 seconds and 2.5 minute 72°C extension for 30 cycles. Each RT-PCR reaction contained 150 ng of RNA template and 100 ng each of either *AtDEG15* gene-specific primers (forward: 5' GTC GAC ATG GAT GTG TCT AAA GTT GTC 3' and reverse: 5' CTC GAG GGC ACA AAT TAT GCA AAG AAG 3'), or *β-tubulin* gene-specific primers (forward: 5' ATA CAG AAC AAG AAC TCG TCT TAC 3' and reverse: 5' CTC TTC TTC TTC AAC ATC ATA CTC 3').

Western blot analysis. Whole plant extracts were prepared from 2-week old wild-type, *atlon2-3* and d*eg15* seedlings by homogenization in 2X (Laemmli) sample buffer using 200 μl/100 μg plant tissue and boiled for 5 min. at 100°C. The extract (0.5 μg) was separated by 10% SDS-PAGE and blotted onto an Immobilon-P PVDF membrane (Millipore). The blot was probed with plant anti-THL (PED1) polyclonal antibodies to detect the presence of precursor and mature forms of thiolase. Secondary antibody detection was performed with goat anti-rabbit IgG secondary antibody conjugated to horseradish peroxidase (BioRad).

***In vitro* protease assays.** Purified recombinant MBP-AtDEG15 or thermolysin (in 5 mM $CaCl_2$) was added in excess of 10X the amount of radiolabeled substrate (GLO, THL, ASP3, and all SDM mutants) in 50 mM Hepes, pH 8.0, 115 mM NaCl and 0.2 mM DTT at 37°C for 4 hours. Reactions were stopped by the addition of an equal volume of 2X (Laemmli) sample buffer, followed by boiling for 5 min. at 100°C. 10μl of each reaction product was separated by 10% SDS-PAGE and visualized by autoradiography following 12-16 overnight exposure at -70°C. The concentration of each radiolabelled protein used in these experiments was based on a calculation that considered the following: counts of radioactivity (in cpm) present in each *in vitro* translation reaction, divided by the specific activity of ^{35}S/ molecule of methionine (in cpm), divided by the number of molecules of methionine present in each molecule of protein, divided by the specific number of molecules found in a mole of protein (6.02×10^{23} molecules),

multiplied by the molecular weight of each protein (in g/mole). For example, if protein A has 10 methionines, 5 x 10^5cpm/μl, and a molecular weight of 50000g/mole, then it's concentration would be determined as follows: (5 x 10^4cpm/μl) X (1 met/4.33x10^{-7}cpm) X 1 molecule protein/10 met) X (1 mole/6.02 x 10^{23}) X (50000g/mole)= 959 x 10^{-12}g/μl = .959ng/μl

Other reagents. Seeds for the T-DNA insertion line Salk_043857, with a potential mutation in the protease *AtLON2,* were purchased from the Arabidopsis Biological Resource Center at Ohio State University. T-DNA insertion mutants (*atlon2-3*) were identified by PCR amplification of DNA extracted from the leaves of germinated seedlings and confirmed by sequencing (Johnson and Olsen, unpublished data, not shown). Anti-THL (PED1) crude serum was a kind gift of Dr. Bonnie Bartel (Rice University, Houston Texas). The antibody was raised in rabbit against a fusion protein produced in pGEX-4T that included the carboxyl terminal 350 amino acid residues of AtTHL. Dr. Stanley R. Terlecky (Wayne State University, Detroit Michigan) generously donated the anti-SKL antiserum used to detect purified recombinant AtDEG15. For Western blots, anti-PED1 and anti-SKL antibodies were used at a 1:10,000 dilution in 1X phosphate-buffered saline (PBS) containing 0.05% Tween-20 and 5% nonfat dry milk (PBST). Anti-MBP was purchased from New England Biolabs (Ipswich, MA) and diluted 1: 75,000 in PBST for immunoblot analysis. Goat anti-rabbit IgG secondary antibody conjugated to horseradish peroxidase was purchased from BioRad (Hercules, CA) and diluted 1:100,000 in PBST for immunoblot analysis.

RESULTS

AtDEG15 imports into the isolated glyoxysomes of pumpkins (*Cucurbita pepo*) in vitro. Using RT-PCR we isolated and cloned *DEG15* from Arabidopsis. In vitro transcription, followed by in vitro translation of [^{35}S]-radiolabeled protein resulted in a 70kDa protein product (Figure 1A, left). Western blot analysis using an anti-SKL antibody immunologically recognized the 70 kDa band (Figure 1A, right).

To confirm the peroxisome localization of AtDEG15, suggested by the PTS1 sequence, –SKL, present at its carboxyl terminus, in vitro peroxisomal protein import assays were performed using glyoxysomes isolated from pumpkin cotyledons and protease resistance as the hallmark of protein import into glyoxysomes (i.e. proteins protected by the glyoxysomal membrane are not degraded by subsequent protease digestion). In each import experiment, all protease-protected protein was considered as imported. The results of a typical import experiment are shown in Figure 1B. The pattern of AtDEG15 import into peroxisomes was similar to that of the control peroxisomal protein glycolate oxidase (GLO), a PTS1 photorespiration enzyme whose import has been previously characterized (Brickner et al., 1997; Brickner and Olsen, 1998). Lane 1 represents all protein bound to the membrane or imported into the organelle. Protease was added to the samples shown in lane 2 to degrade proteins not protected by the peroxisome membrane, leaving only protease-protected, imported proteins. The import reaction was also performed at 4°C (lane 3) to

demonstrate that under conditions not conducive to import, the amount of protease added to the samples is enough to completely degrade unprotected, not imported, protein. From these results it is clear that AtDEG15 imports into peroxisomes (Figure 1).

Thiolase (THL) is not processed in *deg15* knockout mutants in Arabidopsis. To assess the physiological role of AtDEG15, a T-DNA insertion mutant line was purchased from the ABRC stock center: Salk_007184. Genotypic analysis of plants revealed a DNA product consistent with a T-DNA insertion in the fourth intron of *AtDEG15* (At1g28320). PCR amplification of genomic DNA extracted from the leaves of two-week-old mutant plants with either gene-specific left or right primers and the T-DNA specific primer yielded 600 bp and 800 bp products (Figure 2A, panel 2), whereas PCR analysis of genomic DNA extracted from the wild-type tissue resulted in a single product of 1000bp (Figure 2A, panel 1). RT-PCR confirmed that *AtDEG15* was not expressed in these mutants (Figure 2B, lane 4). Immunoblot analysis performed with anti-THL antibodies revealed that THL was not processed to its mature form in these *atdeg15* knockout plants (Figure 2C). Interestingly, these seeds appear to have sucrose-dependent germination; only 25% of mutant seedlings planted on sucrose germinated as compared to the 94% wild-type seedlings germinated at the same time and under the same conditions (Figure 3). By 4-8 weeks, no detectable differences between the growth of the wild-type and mutant plants were observed.

AtDEG15 directly processes thiolase in vitro. Full-length MBP- AtDEG15 was expressed in *E. coli*. Purified recombinant MBP-AtDEG15 was resolved by 10% SDS-PAGE and assayed by Western blotting with anti-MBP and anti-SKL antibodies. A 119 kDa band was detected with both antibodies, consistent with the calculated size expected for an amino-terminal tagged MBP-AtDEG15 fusion protein product (Figure 4A). To assess the *in vitro* proteolytic activity of AtDEG15 with PTS2 proteins, purified, recombinant MBP- AtDEG15 was incubated with the radiolabeled substrates GLO (PTS1), IL (PTS1), and precursor THL (PTS2). Upon incubation with AtDEG15, THL was proteolytically cleaved, as evidenced by the appearance of a distinct lower molecular weight band migrating at 47kDa, the size reported for the endogenous mature form found in Arabidopsis (Figure 4B, THL panel, lane 3). AtDEG15 showed no proteolytic activity when incubated with the PTS1 proteins GLO and IL (Figure 4B, GLO and IL panels, lane 3). Total proteolytic digestion was obtained when incubating each protein in the presence of the nonspecific metalloproteinase thermolysin (Figure 4B, lane 4).

In vivo processing of precursor PTS2 proteins occurs at a conserved cysteine residue located at the carboxyl terminal end of their presequences (Table 1). Site-directed mutagenesis studies indicate that changing this conserved residue to glycine or phenylalanine results in the inhibition of processing of chimeric proteins, possessing the amino-terminal presequence of glyoxysomal citrate synthase (gCS) fused to β-glucuronidase (GUS), subsequent to their import into microbodies in transgenic plants (15, 16, 18). To test the importance of this conserved cysteine residue for AtDEG15 specific cleavage of

thiolase, site-directed mutagenesis was performed to change the cysteine (C34), located 19 amino acids downstream of the PTS2 sequence, to glycine. As a direct result of this mutation, proteolytic processing of thiolase by AtDEG15 *in vitro* was hindered (Figure 4B, bottom panel lane 3). These results suggest that AtDEG15 is the processing protease for THL in Arabidopsis.

Aspartate Aminotransferase 3 (ASP3) is a PTS2 dependent peroxisome matrix enzyme that is processed by AtDEG15 *in vitro*. Aspartate aminotransferase (EC 2.6.1.1; AspAT) catalyzes the reversible reaction: aspartate + α-ketoglutarate ←→ oxaloacetate + glutamate. In plants, AspAT exists as multiple isozymes localized to different subcellular compartments. For example, in maize and cucumber (13, 23, 38), specific AspAT isozymes have been associated with the mitochondrion, chloroplast, glyoxysome and cytosol. In Arabidopsis, 5 AspAT isozymes have been identified that are targeted to different subcellular compartments (Figure 5A): ASP1 (mitochondrial), ASP2 and ASP4 (cytosolic), ASP5 (chloroplastic). ASP3 is predicted to encode either a plastid or peroxisomal enzyme based on analysis of its putative transit peptide sequences (5). Analysis of the amino terminus of ASP3 reveals an obvious nonapeptide sequence, -RIGALLRHL- (Figure 5B), consistent with that of PTS2 sequences currently identified in plants (36). To investigate the import of ASP3 into peroxisomes, *in vitro* import assays were performed. The results indicate that ASP3 imports into peroxisomes in a manner similar to the previously characterized PTS2 protein THL (14) (Figure 5C). Radiolabeled ASP3 becomes

protease-protected after incubation with isolated pumpkin glyoxysomes and subsequent protease treatment (Figure 5C, bottom panel lane 2). In our import experiments, there was not always an observed distinction between precursor and processed forms of imported PTS2 proteins although this difference is clear, at least for thiolase, in the representative gel of the import shown here. This is possibly because processing of PTS2 proteins can occur at any time after import and although there is much evidence that the processing of PTS2 proteins occurs in vivo, the temporal sequence of proteolytic cleavage and intracellular import has yet to be determined.

In plants, the first three of the four residues of the original PTS2 nonapeptide consensus sequence are highly conserved; positions 1, 8 and 9 are R, H, and L, respectively (36). To determine whether the putative PTS2 signal for ASP3 is functional, the R in the first position of the nonapeptide was changed to an A using site-directed mutagenesis. As a control for PTS2-dependent import, the R in the first position in the PST2 sequence of THL was also mutated to an A. These mutations resulted in loss of import for both THL and ASP3 (Figure 5C, bottom panel, lane 5), indicating that ASP3 is a PTS2-dependent peroxisome matrix enzyme.

The amino acid sequence of ASP3 does not contain a conserved cysteine residue near the carboxyl terminus of its PTS2 presequence (Figure 5B). Since this is the first time, to our knowledge, that ASP3 peroxisomal import has been characterized, it remains to be determined whether ASP3 is cleaved following import. While we have observed protease-protected ASP3 migrating at a lower

molecular weight in our in vitro assays (data not shown), we cannot conclude that this shift in mobility is necessarily due to a processing event because the observation of precursor and processed forms of imported PTS2 proteins in our in vitro assays remains unpredictable (14). To address the question of whether ASP3 is processed, we examined the proteolytic activity AtDEG15 in the context of its ability to cleave ASP3 *in vitro*. Incubation of purified recombinant MBP-AtDEG15 resulted in the cleavage of ASP3. Visualization of the cleavage product by autoradiography revealed a lower molecular weight band, migrating at 43kDa, after direct incubation with AtDEG15 (Figure 5D, WT panel, lane 2).

To investigate the specificity of the AtDEG15 cleavage recognition site in ASP3, site-directed mutagenesis was used to create three different mutagenic constructs in the pZL1 expression vector containing the full-length cDNA for *ASP3*: S41 to G41, S47 to G47, and C148 to G148. Each of the three mutations represented potential sites for the cleavage of precursor ASP3 into its mature form (Figure 5D). Subsequent to incubation with purified recombinant MBP-AtDEG15, all of the potential cleavage site mutants were processed *in vitro* (Figure 5D, lanes 4,6, and 8). Although it is clear from our results that ASP3 was processed to its mature form, this AtDEG15-mediated cleavage does not occur at any of the cleavage sites we predicted.

***In vitro* AtDEG15-mediated processing of PTS2 proteins occurs independently from their targeting to glyoxysomes.** To investigate the extent to which the PTS2 sequence plays a role in the recognition and subsequent

cleavage of PTS2 proteins by AtDEG15, the loss-of-import R-to-A variants from THL and ASP3 were each incubated with purified recombinant AtDEG15. Figure 6 shows that AtDEG15 is capable of processing these variants equally as well as their import competent partners. As expected, the cleavage mutants of both THL and ASP3 show import competency when assayed in our *in vitro* import system (data not shown). These results indicate that AtDEG15 processing of PTS2 proteins is not dependent upon the recognition of a functional PTS2.

DISCUSSION

Proteins are targeted to the peroxisome by a PTS2 less frequently than by its predominant counterpart, the PTS1. Plant PTS2-containing proteins account for about 10% of all proteins targeted to the peroxisome matrix (36). In plants and mammals, PTS2 proteins are synthesized and imported as precursors with larger molecular weight masses than those of the mature proteins (11, 12, 17, 18, 20, 21, 31, 33, 41).

Using RT-PCR, we isolated a 76kDa peroxisomal member of the DegP protease family in Arabidopsis, AtDEG15 (At1g28320), which directly processed PTS2 proteins *in vitro*. In addition to a trypsin-like serine protease domain, AtDEG15 contains a clearly defined, extreme carboxyl terminal PTS1 sequence, SKL, and was imported to glyoxysomes *in vitro* (Figure 1). AtDEG15 is involved in specifically processing PTS2 proteins. Consistent with previously published evidence concerning the processing of the PTS2 protein gMDH (12, 20), a knockout mutation resulting in the lack of expression of AtDEG15 also prevents processing of the classic PTS2-containing protein thiolase to its mature form (Figure 2). In addition, we demonstrate direct proteolytic activity *in vitro,* where incubation of recombinant purified AtDEG15 with thiolase resulted in the direct processing of this enzyme to a lower molecular weight consistent with the size reported for its endogenous, mature form (Figure 3). Furthermore, this AtDEG15-mediated processing of thiolase was dependent on the cysteine residue located at amino acid position 34, immediately downstream of its PTS2; the exact

processing site for reported thiolase in Arabidopsis (16). Our results are partially consistent with those reported for the AtDEG15 mammalian homolog, Tysnd1 (20). These authors demonstrated that Tysnd1 was directly responsible for both the cysteine-dependent removal of the PTS2-containing leader peptide from prethiolase and for specific processing of all PTS1 proteins involved in the peroxisomal β-oxidation pathway of fatty acids in mammals (20).

The third isozyme of aspartate aminotransferase (ASP3) was shown to be a bona fide PTS2-dependent peroxisome enzyme in Arabidopsis (Figure 5C). AtDEG15 was also able to process ASP3 to a lower molecular weight form (Figure 5D) although the identity of the precise cleavage recognition site in ASP3 has yet to be determined. An alignment of the 5 aspartate aminotransferase (ASPAT) isozymes identified in Arabidopsis, specifically focusing on those that are targeted to organelles, reveals a 65% sequence conservation in the region downstream of the known amino-terminal presequence cleavage sites for ASPATs targeted to the chloroplast (ASP5) and mitochondria (ASP1) (Figure 7). In addition, alignment of this same region amongst the ASP3 homologs found in Arabidopsis, rice, and soybean shows 97% sequence conservation (Figure 8). Therefore, it is reasonable to predict that the AtDEG15 cleavage recognition site is probably located within the seventeen amino acid residues immediately downstream of the PTS2 sequence because elimination of these non-conserved amino acids would likely not change any conserved domain structure between the ASPATs that also possibly contribute to conserved function.

The physiological relevance of processing of PTS2-containing proteins in the peroxisomes of plants and mammals is not yet understood. One theory is that processing is a necessary mechanism for the activation of PTS2 enzymes within the matrix of peroxisomes. Indeed, in this study, we observed that AtDEG15 knockout mutants in Arabidopsis have a sucrose-dependent germination phenotype (Figure 3), similar to other PTS2 import defective mutants (43). Whereas the latter phenotype is due to an import deficiency that results in a lack of resident PTS2 proteins in the matrix, the former would imply a lack of enzyme function, since it is clear that PTS2 import is normal in *atdeg15* knockout mutants. However, recombinant proteins from both the full-length cDNA of the glyoxysomal thiolase from *Brassica napus* and the truncated version, lacking the amino-terminal targeting signal, have comparable activity when expressed in *E. coli* (30). Also, processing events are not present in yeast, yet yeast PTS2 proteins are fully functional. Therefore, it is likely that PTS2 enzyme function is not a consequence of processing.

PTS2 protein import is characterized by the binding of the PTS2 sequence to the PTS2 receptor PEX7, which facilitates PTS2 protein entry and translocation into the peroxisome matrix followed by the recycling of the import receptor back out into the cytosol for further rounds of PTS2 import (21, 29). Although PEX7 function requires the assistance of several species-specific auxiliary proteins (21, 25, 34, 35, 39, 40, 42, 43), PEX7 binding alone is essential for PTS2 recognition and delivery of proteins into the peroxisome matrix. Perhaps, the subsequent processing of PTS2 presequences could aid in the

dissociation of PEX7 from its cargo on the matrix side of the peroxisome membrane to liberate PEX7 for recycling. A caveat to this theory comes from PTS2 import in yeast: evidence of recycling of PEX7 is reported within these species (6), although no apparent PTS2 protein processing mechanism exists.

One final consideration for the physiological relevance of PTS2 protein processing concerns the preservation of evolutionarily conserved roles for proteins that have evolved to require different modes of import. Both targeting pathways have been identified in highly divergent eukaryotes - from trypanosomes, to yeasts, plants and mammals. Surprisingly, not all peroxisome enzymes have maintained the same mechanism of targeting throughout evolution. In fact, examination of the same peroxisomal proteins from species to species shows evidence for target signal switching of PTS1 and PTS2 proteins (27). For example, plant PTS2 proteins malate dehydrogenase and citrate synthase have clearly defined, experimentally validated PTS1s in *S. cerevisiae* (22, 26). Likewise, acyl-CoA-oxidase is targeted to the peroxisome by a PTS1 signal in both *P. pastoris* and mammals, but it is a PTS2 protein in plants (7). The most dramatic example of target switching lies within the species *C. elegans*. Orthologs of proteins required in the PTS2 import pathway are absent from the genome of *C. elegans* (27). In fact, the entire PTS2 targeting pathway is absent in this species (27). Not surprising, every PTS2-containing protein found in other species has PTS1-containing homologs in *C. elegans*. In light of target switching, it is reasonable to propose that PTS2 protein processing could serve as a mechanism to maintain identical enzyme-substrate interactions and multiple

enzyme complex formations responsible for mediating the same functions regardless of the position of the signal sequence from species to species. As a result of cleavage, PTS2 proteins from one species would maintain the same contact surfaces at their amino terminus as their PTS1 orthologs present in other species.

Regardless of the hypothesized physiological role of processing for PTS2-containing peroxisome matrix proteins in plants and mammals, the first step towards understanding its purpose comes from identifying and characterizing the protein responsible. In this study we have cloned, purified, and examined the direct PTS2-specific proteolytic activity of AtDEG15 in Arabidopsis. Our studies directly show that AtDEG15 is a PTS2 processing protease.

FUTURE DIRECTIONS

Subsequent to our initial identification and characterization of AtDEG15 as the PTS2 processing protease, is a full examination of the factors that influence this cleavage. First, a conserved cysteine residue 35 to 45 amino acids downstream of the PTS2 has been suggested for the cleavage site of PTS2-containing precursor proteins (11, 12, 15, 18). But what other factors does AtDEG15 require that determines the protein-protein interaction required for recognition and specific cleavage of PTS2-containing precursor proteins? Using deletion constructs, mutagenic analyses, and protease assays, the functional organization of both AtDEG15 and the amino terminus of PTS2-containing proteins can be elucidated.

Second, the watermelon homolog of AtDEG15 was partially purified and identified as a glyoxysomal processing protease (GPP) (12). Consistent with our findings, these authors also attribute the specific cleavage of PTS2-carrying proteins to this DegP protease. However, in watermelon, DegP15 is proposed to function in two forms, a 72kDa monomer and a 114kDa dimer whose equilibrium can be shifted in the presence of Ca^{2+} in favor of the dimeric GPP/DEGP15 form, reportedly responsible for cleavage of the PTS2 presequence of malate dehydrogenase at the proper, cysteine-containing location (12). The monomer, on the other hand, acts as a general peptidase that cleaves denatured peroxisome matrix proteins (12). With our in vitro protease assays, we demonstrated AtDEG15 cleavage of PTS2 leader peptide sequences in the

absence of calcium. Although these results suggest that AtDEG15 is able to specifically process PTS2 proteins in the absence of calcium, AtDEG15-dependent processing may be increased by the addition of calcium. Indeed when calcium is added to import of PTS2 proteins (THL and ASP3) in vitro, there is an increase of protease-protected, imported protein that migrates at the lower molecular weight consistent with processed, mature forms (Williams and Olsen, unpublished data).

Third, the mammalian homolog of AtDEG15, Tysnd1, is reported to undergo intracellular amino-terminal processing in a transient overexpression assay (20). This cleavage event resulted in the generation of a smaller molecular weight, catalytically active form. This suggests that Tysnd1 could be synthesized in the cytosol as an inactive precursor that is cleaved to an active form upon entry into the peroxisome matrix. These results are consistent with the idea that the PTS2 processing protease may undergo catalytic autoactivation; a common mechanism found among serine proteases (8). It may be interesting to examine whether or not AtDEG15 undergoes this catalytic activation both in vitro and in vivo, whether an additional enzyme present within the peroxisome matrix or self-catalysis mediates this cleavage and further, to determine if this potential catalytic cleavage is necessary to promote AtDEG15 cleavage of PTS2 proteins.

Finally, what is the identity of the protein responsible for proteolytic degradation of the precursor sequence subsequent to its liberation from the amino terminus of the mature PTS2 protein by AtDEG15? Given the amount of precursor protein that must be processed after PTS2 import, it is conceivable that

digestion of the precursor sequence is absolutely required to prevent an accumulation that may be toxic to the peroxisome matrix environment. An answer to this question, however, depends on knowing more about the identity of the degradation activity that occurs within peroxisomes. In chloroplasts, a novel activity, separate from the stromal processing protease has been shown (37). Perhaps a likely candidate for this activity will be uncovered as the proteomic identity of the peroxisome matrix is revealed.

ACKNOWLEDGEMENTS

This work was supported in part by a fellowship from Pfizer/Rackham Graduate School, University of Michigan, to A.L.W. The authors thank Dr. Bonnie Bartel (Rice University) and Dr. Stanley Terlecky (Wayne State University) for generously sharing reagents.

FOOTNOTES

The discussion of future directions for this work is written in fulfillment of dissertation requirements and is not included as part of the manuscript to be submitted for publication.

Plants and mammals

Enzyme Species	PTS2 sequence (cleavage recognition site*)	Mature subunit
Malate dehydrogenase		
Watermelon	Q**RIARISAHL**HPPKSQMEESSALRRAN**C**R*	AKGGAPGFKVAI
Pumpkin	E**RIARISAHL**PPKSQMEEGSVLRRAN**C**R*	AKGGAPGFRVAI
Alfalfa	S**RITRIASHL**NPPNLKMNEHGGSSLTNVH**C**R*	AKGGTPGFKVAI
Rice	R**RMERLASHL**RPPASQMEESPLLRGSN**C**R*	AKGAAPGFKVAI
Rapeseed	K**RIAMISAHL**QPSFTPQMEAKNSVMGLES**C**R*	AKGGNPGFKVAI
Arabidopsis (At5g09660)	Q**RIARISAHL**TPQMEAKNSVIGREN**C**R*	AKGGNPGFKVAI
Arabidopsis (At2g22780)	Q**RIARISAHL**NPPNLHNQIADGSGLNRVA**C**R*	AKGGSPGFKVAI
Citrate synthase		
Pumpkin	RH**RLAVLAAHL**SAASLEPPVMASSLEAH**C**V*	SAQTMVAPPEL
Arabidopsis (At2g42790)	RA**RLAVLSGHL**SEGKQDSPAIERW**C**T*	SADTSVAPLGS
Arabidopsis (At3g58740)	RA**RLAVLNAHL**TVSEPNQVLPAIEPW**C**T*	SAHITAAPHGS
Acyl CoA oxidase		
Pumpkin	R**RIERLSLHL**TPIPLDDSQGVEMET**C***	AAGKAKAKIEVD
Arabidopsis (At5g65110)	R**RIQRLSLHL**SPSLTLSPSLPLVQTET**C***	SARSKKLDVNGE
3-keto-acyl-CoA thiolase		
Cucumber	N**RQSILLHHL**RPSSSAYTNESSLSASV**C***	AAGDSASY
Pumpkin	N**RQSILLHHL**RPSSSAYSHESSLSASV**C***	AAGDSASY
Mango	N**RQSILLHHL**RPSNSSSHNYESALAASV**C***	AAGDSAAY
Rapeseed	E**RQRVLLEHL**RPSSSSSHSFEGSLSASA**C***	LAGDSAAY
Arabidopsis (At5g48880)	E**RQRVLLEHL**RPSSSSSHNYEASLSASA**C***	LAGDSAAY
Rat	H**RLQVVLGHL**AGRPESSSALQAAP**C***	SAGFPQAS
Human	Q**RLQVVLGHL**RGPADSGWMPQAAP**C***	LSGAPQAS

Table 3.1. Consensus sequences of known PTS2 matrix proteins in mammals and plants. The PTS2 is underlined and indicated in bold. The conserved Cys near the cleavage site for recognition by the peroxisomal processing peptidase in plants and mammals is indicated in bold. Adapted from Helm (2007).

Protein	Mutation	Primer pairs used	
		FORWARD	**REVERSE**
THL	R7A	5’ GAG AAA GCG ATC GAG GCA CAA CGC GTT CTT C 3’	5’ GAA GAA CGC GTT GTG CCT CGA TCG CTT TCT C 3’
	C34G	5’ CTA TCT GCT TCT GCT GGC TTG GCT GGG GAC 3’	5’ GTC CCC AGC CAA GCC AGC AGA AGC AGA TAG 3’
ASP3	R15A	5’ TCT TCT TCT TCC GAT CGC GCT ATC GGT GCT CTG CTC C 3’	5’ GGA GCA GAG CAC CGA TAG CGC GAT CGG AAG AAG AAG A3’
	S41G	5’ CTT TAT GCA TCT CCG ACA GGC GGA GGC ACC GGT GGT TCT G 3’	5’ CAG AAC CAC CGG TGC CTC CGC CTG TCG GAG ATG CAT AAA G 3’
	S47G	5’ CAT CGG GAG GCA CCG GTG GTG GAG TTT TCT CTC ATC TTG TTC 3’	5’GAA CAA GAT GAG AGA AAA CTC CAC CAC CGG TGC CTC CCG ATG 3’
	C148G	5’ CGG ATT ACC ACC GTG GAG GGA TTG TCT GGT ACT GGT TCT C 3’	5’ GAG AAC CAG TAC CAG ACA ATC CCT CCA CGG TGG TAA TCC G 3’

Table 3.2. THL and ASP3 primers. THL, thiolase; ASP3, aspartate aminotransferase 3.

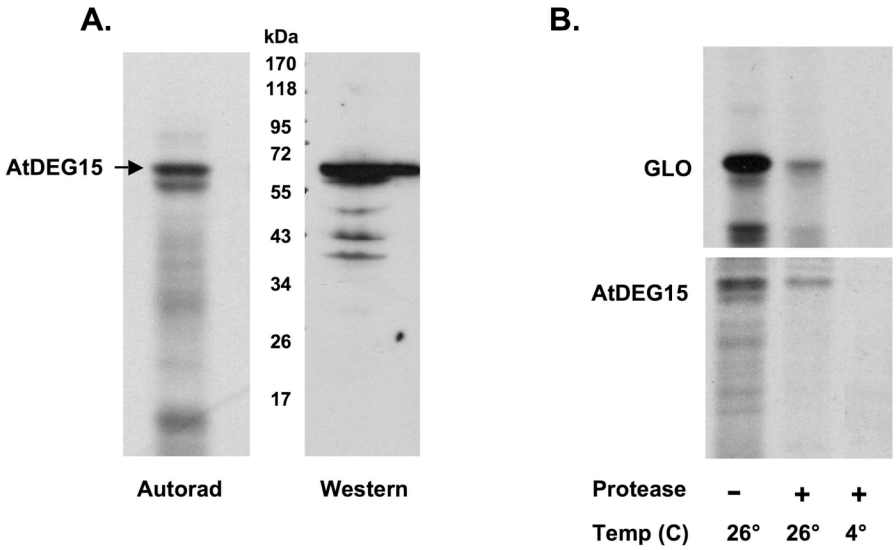

Figure 3.1. AtDEG15 imports into isolated pumpkin glyoxysomes *in vitro*. A) RT-PCR was used to clone *AtDEG15* into TOPO vector pCRII. *In vitro* transcription with T7 polymerase followed by *in vitro* translation produced [^{35}S-met]-radiolabeled AtDEG15 protein. Samples were analyzed by SDS-PAGE and visualized by autoradiography (left) and immunologically identified by Western blot analysis (right) using an anti-SKL antibody. B) Isolated glyoxysomes were incubated with the radiolabeled proteins AtDEG15 and GLO (glycolate oxidase) under standard import conditions, as described in Materials and Methods. Following import, some samples were incubated with the protease thermolysin. Intact glyoxysomes were reisolated and samples were prepared for analysis by SDS-PAGE. A typical autoradiograph is shown. These results are from a representative experiment that was repeated at least 3 times. Both proteins were protease protected, consistent with peroxisomal localization.

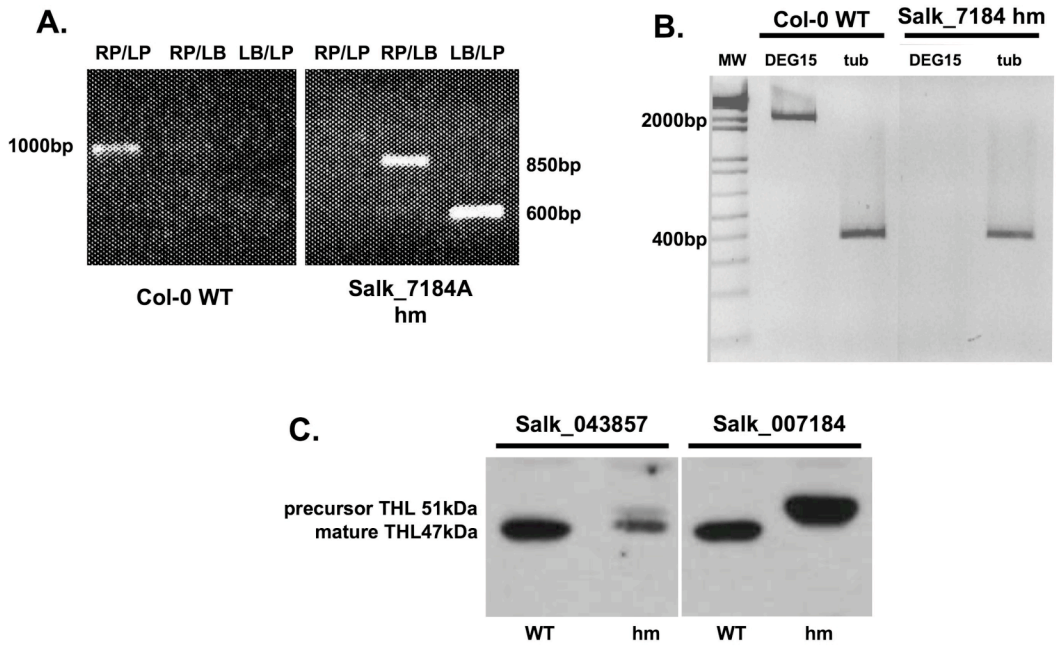

Figure 3.2. Thiolase is not processed in plants from a homozygous T-DNA knockout mutation (7184A) in the At*DEG15* gene. A) Genotypic analysis was performed on wild-type (Col-0) and mutant (7184A) plant DNA with primers specific to *AtDEG15* (RP/LP) and the T-DNA insertion (LB). The results from the PCR amplification of DNA extracted from both the wild-type and the T-DNA insertion mutant are shown. B) Results from reverse transcription followed by PCR of RNA extracted from the leaves of wild-type and the T-DNA insertion mutant is shown. Primers specific to *AtDEG15* and *β-tubulin* are indicated as 15 and tub, respectively. C) Western blot analysis of protein extracts from wild-type and mutant plants probed with anti-thiolase antibodies. WT, wild type; hm, homozygous

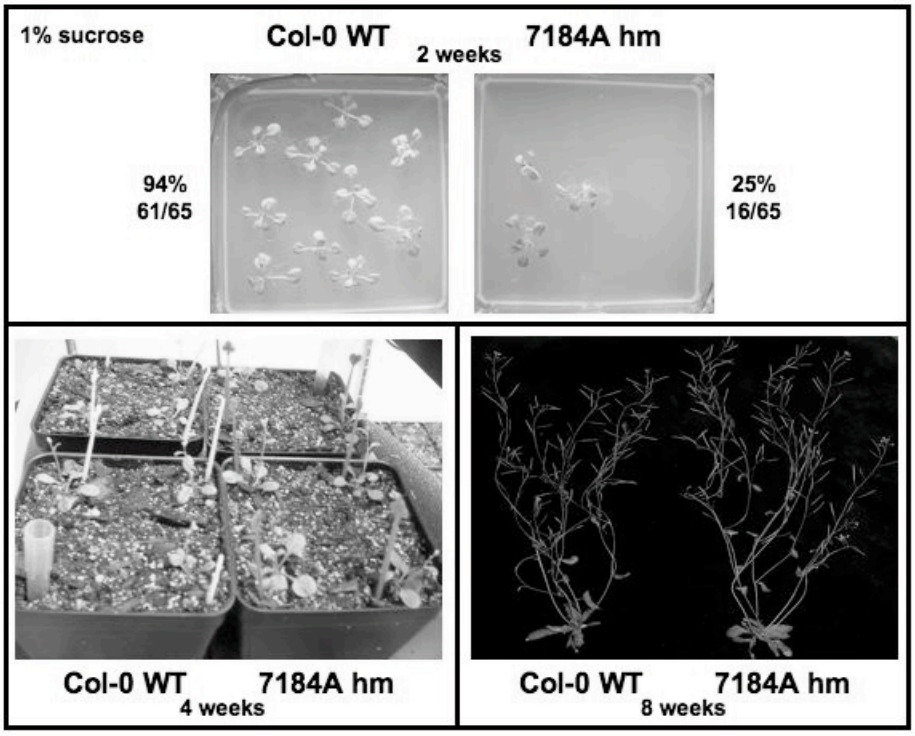

Figure 3.3. Plants with a homozygous mutation in At*DEG15* germinate poorly and require sucrose to germinate. Seeds from wild type (Col-0) and homozygous mutants were germinated on 1% sucrose-supplemented growth media. Seeds were incubated under 16-hour light/ 8-hour dark conditions at 22°C. After 2 weeks, seedlings germinated on sucrose-supplemented media were transferred to fertilized soil and incubated under 16-hour light/ 8-hour dark conditions at 22°C. A representative picture of growth stages at 2, 4 and 8 weeks are shown.

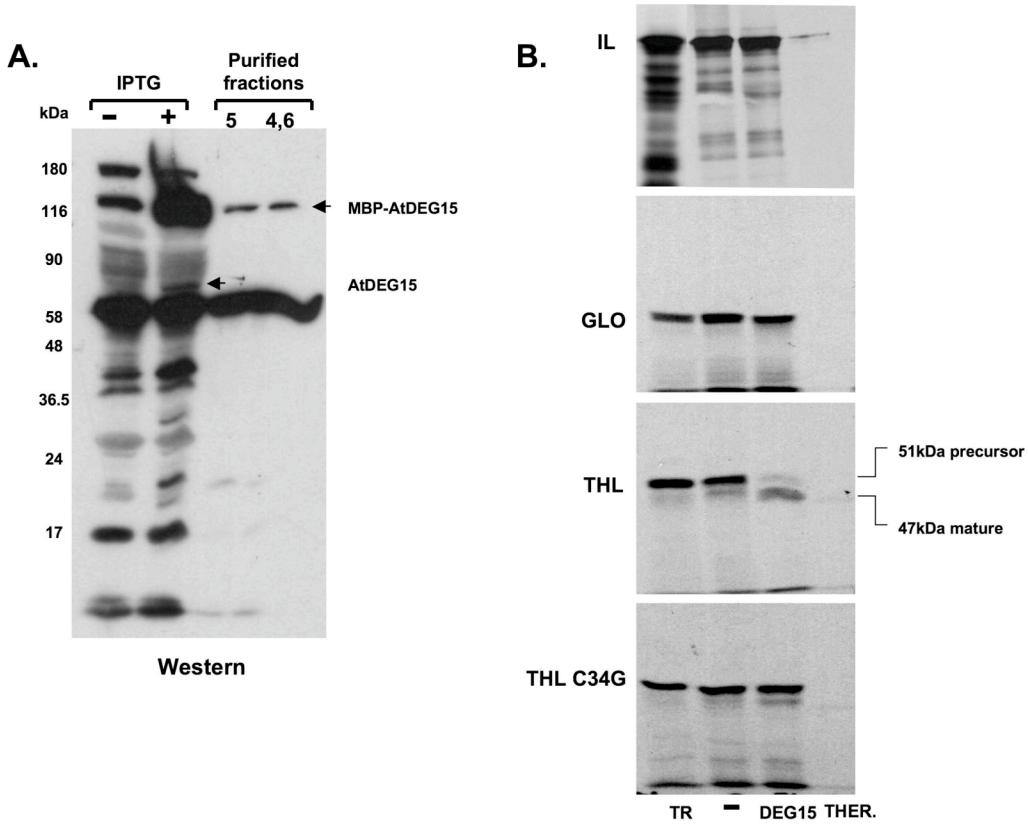

Figure 3.4. Recombinant AtDEG15 processes thiolase (THL), but not PTS1 proteins GLO and IL *in vitro*. A) Full-length AtDEG15 fused to an amino terminal MBP tag was expressed in *E. coli*. MBP-AtDEG15 was purified by affinity chromatography on amylose resin and resolved by SDS-PAGE. The indicated samples were analyzed by Western blot analysis with anti-SKL antibodies. B) **Top three panels**: radiolabeled proteins IL (isocitrate lyase; PTS1), GLO (glycolate oxidase; PTS1) and THL (thiolase; PTS2) were incubated without and with protease (either AtDEG15 or the protease thermolysin). **Bottom panel:** the highly conserved cysteine residue at the cleavage site in thiolase (amino acid position 34) was changed by site-directed mutagenesis to a glycine residue. Radiolabeled protein from the C34G mutant was incubated without and with protease (either AtDEG15 or the protease thermolysin). All samples were prepared for analysis by SDS-PAGE. A typical autoradiograph is shown. These results are from a representative experiment that was repeated at least 3 times. TR, in vitro translated, radiolabeled protein; "-", no protease added; DEG15, AtDEG15 added; THER, thermolysin added

A.

Name	AGI number	Localization
ASP1	At2g30970	mitochondria
ASP2	At5g19550	cytosol
ASP3	At5g11520	*plastid/peroxisome*
ASP4	At1g62800	cytosol
ASP5	At4g31990	plastid

B.

```
  1 mktthfssss ssdrrigall rhlnsgsdsd
 31 nlsslyaspt sggtggsvfs hlvqapedpi
 61 lgvtvaynkd pspvklnlgv gayrteegkp
 91 lvlnvvrkae qqlindrtri keylpivglv
121 efnklsakli lgadspaire nrittvecls
151 gtgslrvgge flakhyhqkt iyitqptwgn
181 hpkiftlagl tvktyryydp atrglnfqgl
211 ledlgaaapg sivllhacah nptgvdptiq
241 qweqirklmr skglmpffds ayqgfasgsl
271 dtdakpirmf vadggeclva qsyaknmgly
301 gervgalsiv cksadvagrv esqlklvirp
331 mysppihga sivavilrdk nlfnewtlel
361 kamadriism rkqlfealrt rgtpgdwshi
391 ikqigmftft glnpaqvsfm tkeyhiymts
321 dgrismagls sktvphlada ihavvtkav
```

C.

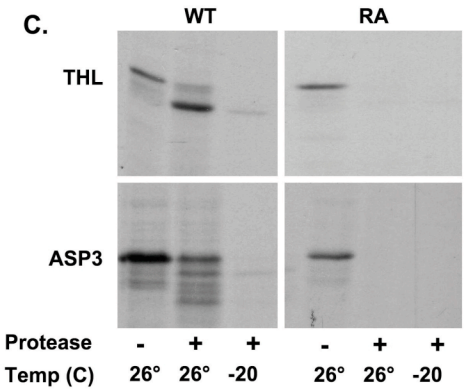

D.

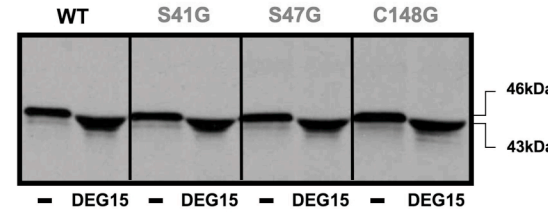

Figure 3.5. The PTS2-dependent peroxisome protein AtASP3 is also processed by AtDEG15 *in vitro*. A) The five ASPAT isozymes from Arabidopsis, the gene locus, and intracellular protein locations are shown. The putative peroxisome enzyme encoded by At5g11520, ASP3, is indicated in red. B) The complete amino acid sequence for AtASP3. The amino-terminal PTS2 sequence is shown in bold and underlined. The amino acid residues at the potential cleavage sites of ASP3 are indicated in bold red. C) Isolated glyoxysomes were incubated with the radiolabeled proteins THL, ASP3, or their respective PTS2 mutants (RA) under standard import conditions, as described in Materials and Methods. Following import, all samples were incubated with the protease thermolysin. Intact glyoxysomes were reisolated and samples were analyzed by SDS-PAGE. Note that placing an alanine residue in the first position of the signal sequence abolished the PTS2-directed targeting and that there is no protease-protected mutant protein for either THLRA or ASP3RA (lane 5). Only wild-type proteins with their PTS2 fully intact were protease protected (lane 2), consistent with peroxisome localization. D) Site-directed mutagenesis was used to change each putative cleavage site (S41, S47 and C148) to a glycine residue. Radiolabeled protein was synthesized from wild-type ASP3 and each mutant (S41G, S47G and C148G). Each radiolabeled protein was incubated without and with protease (either purified, recombinant AtDEG15 or the general protease thermolysin). Samples were analyzed by SDS-PAGE. A typical autoradiograph is shown. These results are from a representative experiment repeated at least 3 times. TR, translated protein; "-", no protease added; DEG15, AtDEG15 added; THER, thermolysin added

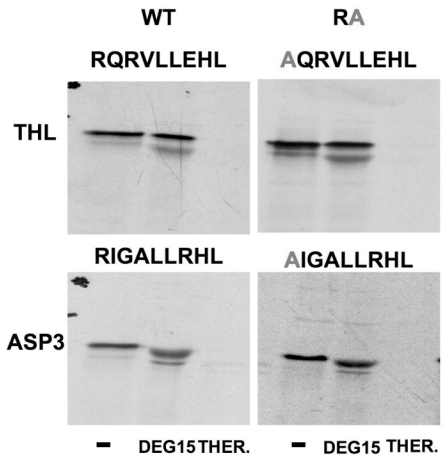

Figure 3.6. Mutants lacking a functional PTS2 are still processed by AtDEG15 *in vitro*. Radiolabeled proteins from THL, ASP3, and the RA import mutants were each incubated without and with protease (either purified, recombinant AtDEG15 or the protease thermolysin). Samples were prepared for analysis by SDS-PAGE. A typical autoradiograph is shown. These results are from a representative experiment repeated at least 3 times. The PTS2 sequence of each protein is shown; mutated residues are red. WT, wild type; RA, PTS2 mutants; "-", no protease added; DEG15, AtDEG15 added; THER, thermolysin added

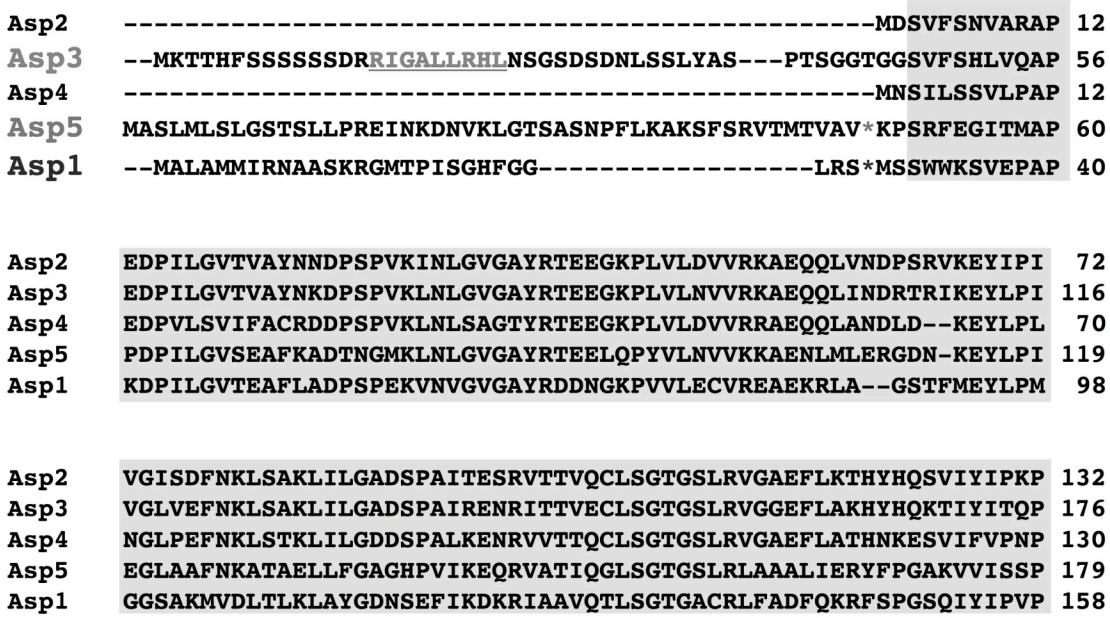

Figure 3.7. Sequence alignment of the ASPAT isozymes found in Arabidopsis. The amino terminal sequences of the ASPAT isozymes found in Arabidopsis are shown. Black, green, blue, and red names indicate cytosolic, plastidic, mitochondrial, and peroxisomal localizations, respectively. Asterisks indicate the cleavage recognition sites for plastid and mitochondrial ASPATs. The PTS2 sequence for the peroxisomal ASPAT, ASP3, is bold, underlined, and shown in red. Blue-shaded boxes indicate areas of sequence conservation. Data were obtained using ClustalW, a web-based EBI server for multiple sequence alignment (www.ebi.ac.uk/clustalw/).

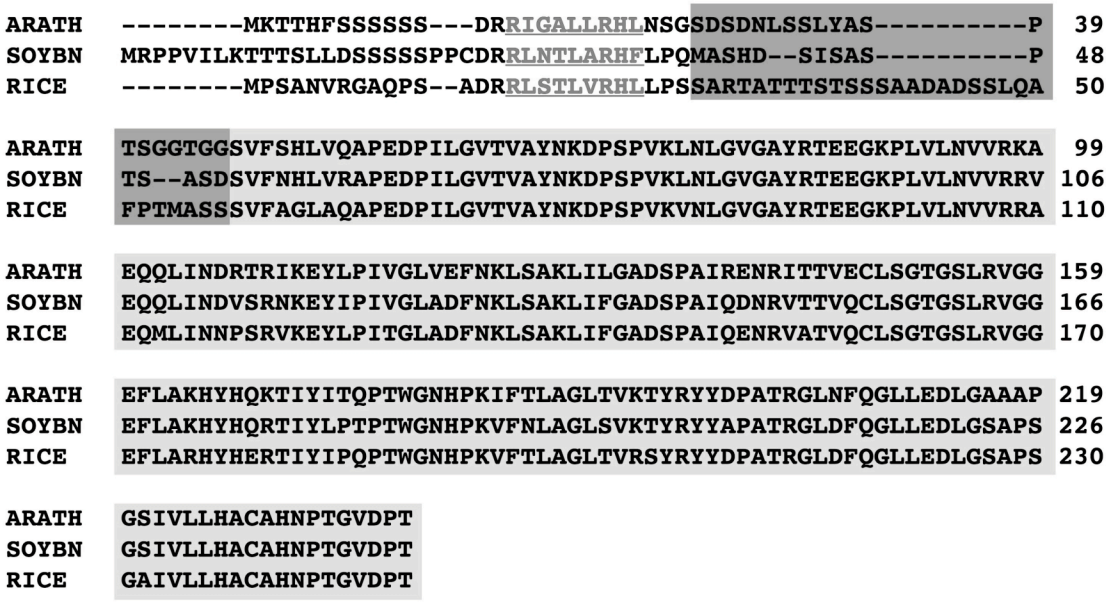

Figure 3.8. Sequence alignment of some plant ASP3 homologs. The amino terminal sequences of the ASP3 homologs from Arabidopsis, rice, and soybean are shown. The PTS2 sequences are bold, underlined, and shown in red. Lilac shading indicates areas of non-conserved amino acid sequence, and blue shading indicates areas of high sequence conservation. Data were obtained using ClustalW, a web-based EBI server for multiple sequence alignment (www.ebi.ac.uk/clustalw/).

REFERENCES

1. **Authier, F., J. J. Bergeron, W. J. Ou, R. A. Rachubinski, B. I. Posner, and P. A. Walton.** 1995. Degradation of the cleaved leader peptide of thiolase by a peroxisomal proteinase. Proc Natl Acad Sci U S A **92:**3859-63.
2. **Balfe, A., G. Hoefler, W. W. Chen, and P. A. Watkins.** 1990. Aberrant subcellular localization of peroxisomal 3-ketoacyl-CoA thiolase in the Zellweger syndrome and rhizomelic chondrodysplasia punctata. Pediatr Res **27:**304-10.
3. **Brickner, D. G., J. J. Harada, and L. J. Olsen.** 1997. Protein transport into higher plant peroxisomes. In vitro import assay provides evidence for receptor involvement. Plant Physiol **113:**1213-21.
4. **Comai, L., R. A. Dietrich, D. J. Maslyar, C. S. Baden, and J. J. Harada.** 1989. Coordinate expression of transcriptionally regulated isocitrate lyase and malate synthase genes in Brassica napus L. Plant Cell **1:**293-300.
5. **Coruzzi, G. M.** 2003. Primary N-assimilation into Amino Acids in Arabidopsis. *In* E. M. Chris Somerville (ed.), The Arabidopsis Book. American Society of Plant Biologists, Rockville, MD.
6. **Elgersma, Y., M. Elgersma-Hooisma, T. Wenzel, J. M. McCaffery, M. G. Farquhar, and S. Subramani.** 1998. A mobile PTS2 receptor for peroxisomal protein import in Pichia pastoris. J Cell Biol **140:**807-20.
7. **Froman, B. E., P. C. Edwards, A. G. Bursch, and K. Dehesh.** 2000. ACX3, a novel medium-chain acyl-coenzyme A oxidase from Arabidopsis. Plant Physiol **123:**733-42.
8. **Gal, P., V. Harmat, A. Kocsis, T. Bian, L. Barna, G. Ambrus, B. Vegh, J. Balczer, R. B. Sim, G. Naray-Szabo, and P. Zavodszky.** 2005. A true autoactivating enzyme. Structural insight into mannose-binding lectin-associated serine protease-2 activations. J Biol Chem **280:**33435-44.
9. **Gietl, C., B. Wimmer, J. Adamec, and F. Kalousek.** 1997. A cysteine endopeptidase isolated from castor bean endosperm microbodies processes the glyoxysomal malate dehydrogenase precursor protein. Plant Physiol **113:**863-71.
10. **Greenwood, J. S., M. Helm, and C. Gietl.** 2005. Ricinosomes and endosperm transfer cell structure in programmed cell death of the nucellus during Ricinus seed development. Proc Natl Acad Sci U S A **102:**2238-43.
11. **Hayashi, H., L. De Bellis, K. Yamaguchi, A. Kato, M. Hayashi, and M. Nishimura.** 1998. Molecular characterization of a glyoxysomal long chain acyl-CoA oxidase that is synthesized as a precursor of higher molecular mass in pumpkin. J Biol Chem **273:**8301-7.
12. **Helm, M., C. Luck, J. Prestele, G. Hierl, P. F. Huesgen, T. Frohlich, G. J. Arnold, I. Adamska, A. Gorg, F. Lottspeich, and C. Gietl.** 2007. Dual specificities of the glyoxysomal/peroxisomal processing protease Deg15 in higher plants. Proc Natl Acad Sci U S A **104:**11501-6.

13. **Huang, A. H., K. D. Liu, and R. J. Youle.** 1976. Organelle-specific Isozymes of Aspartate-alpha-Ketoglutarate Transaminase in Spinach Leaves. Plant Physiol **58:**110-113.
14. **Johnson, T. L., and L. J. Olsen.** 2003. Import of the peroxisomal targeting signal type 2 protein 3-ketoacyl-coenzyme a thiolase into glyoxysomes. Plant Physiol **133:**1991-9.
15. **Kato, A., M. Hayashi, M. Kondo, and M. Nishimura.** 1996. Targeting and processing of a chimeric protein with the N-terminal presequence of the precursor to glyoxysomal citrate synthase. Plant Cell **8:**1601-11.
16. **Kato, A., M. Hayashi, M. Kondo, and M. Nishimura.** 2000. Transport of peroxisomal proteins synthesized as large precursors in plants. Cell Biochem Biophys **32 Spring:**269-75.
17. **Kato, A., M. Hayashi, Y. Takeuchi, and M. Nishimura.** 1996. cDNA cloning and expression of a gene for 3-ketoacyl-CoA thiolase in pumpkin cotyledons. Plant Mol Biol **31:**843-52.
18. **Kato, A., Y. Takeda-Yoshikawa, M. Hayashi, M. Kondo, I. Hara-Nishimura, and M. Nishimura.** 1998. Glyoxysomal malate dehydrogenase in pumpkin: cloning of a cDNA and functional analysis of its presequence. Plant Cell Physiol **39:**186-95.
19. **Kikuchi, M., N. Hatano, S. Yokota, N. Shimozawa, T. Imanaka, and H. Taniguchi.** 2004. Proteomic analysis of rat liver peroxisome: presence of peroxisome-specific isozyme of Lon protease. J Biol Chem **279:**421-8.
20. **Kurochkin, I. V., Y. Mizuno, A. Konagaya, Y. Sakaki, C. Schonbach, and Y. Okazaki.** 2007. Novel peroxisomal protease Tysnd1 processes PTS1- and PTS2-containing enzymes involved in beta-oxidation of fatty acids. Embo J **26:**835-45.
21. **Lazarow, P. B.** 2006. The import receptor Pex7p and the PTS2 targeting sequence. Biochim Biophys Acta **1763:**1599-604.
22. **Lewin, A. S., V. Hines, and G. M. Small.** 1990. Citrate synthase encoded by the CIT2 gene of Saccharomyces cerevisiae is peroxisomal. Mol Cell Biol **10:**1399-405.
23. **Liu, K. D., and A. H. Huang.** 1977. Subcellular Localization and Developmental Changes of Aspartate-alpha-Ketoglutarate Transaminase Isozymes in the Cotyledons of Cucumber Seedlings. Plant Physiol **59:**777-782.
24. **Lubben, T. H., and K. Keegstra.** 1986. Efficient in vitro import of a cytosolic heat shock protein into pea chloroplasts. Proc Natl Acad Sci U S A **83:**5502-5506.
25. **Matsumura, T., H. Otera, and Y. Fujiki.** 2000. Disruption of the interaction of the longer isoform of Pex5p, Pex5pL, with Pex7p abolishes peroxisome targeting signal type 2 protein import in mammals. Study with a novel Pex5-impaired Chinese hamster ovary cell mutant. J Biol Chem **275:**21715-21.
26. **McAlister-Henn, L., J. S. Steffan, K. I. Minard, and S. L. Anderson.** 1995. Expression and function of a mislocalized form of peroxisomal malate dehydrogenase (MDH3) in yeast. J Biol Chem **270:**21220-5.

27. **Motley, A. M., E. H. Hettema, R. Ketting, R. Plasterk, and H. F. Tabak.** 2000. Caenorhabditis elegans has a single pathway to target matrix proteins to peroxisomes. EMBO Rep **1:**40-6.
28. **Mullen, R. T.** 2002. Targeting and Import of Matrix Proteins into Peroxisomes. Kluwer Academic Publishers, Netherlands.
29. **Nair, D. M., P. E. Purdue, and P. B. Lazarow.** 2004. Pex7p translocates in and out of peroxisomes in Saccharomyces cerevisiae. J Cell Biol **167:**599-604.
30. **Olesen, C., K. K. Thomsen, I. Svendsen, and A. Brandt.** 1997. The glyoxysomal 3-ketoacyl-CoA thiolase precursor from Brassica napus has enzymatic activity when synthesized in Escherichia coli. FEBS Lett **412:**138-40.
31. **Olsen, L. J.** 1998. The surprising complexity of peroxisome biogenesis. Plant Mol Biol **38:**163-89.
32. **Olsen, L. J., S. M. Theg, B. R. Selman, and K. Keegstra.** 1989. ATP is required for the binding of precursor proteins to chloroplasts. J Biol Chem **264:**6724-9.
33. **Osumi, T., T. Tsukamoto, S. Hata, S. Yokota, S. Miura, Y. Fujiki, M. Hijikata, S. Miyazawa, and T. Hashimoto.** 1991. Amino-terminal presequence of the precursor of peroxisomal 3-ketoacyl-CoA thiolase is a cleavable signal peptide for peroxisomal targeting. Biochem Biophys Res Commun **181:**947-54.
34. **Otera, H., T. Harano, M. Honsho, K. Ghaedi, S. Mukai, A. Tanaka, A. Kawai, N. Shimizu, and Y. Fujiki.** 2000. The mammalian peroxin Pex5pL, the longer isoform of the mobile peroxisome targeting signal (PTS) type 1 transporter, translocates the Pex7p.PTS2 protein complex into peroxisomes via its initial docking site, Pex14p. J Biol Chem **275:**21703-14.
35. **Purdue, P. E., X. Yang, and P. B. Lazarow.** 1998. Pex18p and Pex21p, a novel pair of related peroxins essential for peroxisomal targeting by the PTS2 pathway. J Cell Biol **143:**1859-69.
36. **Reumann, S.** 2004. Specification of the peroxisome targeting signals type 1 and type 2 of plant peroxisomes by bioinformatics analyses. Plant Physiol **135:**783-800.
37. **Richter, S., and G. K. Lamppa.** 2002. Determinants for removal and degradation of transit peptides of chloroplast precursor proteins. J Biol Chem **277:**43888-94.
38. **Scandalios, J. G., J. C. Sorenson, and L. A. Ott.** 1975. Genetic control and intracellular localization of glutamate oxaloacetic transaminase in maize. Biochem Genet **13:**759-69.
39. **Schliebs, W., and W. H. Kunau.** 2006. PTS2 co-receptors: diverse proteins with common features. Biochim Biophys Acta **1763:**1605-12.
40. **Sichting, M., A. Schell-Steven, H. Prokisch, R. Erdmann, and H. Rottensteiner.** 2003. Pex7p and Pex20p of Neurospora crassa function together in PTS2-dependent protein import into peroxisomes. Mol Biol Cell **14:**810-21.

41. **Swinkels, B. W., S. J. Gould, A. G. Bodnar, R. A. Rachubinski, and S. Subramani.** 1991. A novel, cleavable peroxisomal targeting signal at the amino-terminus of the rat 3-ketoacyl-CoA thiolase. Embo J **10:**3255-62.
42. **Titorenko, V. I., J. J. Smith, R. K. Szilard, and R. A. Rachubinski.** 1998. Pex20p of the yeast Yarrowia lipolytica is required for the oligomerization of thiolase in the cytosol and for its targeting to the peroxisome. J Cell Biol **142:**403-20.
43. **Woodward, A. W., and B. Bartel.** 2005. The Arabidopsis peroxisomal targeting signal type 2 receptor PEX7 is necessary for peroxisome function and dependent on PEX5. Mol Biol Cell **16:**573-83.

CHAPTER FOUR

Peroxisome matrix protein import: the study of putative dual-signaled peroxisome matrix proteins

ABSTRACT

To date, all models of peroxisome matrix protein import agree that each respective receptor PEX5 or PEX7 binds to a distinct, newly synthesized protein in the cytosol bearing either a Peroxisome Targeting Signal (PTS) 1 protein or PTS2, respectively. The receptor/cargo complex follows a distinct pathway that converges at the docking site on the peroxisome membrane, after which the cargo is translocated into the matrix and the receptor is recycled to the cytosol for further rounds of import. Two proteins found in *Arabidopsis thaliana* have been identified that possess both a putative PTS1 and a PTS2: long-chain acyl-CoA synthetase 7 (LACS7) and alpha-crystallin domain-containing protein 31.2 (ACD31.2). While both proteins have been localized to peroxisomes, the PTS responsible for their localization remains unclear. Using mutagenic analysis and a standard *in vitro* protein import assay, the import of each protein and the role that each of its putative PTSs plays in this subcellular localization was characterized. For both proteins ACD31.2 or LACS7, either the PTS1 or PTS2

alone was sufficient to direct import into the peroxisome matrix. Removal of both signals totally abolished peroxisomal import of ACD31.2 and LACS7.

INTRODUCTION

Peroxisomal matrix protein import is accomplished when a single targeting sequence, present on newly synthesized peroxisome matrix proteins is bound by a specific receptor in the cytosol that facilitates import. In the case of PTS2 protein import, additional interactions between the PTS2 receptor PEX7 and other co-factors are required to complete the PTS2-dependent import process (27). Nevertheless, it remains clear that most peroxisome matrix protein import is directed by an independent interaction between one targeting signal (PTS1 or PTS2) and its specific targeting pathway receptor (PEX5 or PEX7, respectively) (2, 5, 9, 14, 22, 31, 33). Interestingly, a few unique enzymes predicted to be associated with peroxisomes have been identified that contain both a putative PTS1 and PTS2.

PEX8, the yeast importomer complex linker protein, contains both a PTS1 and a PTS2 sequence (23, 29, 30). Studies involving PEX8 from *Hansenula polymorpha* first revealed that both the PTS1 and its interaction with PEX5 are required for targeting of PEX8 (34). Also, deletion of the PTS2 motif on PEX8 results in PEX5-directed PTS1 import (34). Similarly, PEX8 lacking its PTS1 sequence is imported via the PTS2 pathway. In this case, the targeting depends on both PEX7 and its auxillary protein PEX20 (15, 28, 34).

Two proteins identified in *Saccharomyces cerevisiae,* Dci1 and Eci1, belong to the isomerase/hydratase family and share 50% sequence identity. Both of these proteins are localized to peroxisomes, and both contain sequences at

their carboxyl and amino-termini that resemble PTS1 and PTS2, respectively (13, 32). PTS1-dependent targeting of both Eci1 and Dci1 has been demonstrated in wild-type cells (32). Surprisingly, although Eci1 peroxisomal targeting does in fact require the PEX5-dependent PTS1 pathway, it does not require a PTS1 of its own (32). It has been suggested that the PEX5-dependent import of Eci1 is due to interaction and co-import with its partner Dci1 (32).

Long-chain acyl-CoA synthetase (LACS) activities are critically involved in the breakdown of the stored lipid reserves to release free fatty acids and feed the β-oxidation cycle in peroxisomes. Two genes, *LACS6* and *LACS7*, from *Arabidopsis thaliana* have been identified that code for peroxisomal LACS proteins. While LACS6 is targeted by a single peroxisomal targeting sequence (PTS2), LACS7 possesses both a predicted PTS1 (SKL) as well as a PTS2 (RLx_5HI) (7) (Figure 1C). Subcellular localization studies of PTS fusions to the green fluorescent protein (GFP) reveal that localization of LACS7 is dependent on both PTS1 and PTS2 (7). Yeast two-hybrid analysis and co-immunoprecipitation show LACS7 interactions with the PTS1 receptor PEX5 (1), indicative of PTS1-dependent import. No interaction with PEX7 was detected, although a clear PTS2 signal is present at the amino terminus of the protein. Still, both the PTS1 and PTS2 of LACS7 appear necessary to direct its peroxisome entry. For this reason, further characterization of LACS7 import is needed.

Among the results of a screen for novel low-abundance proteins of plant peroxisomes were two genes identified in the Arabidopsis genome (At5g37670 or Hsp15.7 and At1g06460 or ACD31.2) (26), encoding two predicted proteins

possessing both an α-crystallin domain, characteristic of small heat-shock proteins, and putative targeting signals for plant peroxisomes (24). ACD31.2 (At1g06460) carries both a predicted PTS2 nonapeptide (RLx_5HF) and a predicted PTS1 tripeptide (PKL), both of which have been defined as minor PTS peptides that indicate peroxisome targeting (17, 24) (Figure 1). Double-labeling experiments using full-length fusion proteins with enhanced yellow fluorescent protein, as well as deletion and mutagenic constructs lacking the putative targeting domains, suggest that Hsp15.7 and ACD31.2 are targeted to the peroxisome matrix by a functional PTS1 (SKL) and a functional PTS2 (RLX_5HF), respectively (17). Though these experiments provide some evidence for PTS2-dependent peroxisome localization of ACD31.2, further biochemical investigation will be useful to assess whether dual-PTS-containing enzymes are capable of peroxisome import using one, both, or neither of their putative PTSs.

Using an *in vitro* peroxisome protein import assay, we examined the import characteristics of both ACD31.2 and LACS7. Both are peroxisome matrix proteins that become protease-protected after incubation with isolated glyoxysomes under standard import conditions. Removal of the PTS1 did not significantly affect the import of either protein into peroxisomes *in vitro*, though the import efficiency of ACD31.2 was slightly decreased. Likewise, mutations of the PTS2 signal that result in loss of import of PTS2 protein ASP3, did not significantly affect the PTS2-dependent import of ACD31.2 or LACS7. When the PTSs were simultaneously disabled for both ACD31.2 and LACS7, peroxisomal import was abolished. These results suggest that both ACD31.2 and LACS7

were capable of peroxisome protein import directed by either of their PTS1 or their PTS2.

MATERIALS AND METHODS

DNA constructs Plasmids containing the full-length cDNA inserts for isocitrate lyase (IL) from *Brassica napus,* spinach (*Spinacia oleracea*), glycolate oxidase (GLO), and thiolase (THL) from Arabidopsis were previously described (3, 4, 12). The plasmids *pASP3* and *pACD31.2*, containing the full-length cDNA insert coding for aspartate aminotransferase 3 (*ASP3*) and *ACD31.2* in the pZL1 expression vector, were each obtained from the Arabidopsis Biological Resource Center (EST stocks 136A4T7 and 31B9T7; GenBank accession nos. P46644 and T04728; Arabidopsis Genome Initiative locus At5g11520 and At1g06460, respectively).

To clone *LACS7*, the full-length gene was PCR-amplified from an Arabidopsis cDNA library, λ-Yes (6) using the following *LACS7* gene-specific primers: forward- 5' CAC CAT GGA ATT TGC TTC GCC GG 3' and reverse- 5' TCA CAG TTT AGA AGG AAT GGG GTT CGA GGC 3'. Following PCR amplification, full-length *LACS7* cDNA was cloned into the Gateway entry vector pENTR SD/D-TOPO according to the manufacturer's instructions (Invitrogen). Plasmids containing *LACS7* were isolated and the inserts confirmed by sequencing. Subsequently, an expression construct encoding full-length LACS7 fused with an amino-terminal GST in vector pDEST15 was made by recombination using the LR Clonase II enzyme according to the manufacturer's instructions (Invitrogen). Transformants were screened by PCR amplification

using *LACS7* gene-specific primers. DNA sequencing was used to confirm all DNA constructs.

PTS1-deletion constructs were created by restriction enzyme digestion with the appropriate enzyme to cleave several amino acids from the carboxyl terminus of the full-length DNA constructs. Restriction enzymes (Promega) used and the resulting deletion constructs for each protein are given in Table 1. All PTS2 mutant constructs were obtained using the Site-Directed Mutagenesis kit (Statagene); mutations and primers are shown in Table 2.

Preparation of [^{35}S-met]-radiolabeled peroxisome proteins. To synthesize radiolabeled GLO, THL, ASP3, ACD31.2 and LACS7 proteins, all DNA templates were linearized with an appropriate restriction enzyme such that a single cleavage occurred 3' to the coding region to be transcribed/translated (GLO, HindIII; THL, ASP3 and ACD31.2, NotI or XbaI; LACS7, NheI). Transcription of the linearized DNA with SP6 RNA polymerase for pGLO and T7 RNA polymerase for all others was performed as described previously (16, 21). Radiolabeled proteins were synthesized in a cell-free wheat germ lysate system in the presence of L- methionine, [^{35}S] (specific activity 43.5 TBq/mmol) purchased from MP Biomedicals, Inc. (Irvine, CA). The efficiency of translation was assessed by trichloroacetic acid precipitation onto glass fiber filters, followed by ethanol washes and quantitation in a liquid scintillation counter (model LS 6800, Beckman Coulter, Fullerton, CA). Radiolabeled THL and ASP3 were synthesized in their full-length precursor protein forms. Radiolabeled LACS7 was

synthesized with an amino-terminal GST fusion tag attached to the full-length protein product.

Isolation of pumpkin glyoxysomes. Pumpkin seeds (*Cucurbita pepo* var Connecticut Fields) purchased from Siegers Seed Co. (Zeeland, MI) seedlings were grown in moist vermiculite for 5-to-7 days in the dark at 25°C. Approximately 25-40 g cotyledons were harvested manually in dim light and glyoxysomes were isolated by slight modification of the procedure described previously (3). Initial homogenization occurred with three 3-second bursts using a Waring blender. Filtration was performed through one layer of Miracloth (Calbiochem). The final glyoxysomal pellet was resuspended in isolation buffer to a final concentration of 20 mg/ml total protein.

***In vitro* Import Assays.** Standard *in vitro* import reactions were initiated by the addition of 200 μg isolated glyoxysomes to 500,000 cpm trichloroacetic acid precipitable, radiolabeled protein in the presence of import buffer (25 mm MES-KOH, pH 6, 500 mM sucrose, 10 mM KCl, 1 mM $MgCl_2$ and 5 mM MgATP) in a final volume of 200 μl. Import reactions were performed at 26°C for 30 min. in the case of PTS1 protein import, and 1 hour in the case of PTS2 protein import. Following incubation, the import reactions were treated with thermolysin (freshly dissolved in import buffer containing 5 mM $CaCl_2$) to completely digest proteins that were not imported. Protease treatments were incubated for 30 min. on ice; reactions were stopped by the addition of EDTA (25 mM final concentration) to

inhibit the thermolysin. After protease treatment, the glyoxysomes were repurified on a 0.7 M sucrose, solubilized in 1X (Laemmli) sample buffer, subjected to 10% SDS-PAGE and visualized by autoradiography after a 12-16 hour overnight exposure at -70°C. Some samples (as indicated in the figures) were incubated at -20°C during import to provide negative import controls. The protein from these samples was fully digested after treatment with thermolysin and not recovered by the subsequent repurification of glyoxysomes on sucrose. In cases where import efficiency is reported, import levels were determined as described previously (12).

RESULTS

ACD31.2 and LACS7 imported into isolated glyoxysomes of pumpkins *(Cucurbita pepo) in vitro* despite the removal of their putative PTS1. *In vitro* synthesis of [^{35}S-met]-radiolabeled protein, using a cell-free wheat germ lysate system, was carried out. Visualization of radiolabeled proteins by autoradiography is shown in Figure 2. To study the import characteristics of ACD31.2 and LACS7, *in vitro* import assays were performed by incubation of radiolabeled import proteins with glyoxysomes isolated from etiolated pumpkin cotyledons. Protease resistance was used as the hallmark of protein import (i.e., proteins protected by the glyoxysomal membrane are not degraded by exogenous protease digestion). In each import experiment, all protease-protected protein was considered as imported. The results of a typical import experiment are shown in Figure 2A, full-length GLO. The pattern of ACD31.2 and LACS7 import into peroxisomes was similar to that of the control PTS1 photorespiration enzyme, glycolate oxidase (GLO), whose import has been previously characterized (Brickner et al., 1997; Brickner and Olsen, 1998). Lane 2 represents all protein bound to the membrane or imported into the organelle. Protease was added to the samples shown in lane 3 to degrade proteins not protected by the glyoxysome membrane, leaving only protease-protected, imported protein. Import reactions were also performed at -20°C (lane 4) to demonstrate that under conditions not conducive to import, the amount of

protease added to the samples was enough to completely digest unprotected protein.

Truncated GLO, ACD31.2, and LACS7 proteins lacking 46, 15, and 106 amino acids from the carboxyl terminus, respectively, were created by restriction enzyme digestion (Table 1). Results from standard import reactions with isolated pumpkin glyoxysomes revealed a loss of import of GLO lacking the PTS1 signal (Figure 2A, GLO panel, lane 6). In contrast, ACD31.2 and LACS7 carboxyl terminal truncation mutants showed no significant loss of import competency (Figure 2A, ACD31.2 and LACS7 panels, lane 6). These results indicate that both ACD31.2 and LACS7 are capable of peroxisomal import in the absence of their putative PTS1.

Mutations in the PTS2 sequence that inhibit the import of PTS2 proteins THL and ASP3 did not affect the import of ACD31.2 or LACS7. The results of a typical PTS2 protein import experiment are shown in Figure 3. The pattern of ACD31.2 and LACS7 import into peroxisomes was similar to that of control proteins thiolase (THL), the PTS2 β-oxidation enzyme (12), and aspartate amino transferase 3 (ASP3), the PTS2-containing enzyme responsible for transferring an amino group to ketoacids (Williams and Olsen, unpublished data), whose import has been previously described (12; Chapter 3, this thesis). All protein remained protease-protected (Figure 3, lane 3).

In plants, three of the four residues from the PTS2 nonapeptide consensus sequence are highly conserved; positions 1, 8 and 9, which are R, H

and L, respectively (24). In previous studies to determine functionality of the PTS2, site-directed mutagenesis was used to change the R in the first amino acid position of the nonapeptide to an A (see Chapter 3, this thesis). These mutations resulted in the loss of import for both THL and ASP3; no protease-resistant protein was observed following import *in vitro* (Figure 3, THL and ASP3 panels, lane 6). To determine whether the putative PTS2 signal is necessary for import of ACD31.2 and LACS7, site-directed mutagenesis was used to create the same arginine to alanine (R1A) mutations in the first amino acid positions of the putative PTS2 of ACD31.2 and LACS7. Protease-protected protein was observed following import for both the ACD31.2RA and the LACS7RA mutant (Figure 3, ACD31.2 and LACS7 panels, lane 6). Thus, these results indicate that both proteins are capable of import despite mutations in their putative PTS2.

Simultaneous disabling of PTS1 and PTS2 abolished import of both ACD31.2 and LACS7. Restriction digestion with the appropriate enzymes (Table 1) to remove the carboxyl terminus of ACD31.2 and LACS7 was performed on their PTS2 R1A mutants to create double-import-signal mutants. The results of a standard import assay are shown in Figure 4. As expected, no protease-resistant protein was observed following import of these double-signal mutants *in vitro* (lane 2). These results indicate that only when both targeting signals were non-functional was the *in vitro* import of ACD31.2 and LACS7 totally abolished.

DISCUSSION

Most peroxisome matrix proteins are expected to follow an exclusive import pathway directed by either a PTS1 or PTS2. However, unique peroxisome-targeted matrix enzymes have been identified that contain both a PTS1 and PTS2 (23, 28, 30). In Arabidopsis, two genes, *ACD31.2 and LACS7*, have been identified that code for peroxisome enzymes possessing putative redundant PTSs (7, 17). Subcellular localization of PTS-dependent variants of each protein fused to fluorescent tags reveals that localization of LACS7 is dependent on either PTS1 or PTS2 (7), while ACD31.2 is strictly PTS2 dependent (17). Interestingly, studies focused on determining LACS7 binding partners only show interactions with the PTS1 receptor PEX5 (1), indicative of PTS1-dependent import.

Using an *in vitro* biochemical assay reconstituting import into pumpkin glyoxysomes we have examined the import characteristics of ACD31.2 and LACS7. We show that either the PTS1 or the PTS2 alone is sufficient to direct the import of both ACD31.2 and LACS7 into the peroxisome matrix, consistent with localization data previously reported for a similarly dual-targeted protein, PEX8, in yeast (15, 28, 34).

Although the results from our biochemical analysis are also consistent with the fluorescence localization data previously reported for LACS7 (1), some discrepancies remain in the case of ACD31.2. Using an *in vitro* import assay, we demonstrated dependence upon either PTS1 or PTS2 for ACD31.2 import rather

than just the single PTS2 (24). Localization determined by fluorescence microscopy does not distinguish between intra-organelle localization and organelle-membrane association. Type 1 targeting signals that deviate from the canonical sequence also require accessory residues that assist in import (19, 20, 24), therefore careful consideration of the nature of the deletion constructs must be made. In the analysis ACD31.2 localization involving fluorescence microscopy, only the 3 amino acids belonging to the carboxyl terminal PTS1 were eliminated in the deletion construct (24). Thus, the remaining accessory proteins, along with the intact PTS2, could potentially aid in cargo/receptor binding in the cytosol and subsequent association at the peroxisome membrane – a result not easily distinguished by fluorescence microscopy alone. Our biochemical studies utilized constructs with deletions of at least 15 amino acids from the carboxyl terminus; the resulting constructs lacked not only their PTS1 but also potential accessory residues. It is also noteworthy to mention that the construct made to test ACD31.2 import dependence on the PTS2, not only possessed a mutated PTS2 sequence, but also a carboxyl terminal fluorescent tag (24), the presence of which has been previously shown to eliminate PTS1 import (10, 18). Thus, both PTSs were eliminated and mislocalization of ACD31.2 to the cytosol was likely a result of the loss of both signals rather than an insufficient PTS1. In fact, we have shown that the simultaneous elimination of both targeting signals results in the loss of import of both ACD31.2 and LACS7 (Figure 4). Thus, without the need for consideration of where fluorescence tags

should be placed, we were able to eliminate just one PTS at a time and demonstrate that either is sufficient for ACD31.2 import.

Data from the fluorescent analysis of LACS7 localization and our biochemical *in vitro* import assays seem to agree. However, neither result can reconcile the enigma concerning the lack of binding to PEX7 (1). Perhaps the lack of PEX7 interaction could be explained by fusion of the Gal4-binding domain to the amino terminus of LACS7, resulting in a bait protein with a PTS2 sequence located too far from the amino terminus of LACS7 to be an effective targeting sequence. On the other hand, there are documented examples of amino-terminal fusions to enzymes that can still be recognized as PTS2 import proteins in yeast two-hybrid systems (5). In fact, the LACS7 protein used in this study was expressed with a GST fusion attached to its amino-terminus; this fusion protein was able to import into glyoxysomes in a PTS2-dependent manner *in vitro*.

It is interesting to speculate about the requirement of potentially redundant targeting signals. One could speculate that peroxisome import could benefit from two targeting signals during stages of peroxisome biogenesis consistent with changes in the developmental stage of an organism or conditions that might warrant the immediate import of certain proteins (i.e. germination, senescence, stress). In the case of LACS7, dual PTSs could actually prove to be an advantage in times of early germination when rapid peroxisome proliferation and the import of large amounts of enzymes for β-oxidation and the glyoxylate cycle are essential (8, 25). Certainly, the examination of *LACS7* gene expression compared with the expression profile of genes for peroxisomal enzymes involved

in β-oxidation and glyoxylate cycle demonstrates a synchronized induction of both at the onset of germination (25). Thus, it is reasonable to consider the possibility that if the import machinery of one pathway is totally saturated, it is more favorable for a specific protein to carry both targeting signals to ensure its import and subsequent activity inside the organelle via a second pathway. Proteins are targeted to the peroxisome by a PTS2 less frequently than by its predominant partner, the PTS1. In plants, PTS2-containing proteins account for about 10% of all proteins targeted to the peroxisome matrix (24). Therefore one could imagine that proteins carrying both signals are able to default to the PTS2 pathway for import and ensure their proper localization and activity inside the peroxisome.

If this is true, it may be slightly harder to reconcile the usefulness of dual signals for ACD31.2. While it is relatively easy to speculate that the import and putative chaperone activity of ACD31.2 may be upregulated and crucial at times of stress to prevent unspecific aggregation of partially denatured proteins, the results from expression studies by reverse transcription-PCR reveal that AtACD31.2 is constitutively expressed (17). But plants are exceptional among eukaryotes in employing sHsps in the peroxisome matrix to prevent nonspecific aggregation of partially denatured proteins under both physiological and stress conditions. Thus, for ACD31.2, an import strategy similar to the one considered for LACS7 described above may be useful to ensure it's constitutive function; when one pathway is blocked, the other pathway is utilized.

Using our *in vitro* peroxisome import assay, we have studied the import characteristics of two proteins found in *Arabidopsis thaliana* that possess both a putative PTS1 and a PTS2, LACS7 and ACD31.2. Our results suggest that in both cases, ACD31.2 and LACS7, either the PTS1 or PTS2 was sufficient to direct localization into the peroxisome matrix.

FUTURE DIRECTIONS

It is clear that both ACD31.2 and LACS7 are peroxisome matrix enzymes whose localization is dependent on PTS1 and/or PTS2. What remains unclear is an understanding of how these signals might work in a coordinate fashion with their distinct and specific receptors to facilitate import along two different peroxisome import pathways. To better understand these relationships, it is important to rigorously tease out the factors involved in the successful import of these dual-targeted proteins.

Analysis should begin with an in-depth approach to studying the binding relationships between these proteins and their import receptors. Despite the successful identification of thousands of binding partners of various proteins from a variety of organisms, the yeast two-hybrid approach is subject to certain limitations - false negatives due to interference of the fused domains, false positives caused by nonspecific interactions giving rise to biologically irrelevant yeast two-hybrid interactions, inability to detect weak or transient interactions involving low abundance proteins, and low reproducibility. A better and more definitive, approach would be to use over-expressed, purified protein in direct binding interactions *in vitro*. The advantage of this method is that it indicates the reaction between the two participating proteins independent of any other factors that might influence or interfere with their binding.

A more elegant approach to show direct protein-protein interaction between LACS7, ACD31.2 and their import receptors would be to use Flourescence Resonance Energy Transfer (FRET) microscopy. FRET technology relies on the interaction between native proteins and eliminates counterfeit results that could be produced. Plant cells can be transformed with suitable FRET-fluorescence (CFP, YFP, etc.) labeled ACD32.1, LACS7, PEX5 or PEX7 constructs. Using confocal microscopy, FRET is able to capture weak and transient interactions through fluorescent signals that indicate a direct interaction between participating proteins in single living or fixed cells. This technique can be used to answer interesting questions on a wide variety of background conditions. For example, it would be interesting to observe the hierarchy of binding between PEX5, PEX7 as it relates to *in vivo* import of LACS7 or ACD31.2 in wild-type plants in comparison to conditions where PEX5 or PEX7 binding is defective (11).

By establishing the protein-protein interactions that participate in the import of these proteins, one could begin to understand the precise nature by which these proteins import into peroxisomes, especially as it relates to the interactions with the receptors that define specific import pathways.

Protein	RE digestion		
	Enzyme	**CT amino acid truncation**	**Resulting extreme CT tripeptide**
GLO	PstI	46	-AGV
ACD31.2	MspAI	15	-NVS
LACS7	SalI	106	-AIV

Table 4.1. GLO, ACD31.2 and LACS7 PTS1 deletion constructs. The table above lists the PTS1 deletion constructs obtained by restriction digest. The restriction enzymes used to create each construct are shown. The number of amino acids cleaved from the carboxyl terminus (CT) of each protein is given. This number includes the PTS1 tripeptide. Note that the resulting extreme carboxyl terminal tripeptide sequence shown is not a PTS1. These proteins are not expected to be protease protected in an *in vitro* import assay. GLO, glycolate oxidase; ACD31.2, alpha-crystalline domain protein 31.2kDa; LACS7, long-chain acyl-CoA synthetase 7.

Protein	Mutation	Primer pairs used	
		FORWARD	REVERSE
THL	R7A	5’ GAG AAA GCG ATC GAG GCA CAA CGC GTT CTT C 3’	5’ GAA GAA CGC GTT GTG CCT CGA TCG CTT TCT C 3’
ASP3	R15A	5’ TCT TCT TCT TCC GAT CGC GCT ATC GGT GCT CTG CTC C 3’	5’ GGA GCA GAG CAC CGA TAG CGC GAT CGG AAG AAG AAG A3’
ACD31.2	R11A	5’ CAC CGC TCG ACG CGC TCT CGC TGC CTT CGC 3’	5’ GCG AAG GCA GAG AGA GCG CGT CGA GCG GTG 3’
LACS7	R10A	5’ CGC CGG AAC AAC GTG CTC TCG AAA CCA TTC 3’	5’ GAA TGG TTT CGA GAG CAC GTT GTT CCG GCG 3’

Table 4.2. THL, ASP3, ACD31.2 and LACS7 R1A mutants and primers. The positions of the arginines in the protein are given. ASP3, aspartate aminotransferase 3; ACD31.2, alpha-crystalline domain protein 31.2kDa; LACS7, long-chain acyl-CoA synthetase 7.

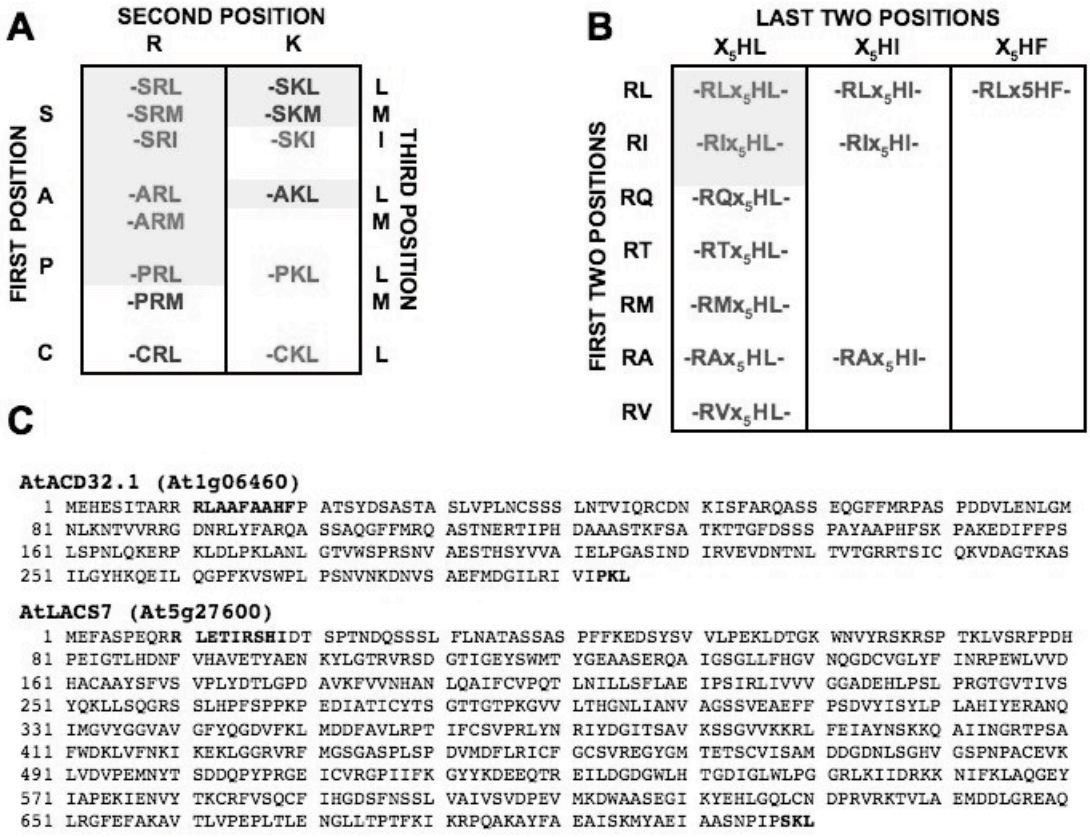

Figure 4.1. Plant PTSs and the protein sequences of ACD31.2 and LACS7. A) The extreme carboxyl terminal tripeptide PTS1 sequences of matrix proteins in plants are shown. B) The amino-terminal PTS2 nonapeptides of matrix proteins in plants are depicted. Major PTS sequences (red, light gray shade) are present in at least 10 sequences and 3 orthologous groups. Minor PTS sequences (blue) are present in at least 2 sequences. Adapted from Reumann (2004). C) The complete amino acid sequences for ACD31.2 and LACS7 are shown. The carboxyl terminal PTS1 and amino-terminal PTS2 sequences are in bold.

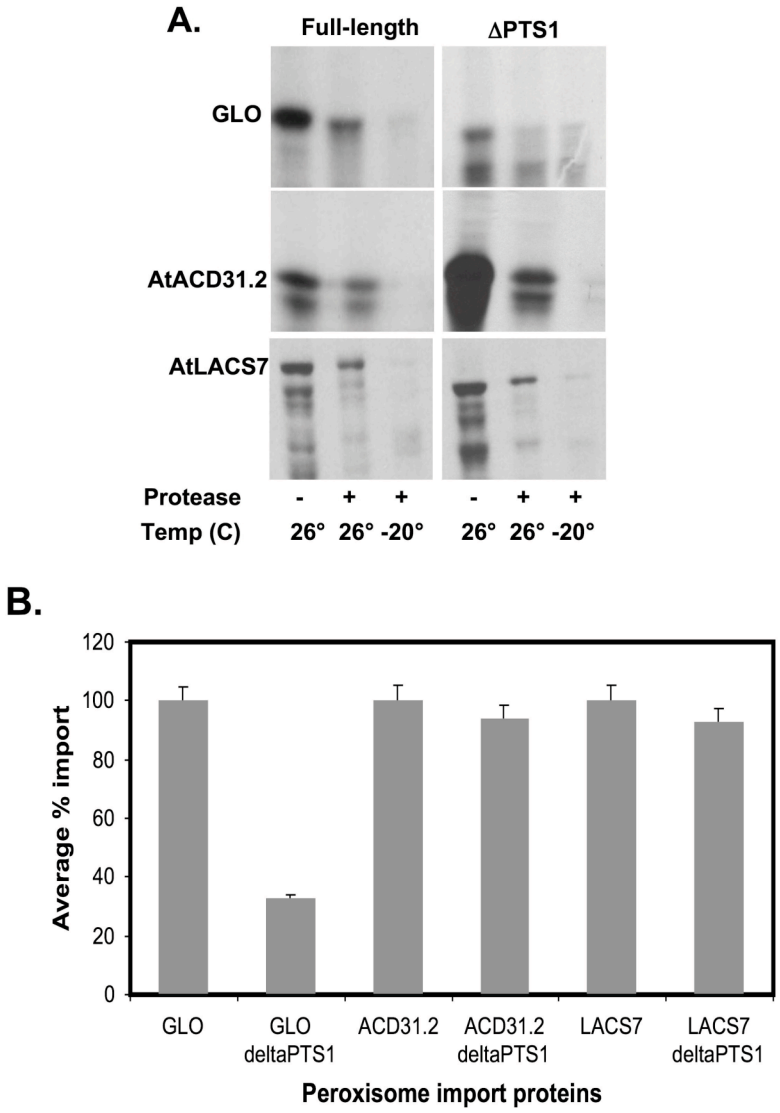

Figure 4.2. Deletion of the PTS1 signal decreased the import of the PTS1 protein GLO, but not ACD31.2 and LACS7 *in vitro*. A) PTS1 deletion constructs were created by restriction enzyme digestion of the full-length genes *GLO, ACD31.2 and LACS7* upstream of their carboxyl terminal ends. The resulting truncated proteins lacked the PTS1. Isolated glyoxysomes were incubated with radiolabeled proteins GLO, ACD31.2, LACS7, and all truncation import mutants (ΔPTS1) for 60 minutes under standard import conditions, as described in Materials and Methods. Samples were prepared for analysis by SDS-PAGE. An autoradiograph after 12 hours' exposure is shown. All full-length proteins were protease-protected, consistent with peroxisomal localization (lane 3). Note that only the removal of the PTS1 from GLO resulted in loss of import (lane 6). B) Import efficiency was quantitated by phosphorimaging analysis. All results are from representative experiments that were repeated at least 3 times. Error bars indicate the standard deviation.

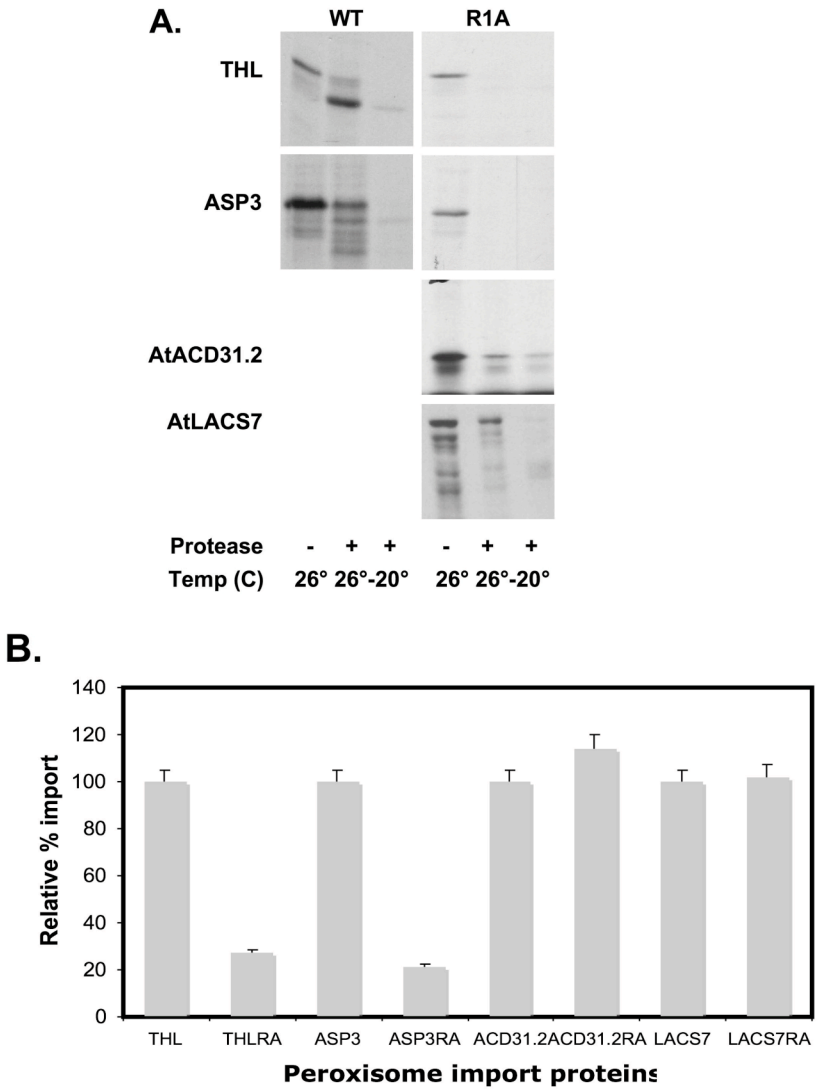

Figure 4.3. Mutating the highly conserved arginine in position 1 of the PTS2 consensus sequence inhibits the import of THL and ASP3, but not ACD31.2 and LACS7. Site-directed mutagenesis was used to change the arginine residue in the first position of each PTS2 sequence in THL, ASP3, ACD31.2 and LACS7 to an alanine. These PTS2 import mutants are indicated in the figure as R1A. Following import under standard import conditions, all samples were incubated with thermolysin for 30 minutes on ice. Intact glyoxysomes were reisolated and samples were prepared for analysis by SDS-PAGE. Note that placing an alanine in the first position of the PTS2 changes the consensus sequence. Except in the case of ACD31.2 and LACS7, PTS2-dependent import of these mutants is decreased. B) Import levels were quantitated by phosphorimaging as described in Materials and Methods. All results are from representative experiments that were repeated at least 3 times. Error bars indicate the standard deviation.

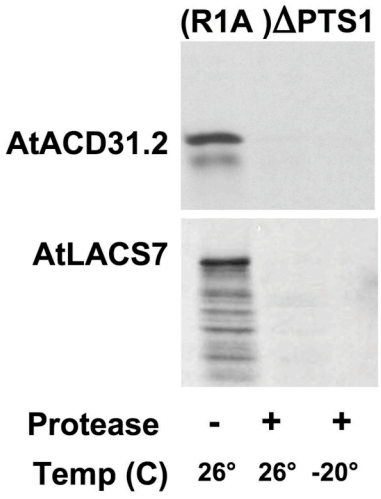

Figure 4.4. Neither ACD31.2 nor LACS7 was imported when both PTSs were disabled. R1A mutants were subjected to restriction digestion with the appropriate enzymes to delete carboxyl terminal regions that include the PTS1. The autoradiograph from a standard import experiment is shown. Note that the elimination of both import signals resulted in protease-sensitivity after standard import incubation at 26°C for 60 minutes. All results are from representative experiments that were repeated at least 3 times.

REFERENCES

1. **Bonsegna, S., S. P. Slocombe, L. De Bellis, and A. Baker.** 2005. AtLACS7 interacts with the TPR domains of the PTS1 receptor PEX5. Arch Biochem Biophys **443:**74-81.
2. **Braverman, N., G. Steel, C. Obie, A. Moser, H. Moser, S. J. Gould, and D. Valle.** 1997. Human PEX7 encodes the peroxisomal PTS2 receptor and is responsible for rhizomelic chondrodysplasia punctata. Nat Genet **15:**369-76.
3. **Brickner, D. G., J. J. Harada, and L. J. Olsen.** 1997. Protein transport into higher plant peroxisomes. In vitro import assay provides evidence for receptor involvement. Plant Physiol **113:**1213-21.
4. **Comai, L., R. A. Dietrich, D. J. Maslyar, C. S. Baden, and J. J. Harada.** 1989. Coordinate expression of transcriptionally regulated isocitrate lyase and malate synthase genes in Brassica napus L. Plant Cell **1:**293-300.
5. **Elgersma, Y., M. Elgersma-Hooisma, T. Wenzel, J. M. McCaffery, M. G. Farquhar, and S. Subramani.** 1998. A mobile PTS2 receptor for peroxisomal protein import in Pichia pastoris. J Cell Biol **140:**807-20.
6. **Elledge, S. J., J. T. Mulligan, S. W. Ramer, M. Spottswood, and R. W. Davis.** 1991. Lambda YES: a multifunctional cDNA expression vector for the isolation of genes by complementation of yeast and Escherichia coli mutations. Proc Natl Acad Sci U S A **88:**1731-5.
7. **Fulda, M., J. Shockey, M. Werber, F. P. Wolter, and E. Heinz.** 2002. Two long-chain acyl-CoA synthetases from Arabidopsis thaliana involved in peroxisomal fatty acid beta-oxidation. Plant J **32:**93-103.
8. **Germain, V., E. L. Rylott, T. R. Larson, S. M. Sherson, N. Bechtold, J. P. Carde, J. H. Bryce, I. A. Graham, and S. M. Smith.** 2001. Requirement for 3-ketoacyl-CoA thiolase-2 in peroxisome development, fatty acid beta-oxidation and breakdown of triacylglycerol in lipid bodies of Arabidopsis seedlings. Plant J **28:**1-12.
9. **Ghys, K., M. Fransen, G. P. Mannaerts, and P. P. Van Veldhoven.** 2002. Functional studies on human Pex7p: subcellular localization and interaction with proteins containing a peroxisome-targeting signal type 2 and other peroxins. Biochem J **365:**41-50.
10. **Gould, S. J., G. A. Keller, N. Hosken, J. Wilkinson, and S. Subramani.** 1989. A conserved tripeptide sorts proteins to peroxisomes. J Cell Biol **108:**1657-64.
11. **Hayashi, M., M. Yagi, K. Nito, T. Kamada, and M. Nishimura.** 2005. Differential contribution of two peroxisomal protein receptors to the maintenance of peroxisomal functions in Arabidopsis. J Biol Chem **280:**14829-35.
12. **Johnson, T. L., and L. J. Olsen.** 2003. Import of the peroxisomal targeting signal type 2 protein 3-ketoacyl-coenzyme a thiolase into glyoxysomes. Plant Physiol **133:**1991-9.
13. **Karpichev, I. V., and G. M. Small.** 2000. Evidence for a novel pathway for the targeting of a Saccharomyces cerevisiae peroxisomal protein

belonging to the isomerase/hydratase family. J Cell Sci **113 (Pt 3):**533-44.

14. **Lazarow, P. B.** 2006. The import receptor Pex7p and the PTS2 targeting sequence. Biochim Biophys Acta **1763:**1599-604.
15. **Leon, S., J. M. Goodman, and S. Subramani.** 2006. Uniqueness of the mechanism of protein import into the peroxisome matrix: transport of folded, co-factor-bound and oligomeric proteins by shuttling receptors. Biochim Biophys Acta **1763:**1552-64.
16. **Lubben, T. H., and K. Keegstra.** 1986. Efficient in vitro import of a cytosolic heat shock protein into pea chloroplasts. Proc Natl Acad Sci U S A **83:**5502-5506.
17. **Ma, C., M. Haslbeck, L. Babujee, O. Jahn, and S. Reumann.** 2006. Identification and characterization of a stress-inducible and a constitutive small heat-shock protein targeted to the matrix of plant peroxisomes. Plant Physiol **141:**47-60.
18. **Miyazawa, S., T. Osumi, T. Hashimoto, K. Ohno, S. Miura, and Y. Fujiki.** 1989. Peroxisome targeting signal of rat liver acyl-coenzyme A oxidase resides at the carboxy terminus. Mol Cell Biol **9:**83-91.
19. **Mullen, R. T., M. S. Lee, and R. N. Trelease.** 1997. Identification of the peroxisomal targeting signal for cottonseed catalase. Plant J **12:**313-22.
20. **Neuberger, G., S. Maurer-Stroh, B. Eisenhaber, A. Hartig, and F. Eisenhaber.** 2003. Motif refinement of the peroxisomal targeting signal 1 and evaluation of taxon-specific differences. J Mol Biol **328:**567-79.
21. **Olsen, L. J., S. M. Theg, B. R. Selman, and K. Keegstra.** 1989. ATP is required for the binding of precursor proteins to chloroplasts. J Biol Chem **264:**6724-9.
22. **Rehling, P., M. Marzioch, F. Niesen, E. Wittke, M. Veenhuis, and W. H. Kunau.** 1996. The import receptor for the peroxisomal targeting signal 2 (PTS2) in Saccharomyces cerevisiae is encoded by the PAS7 gene. Embo J **15:**2901-13.
23. **Rehling, P., A. Skaletz-Rorowski, W. Girzalsky, T. Voorn-Brouwer, M. M. Franse, B. Distel, M. Veenhuis, W. H. Kunau, and R. Erdmann.** 2000. Pex8p, an intraperoxisomal peroxin of Saccharomyces cerevisiae required for protein transport into peroxisomes binds the PTS1 receptor pex5p. J Biol Chem **275:**3593-602.
24. **Reumann, S.** 2004. Specification of the peroxisome targeting signals type 1 and type 2 of plant peroxisomes by bioinformatics analyses. Plant Physiol **135:**783-800.
25. **Rylott, E. L., M. A. Hooks, and I. A. Graham.** 2001. Co-ordinate regulation of genes involved in storage lipid mobilization in Arabidopsis thaliana. Biochem Soc Trans **29:**283-7.
26. **Scharf, K. D., M. Siddique, and E. Vierling.** 2001. The expanding family of Arabidopsis thaliana small heat stress proteins and a new family of proteins containing alpha-crystallin domains (Acd proteins). Cell Stress Chaperones **6:**225-37.

27. **Schliebs, W., and W. H. Kunau.** 2006. PTS2 co-receptors: diverse proteins with common features. Biochim Biophys Acta **1763:**1605-12.
28. **Smith, J. J., and R. A. Rachubinski.** 2001. A role for the peroxin Pex8p in Pex20p-dependent thiolase import into peroxisomes of the yeast Yarrowia lipolytica. J Biol Chem **276:**1618-25.
29. **Wang, X., M. A. McMahon, S. N. Shelton, M. Nampaisansuk, J. L. Ballard, and J. M. Goodman.** 2004. Multiple targeting modules on peroxisomal proteins are not redundant: discrete functions of targeting signals within Pmp47 and Pex8p. Mol Biol Cell **15:**1702-10.
30. **Waterham, H. R., V. I. Titorenko, P. Haima, J. M. Cregg, W. Harder, and M. Veenhuis.** 1994. The Hansenula polymorpha PER1 gene is essential for peroxisome biogenesis and encodes a peroxisomal matrix protein with both carboxy- and amino-terminal targeting signals. J Cell Biol **127:**737-49.
31. **Woodward, A. W., and B. Bartel.** 2005. The Arabidopsis peroxisomal targeting signal type 2 receptor PEX7 is necessary for peroxisome function and dependent on PEX5. Mol Biol Cell **16:**573-83.
32. **Yang, X., P. E. Purdue, and P. B. Lazarow.** 2001. Eci1p uses a PTS1 to enter peroxisomes: either its own or that of a partner, Dci1p. Eur J Cell Biol **80:**126-38.
33. **Zhang, J. W., X. Cai, and P. B. Lazarow.** 1996. Peb1p (Pas7p) is an intra-peroxisomal receptor for the N-terminal, type 2, peroxisomal targeting signal of thiolase. Ann N Y Acad Sci **804:**654-5.
34. **Zhang, L., S. Leon, and S. Subramani.** 2006. Two independent pathways traffic the intraperoxisomal peroxin PpPex8p into peroxisomes: mechanism and evolutionary implications. Mol Biol Cell **17:**690-9.